STUDY ON THE DEVELOPMENT OF THE ALUMINA-RARE EARTH PHOSPHATE MACHINABLE COMPOSITES FOR BIOMEDICAL APPLICATIONS

ABHISHEK BADOLIA

DEPARTMENT OF CERAMIC ENGINEERING
NATIONAL INSTITUTE OF TECHNOLOGY, ROURKELA
ODISHA, INDIA

STUDY ON THE DEVELOPMENT OF THE ALUMINA - RARE EARTH PHOSPHATE MACHINABLE COMPOSITES FOR BIOMEDICAL APPLICATIONS

A Thesis Submitted in Partial Fulfillment of the

Requirement for the Degree

MASTER OF TECHNOLOGY

(RESEARCH)

By

ABHISHEK BADOLIA

612CR302

Under the guidance of

Prof. Ritwik Sarkar

and

Prof. Sumit Kumar Pal

Department of Ceramic Engineering

National Institute of Technology, Rourkela

2015

NATIONAL INSTITUTE OF TECHNOLOGY

Rourkela, INDIA

CERTIFICATE

This is to certify that the thesis entitled, **"STUDY ON THE DEVELOPMENT OF THE ALUMINA - RARE EARTH PHOSPHATE MACHINABLE COMPOSITES FOR BIOMEDICAL APPLICATIONS"** submitted by Mr. Abhishek Badolia (612CR302) for the degree of Master of Technology (Research) in Ceramic Engineering, National Institute of Technology, Rourkela, is a bonafide research work carried out by him under our supervision and guidance. His thesis, in our opinion, is worthy of consideration for the award of degree of Master of Technology (Research) in accordance with the regulation of the institute.

The result embodied in this thesis is original and have not been submitted to any other university or institute for the award of any degree.

Prof. Ritwik Sarkar
Associate Professor
Department of Ceramic Engineering
National Institute of Technology, Rourkela

Prof. Sumit Kumar Pal
Assistant Professor
Department of Ceramic Engineering
National Institute of Technology, Rourkela

Declaration

I declare that this thesis is my own work and has not been submitted in any form for another degree at any university or other institution. Derived Information from the literature of published work of others has been acknowledge in the text and a list of references given.

Date: _23-1-2015_

Abhishek Badolia

CONTENTS

Acknowledgement

ABSTRACT

Alumina, being a ceramic material, is very hard and strong, is a well-known bioinert ceramics, useful for many implant applications. But strong atomic bonding results in poor machinability in alumina, which is a useful and required property for implants as the shape and dimensional accuracy & criticality are very strict. Hence being a poorly machinable material wide applicability of alumina as implant material is restricted.

In the present work, two different grades (C and R) of commercial grade high pure alumina is studied for its machinability (drilling character) by incorporating a weak interphase material, rare earth phosphates (REP`s), namely lanthanum phosphate ($LaPO_4$) and yttrium phosphate (YPO_4). Variation of REP was studied between 10 – 50wt. % for both the aluminas. Both the phosphates were stable and found to remain inert (no reaction with alumina) on sintering upto 1600^oC, making a true composite character of the alumina-REP sintered compositions. Microstructural studies showed well distributed alumina and rare earth phosphates grains after sintering. All the sintered samples were found to be drillable for all the condition. Only a threshold value of REP content was observed at 1600^oC for the higher reactive alumina. Biological studies showed positive results for all the compositions studied. CAl_2O_3 with 30wt. % REP content sintered at 1600^oC was found to be machinable with a densification of >85% and strength >150MPa.

Abbreviations

Al_2O_3	Alumina (CAl_2O_3 & $RCAl_2O_3$)
REO	Rare Earth Oxides
REP	Rare Earth Phosphates
$LaPO_4$	Lanthanum Phosphate
YPO_4	Yttrium Phosphate
H_3PO_4	Phosphoric Acid
XRD	X-ray Diffraction
FTIR	Fourier Transformed Infrared Analysis
FESEM	Field Emission Scanning Electron Microscopy
MTT	3-(4,5-dimethylthiazol-2-yl)-2,5-diphenyltetrazolium bromide
Wt.%	Weight Percent

List of Figures

List of Tables

CHAPTER 1
Introduction

1.1 Ceramic Materials

Ceramic materials defined as inorganic, non-metallic compounds of a metal or a non-metal. Ceramic materials may be crystalline or non-crystalline. They are formed by the action of heat and subsequent cooling. Clay is one of the earliest materials used to produce ceramics, as pottery, but many different ceramic materials are used in domestic, industrial and building products. Ceramic materials tend to be strong, brittle, chemically inert, and non-conductors of heat and electricity, but their properties vary widely. For example, porcelain is extensively used to make electrical insulators but some ceramic compounds act as superconductors. Fig. 1.1 – Fig. 1.2 shows the classifications and applications of ceramic material.
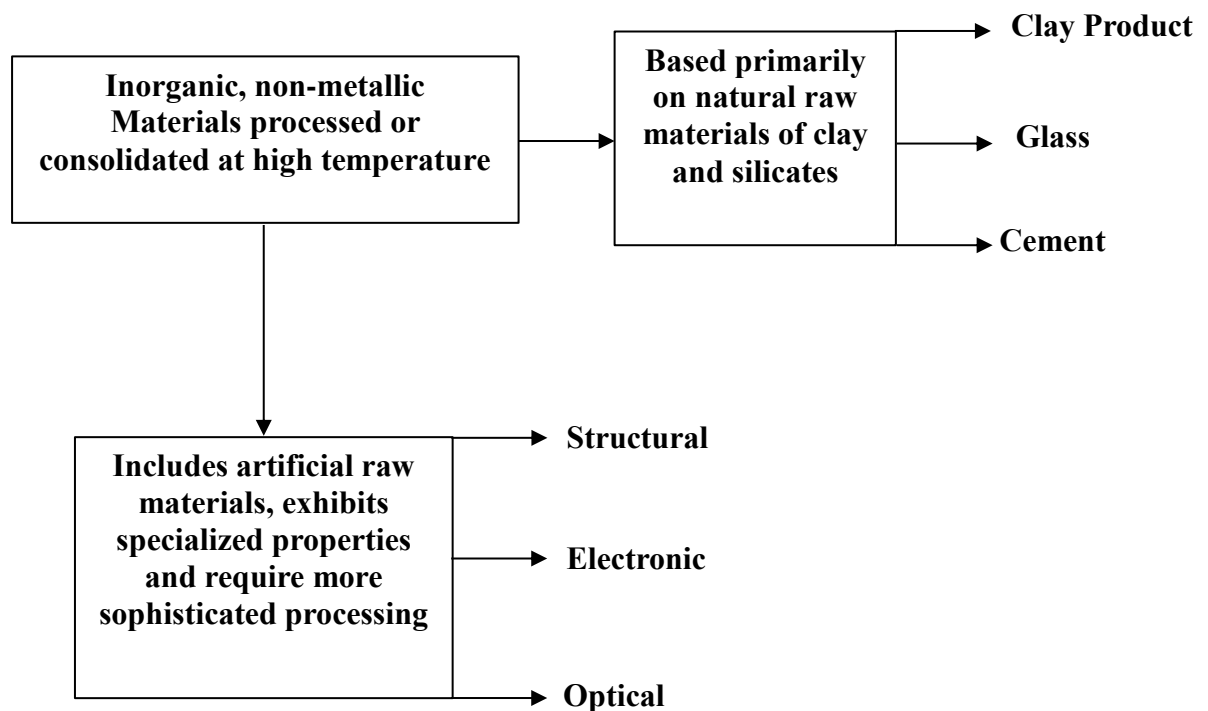
Fig. 1.1: Broad Classifications of Ceramics [1]

Advance Ceramic

Oxide	Nitride	Carbide
▪ **Abrasive** ▪ **Bioceramics** ▪ **Electrical/Electronics** ▪ **Cutting tools** ▪ **Refractory Block** ▪ **Class Additives** ▪ **Nuclear Fuels**	▪ **Rocket Engines** ▪ **Gas Turbines** ▪ **Cutting Tools (steels)** ▪ **Substrate for IC Chips**	▪ **Abrasive** ▪ **Resistance Heating** ▪ **Steel Additives** ▪ **Cutting Tools (Cements)** ▪ **Ceramic Matrix Composites** ▪ **Reinforcing Fibers**
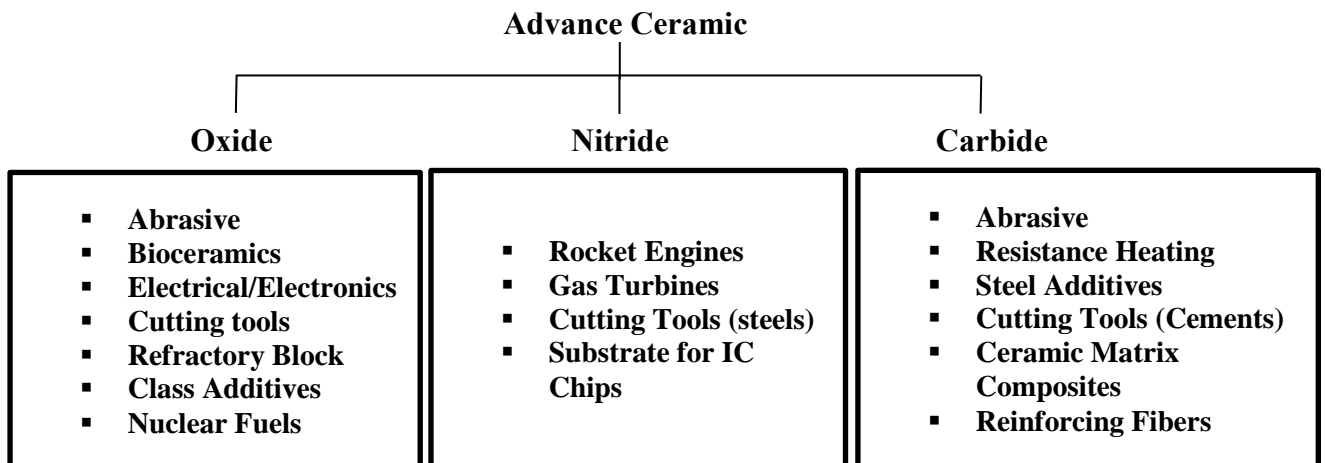
Fig. 1.2: Applications of Advance Ceramic Materials [1]

1.1.1 Properties of Ceramics

1. High hardness, electrical and thermal insulating, chemical stability and high melting temperatures.
2. Brittle, virtually no ductility can cause problems in both processing and performance of ceramic products.
3. Some ceramics is translucent, window glass (based on silica) being the clearest example.

1.1.2. Alumina ceramics

Alumina ceramic is one of the most desirable ceramic for engineering work. Alumina or aluminium oxide is a chemical compound of aluminium and oxygen with the chemical formula Al_2O_3. It usually occurs in its crystalline polymorphic phase α-Al_2O_3, in which it composes the mineral corundum. Al_2O_3 is significant in its use to produce aluminium metal, as abrasive material because of its hardness, and as a refractory material due to the high melting point.

Alumina ceramics are white in color but may vary to different shades depending on the impurities content in them. The color may also be due to the sintering additives. Many industries commercially produce different ranges of highly pure alumina ceramics in the range of 96% – 99.9% purity for various industrial applications [2].

1.1.3. Characteristics of Alumina ceramic

1. Good strength and stiffness.
2. Good hardness and wear resistance.
3. Good corrosion resistance.
4. Good thermal stability.
5. Excellent dielectric properties.

1.1.4 Applications of Alumina Ceramic

1. Medical Prostheses.
2. Electronic Substrates.
3. Thermocouple tubes.
4. Refractories.
5. Wear components.
6. Electrical insulators.
7. Sealing rings.

1.2 Machinable Ceramics

Most of the ceramic components have complex shapes and require a good tolerance and surface finish. Such characteristics are usually achieved by machining, which is both costly and potentially damaging to the strength of the component. Machining is emerging as an inevitable requirement for flexible use of advanced ceramics, especially for structural ceramics. However, the extremely high hardness and brittleness of ceramics make conventional machining very difficult or even impossible. In some cases (especially optical and electronic applications), machining damage may be so intrusive as to necessitate additional polishing operations [3]. In this context, the machining may be seen as a major limiting step in ceramics manufacturing.

In past few years, many researchers have been focused on the improvement of ceramic machinability [4-6]. There are two methods that used for improving the machinability of ceramic materials. One method is to introduce a weak interface or layered structured material in the matrix to facilitate crack deflection, where phase and porosity distribution in three-dimension are controlled and optimized [7-8]. The other method is the structure design

method, where the machinability of ceramics is optimized by adjusting the distribution of phase and porosity [8].

The most popular ceramic based machinable materials are machinable glass-ceramics, consisting of finely dispersed mica platelets in a glass matrix, can be cut and drilled using conventional metal-working tools. The ease of cutting derives from the cleavage of the mica crystals beneath the cutting tool, and material removal by linking of the microcrack. These materials are used in a variety of applications requiring their high-temperature properties, high hardness, electrical or thermal insulation, or dielectric properties, combined with the convenience of machining. However, their high-temperature use is limited by softening of the glass phase or coarsening of the crystallites, usually at temperatures above 800°C [9-10].

Interest in monazite ceramics during the eighties was due to its high temperature stability, high melting point (> 1900°C) greater than that of alumina (Al_2O_3) and low thermal conductivity and diffusivity [11]. After that in mid-nineties search for high temperature, oxidation resistant and weakly bonded interface materials for ceramic composites had also ended up in monazite ceramics, especially rare earth phosphates La, Ce, Y [12]. Due to the identical thermal expansion coefficients of Al_2O_3 and $LaPO_4$ their composites were widely investigated and were found to be chemically inert.

1.3 Biomaterials

In recent years, many definitions have been developed for the term "Biomaterials". The consensus developed by experts in this field is the following: biomaterials (or biomedical materials) are defined as synthetic or natural materials used to replace parts of living system or to function in intimate contact with living tissue [13]. A biomaterial is a substance that has been engineered to take a form which, alone or as part of a system, is used to direct, by control of interactions with components of living systems, the course of any therapeutic or diagnostic procedure, in human or veterinary medicine [14]. Biomaterials are intended to interface with biological systems to evaluate, treat, augment, or replacement of any tissue, organ or function of the body and are now used in a number of different applications throughout the body [15-16]. The significant difference of biomaterials from other classes of materials is their ability to remain in a biological environment without damaging the surroundings and without being hurt in that process.

Biomaterials are solely associated with the health care domain and must have an interface with tissue or tissues components [17].

Significant advancements in the development of medical applications have occurred in last few years, and innovation, and use of ceramic materials for skeletal repair and reconstruction is a major one [15]. The revolution occurred in ceramic to repair and reconstruct the damaged or diseased parts of the body [18]. When ceramics entered in bio-medical field a new class of materials, namely, "Bioceramics" is created. Ceramic materials can be classified as bioinert, bioactive and bioresorbable. Bioinert ceramics such as alumina have high compressive and bending strength and better biocompatibility than metals. Therefore, alumina is used for osteosynthetic devices (alumina monocrystal) or to fabricate bone and joint prosthetic in the 1980`s [19] and due to its bio inertness it shows low reactivity with good mechanical feature (little wear and stability). The most popular applications are in ortho prosthetic joints, and it has proven to be very effective. Dental also uses this material proposed to achieve aesthetic and reliability of dental repair [20].

1.4 Composite Materials

Composite materials define that the working elements that can consider both the structural form and composition of the material constituents follows. A composite material will be substantial framework made out of a mixture or mix of two or more macro-constituents varying in structure and material arrangement and that are insoluble in one another [21].

The principle of composites states that it can be constructed of any grouping of two or more materials such as metallic, organic, or inorganic. While the possible material combinations in composites are almost unrestricted, the constituent forms are more limited. Real constituent structure is utilized as parts of composite material are filaments, particles, lamina or layer and networks. The lattice is the body component, serving to encase the composite and provide for it is mass structure. The filaments, particles, lamina, and fillers are the structural element, and they focus the interior structure of the composites. By and large, yet not, they are the added substance stage. Fig. 1.3 shows the composite material morphology.
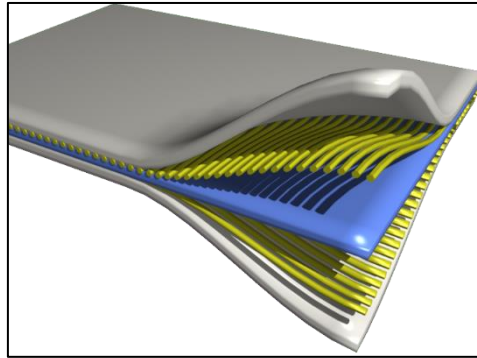
Fig. 1.3: Morphology of Composite Material

1.4.1   Types of Composites

The nature and the structure of composites, a working material can be made. A few order frameworks have been utilized, including characterization (1) by fundamental material mix, e.g. metal-natural or metal-inorganic; (2) by mass material blend, e.g. network frameworks or overlays; (3) by conveyance of the constituents, e.g. persistent or intermittent and (4) by capacities, e.g. electrical or structural. The order framework primarily utilized is focused on the type of the fundamental constituents. This gives five general classes of composites:

1. Fiber composites made out of fiber with or without a matrix.
2. Flake composites, composed of flat flakes with or without a matrix.
3. Particulate composites consisting of particles with or without a matrix.
4. Filled (or skeletal) composites, made out of a ceaseless skeletal framework supplied by a second material.
5. Laminar composites composed of layer or laminar constituent.

The fiber type composites have evoked the most interest among engineers concerned with structural applications. Initially, most work is done with strong, stiff fibers of solid, circular cross section in a much weaker, more flexible matrix. Then development work disclosed the particular advantage offered by metal and ceramic fibers. In structural applications, flakes appear to provide several advantages over fibers.

For example, flake composites containing parallel flakes have a higher theoretical modulus than fiber composites and can be packed closer and with fewer voids. Compared with fibers, flakes are relatively inexpensive and can handled in batch quantitates.

Particulate composites have an additive constituent that is essentially one or two dimensional and macroscopic. Particulate composites differ from the fiber, and flake types in the distribution of the additives constituent are usually random rather than controlled. In the filled composites, there is a continuous 3D structural matrix, infiltrated or impregnated with a second phase filler material. The filler also has a 3D shape determined by the void form. The matrix itself may be an ordered honeycomb, a group cell, or a random sponge-like network of open pores. Laminar or layered composites have been made up of films or sheets, and they are easier to design, produce, standardize and control than another type of composites. The most successful application of the laminar principle has been the development of sandwich materials. Composites materials have many characteristics that differ from those of more conventional engineering materials. Most common construction materials are homogenous and isotropic. In contrast, composite materials are often both in homogeneous (or heterogeneous) and non-isotropic (or anisotropic). Fig. 1.4 shows the different types of composites.
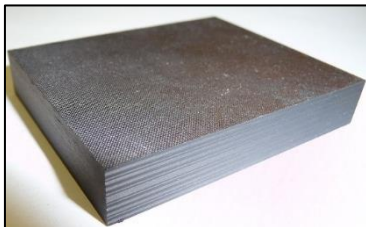
Laminar Composite
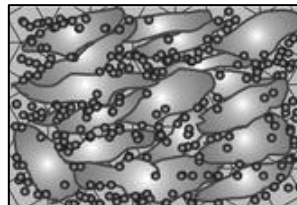
Flake Composite

Fiber Composite

Filled Composite

Fig. 1.4: Different Types of Composites

1.4.2 Alumina and Its Composites

Alumina is widely used as structural materials because of their high melting point and excellent mechanical properties, electrical resistance and chemical durability [22]. The application of alumina ranges from high-speed cutting tools, dental implants, electrical and thermal insulators, wear resistance parts and coatings. Alumina-based nano-sized ceramic composites will demonstrate a novel and favorable properties in comparison with their micro-sized crystalline counterparts [23]. Alumina forms composite with other materials ranging from metals, inter-metallic, to ceramic. The starting materials for composites are carefully selected such that even if a reaction occurs between them, at least two phases must be distinct in the material and the interaction of these phases in the matrix would not affect the properties of the matrix. The starting material for making of composites are carefully selected such that even if a reaction occurs between them, at least two phase must be distinct in the material and the interaction of these phases matrix would not affect the properties of the composites.

1.5 Alumina-Rare Earth Phosphate (REP) Composite

In mid-nineties, search for high temperature, oxidation resistant and weakly bonded interface material for ceramics has resulted in rare earth phosphate compounds like lanthanum phosphate ($LaPO_4$) [24]. Due to identical thermal expansion coefficient of Al_2O_3 and $LaPO_4$, their composites were widely investigated and were found to be chemically inert and machinable. The melting temperature of rare earth phosphates is above 2000°C. Therefore REP's are suitable to the fabricate the composites with Al_2O_3

Lanthanum phosphate ($LaPO_4$) in the Al_2O_3 composite is quite stable, and no reaction occurs between the two phase up to 1600°C as per the provided ratio of La:P. According to Morgan et al., $LaPO_4$ is stable in an alumina matrix, and phases are separated up to 1600°C, and sintered products are machinable also. $LaPO_4$-Al_2O_3 weak interface is reported to deflect the cracks and thus improves machinability [24]. Yttrium phosphate (YPO_4) in the Al_2O_3 based composites also has the similar nature as that of lanthanum phosphate. It is chemically and thermally stable and has no reaction with alumina even at high temperatures. It remains as a separate entity in a mixture of alumina and provides machinable character to alumina ceramic due to the phenomenon of weak interface [24].

Flexible use of advanced ceramics is limited due to high hardness that makes conventional machining very difficult or even impossible. Reduced hardness leads to good machinability. It has reported that lanthanum phosphate has low hardness of 4.2 GPa [25], which is close to that of machinable mica containing glass-ceramic (3 GPa) [26] and layered ternary compounds Ti_3SiC_2 (4-5 GPa) [26]. Many researchers have dedicated their research work to impart machinability in ceramics [12, 15, 16, 20, 24] [28-31].

References

1. J. A. Jacobs, T. F. Kilduff, Engineering Materials Technology, Fourth Edition, Prentice-Hall, Englewood Cliffs, N. J. (1985).

2. Coors Tek Amazing Solution, Alumina Ceramic, England.

3. L. M. Sheppard, The Challenge of Ceramic Machining Continue, Journal of Ceramic Society, Bulletin 71 (11) (1992) 1590-1610.

4. D. G. Grossman, Machinable Glass-Ceramics Based on Tetrasilicic Mica, Journal of Ceramic Society, 55 (9) (1972) 446-449.

5. T. Kusunose, T. Sekino, Y. H. Choa, K. Niihara, Machinability of Silicon Nitride/Boron Carbide Nanocomposites, Journal of American Ceramic Society, 85 (11) (2002) 2689-2695.

6. C. Kawai, A. Yamakawa, Machinability of high strength Porous Silicon Nitride Ceramics, Journal of Japan Ceramic Society, 106 (1998) 1135-1137.

7. R. Wang, Wei Pan, Jain Chen, Minghao Fang, Jun Meng, Materials letters 57 (2002) 822-827.

8. W. Pan and R.G. Wang, Material Engineering 29 (2000) 84-88.

9. C. K. Chyung, G. H. Beall, D. G. Grossman, Electron Microscopy and Structure of Materials, Edited by G. Thomas, R. M. Fulrath, R. M. Fisher, University of California, Berkeley, CA, 1972.

10. C. K. Chyung, G. H. Beall, D. G. Grossman, Flurophlogophic Mica Glass-Ceramics, 10th Processing of International Glass Congress, 1974.

11. Y. Hikichi, T. Nomura, Melting Temperature of Monazite and Xenotime, Journal of American Ceramic Society, 70 (10) (1987) C-252-C-253.

12. P. E. D. Morgan, D. B. Marshall, Functional Interfaces in Oxide-Oxide Composites, Journal of Material Science and Engineering A, 162 (1-2) (1993) 15-25.

13. D. F. Williams, The Williams dictionary of biomaterials, Liverpool, UK: Liverpool Uni. Press, (1999) 368.

14. D. F. Williams, On the nature of biomaterials, Biomaterials, 30 (2009) 5897-5909.

15. S. M. Best, A. E. Porter, E. S. Thian, J. Huang, Bioceramics: Past, Present and for the future, J Eur. Ceram Soc., 28 (2008) 1319-1327.

16. K. D. Jandt, Evolutions Revolutions and trends in biomaterials science – a perspective, Adv. Eng. Mater, 9 (2007) 1038-1050.

17. S. V. Dorozhkin, Bioceramics of calcium orthoposphates, Biomaterials, 31 (2010) 1465-1485.

18. L. L. Hench, Journal of the American Ceramic Society, 74 (7) (1991) 1487-1510.

19. T. Yamamura, Y. Kotoura, K. Kasahara, M. Takahashi, M. Abe, Intraoperative Radiotherapy and Ceramic Prosthesis Replacement for Osteosarcoma, Springer Verlag Tokyo 1989.

20. G. Maccauro, P. R. Iommetti, L. Raffaelli and P. F. Manicone, Chapter 15, Biomaterials Applications for Nanomedicine, November 2011.

21. Introduction to ceramics, W. D. Kingery, H. K. Bowen, D. R. Uhlamann, John Wiley and Sons, New York, 1975.

22. G. B. Kenny, H. K. Bowen, Journal of American Ceramic Society Bulletin 63 (1983) 590.

23. Particulate strengthened Oxide Ceramic-Nanocomposites, K. Niihara, A. Nakahira in advanced structural Inorganic Composites, Edited by P. Vincenzini, Elsevier Science Publishers B. V. 1991, 974.

24. P. E. D. Morgan, D. B. Marshall, Journal of American Ceramic Society, 78 (1995) 1553.

25. Y. Konishi, T. Kununose, P. E. D. Morgan, T. Sekino, K. Niihara, The Science of Engineering Ceramics II, Proceedings 2nd international symposium of Science and Engineering Ceramic 3 (1998) 161-341.

26. D. G. Grossman, Journal of American Ceramic Society 55 (1972) 446.

27. M. W. Barsoun, T. El-Raghy Journal of American Ceramic Society 79 (1996) 1953.

28. C. Ergun, Journal of Materials Processing Technology 199 (2008) 178-184.

29. R. Wang, W. Pan, J. Chen, M. Jiang, Y. Luo, M. Fang, Ceramic International 29 (2003) 19-25.

30. G. Gong, B. Zhang, H. Zhang, W. Li, Ceramic International 32 (2006) 349-352.

31. M. A. Majeed, L. Vijayaraghavan, S. K. Malhotra, R. Krishnamoorthy, Journal of Materials Processing Technology 209 (2009) 2499-2507.

CHAPTER 2

Literature Review

Part A: Bioceramic Era and Alumina
Part B: Machinability
Part C: Rare Earth Phosphates and Ceramic Machinability
Part D: Biological Studies
Part E: Motivation and Objective of the Work
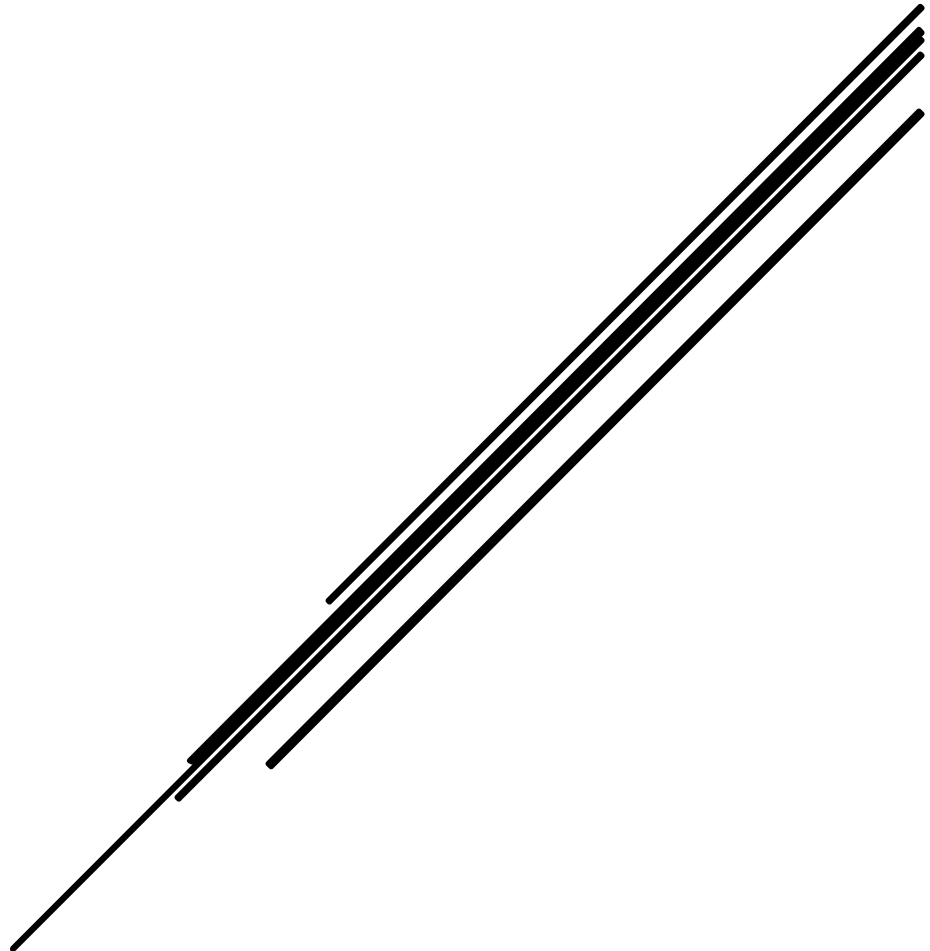
Part A

Bioceramic Era

2.1 The Bioceramics Era

In the last few decades treatment procedure through reconstructive surgeries has changed significantly with the introduction of bioceramics. Bioceramics are a particular class of ceramics that perform tailored functional/biological/chemical activities of the living system [1]. During the past 30-40 years, there has been a significant advancement in the development of medical materials for skeletal repair and reconstruction. The ceramic based materials within this class of medical implants are referred as "bioceramics" [2]. The use of ceramics in vivo as implants is a newly explored area for more than 30 years which are used to alleviate pain and restore function of the diseased/damaged part of the body. Bioceramics are now employed in a number of applications throughout the body. Various parts of the human skeletal structure, which require replacement by prosthetic on damage (Fig. 2.1). According to the type of bioceramics used and their interaction with the host tissue, they can be categorized as either "bioinert", "bioactive" or "bioresorbable". A major contributor to the need for 'spares parts' for the body is a progressive deterioration of tissue with ages. With growing age, the natural hard tissues in our system, which are natural living composites of calcium phosphate-based ceramics and collagen were particularly vulnerable to fracture because the osteoblast become less productive in elderly person that lead to reduction of bone density and strength [3].

The success of bioceramics in hard tissue replacement primarily depends on the fact that natural bone is a supportive living tissues composed of a carbonate containing calcium apatite approx. 60 wt. % in type 1 collagen approx. 30 wt. % matrix. It also contains approx. 10 wt. % water. The mineral component of bone is a form of calcium phosphate/calcium apatite known as hydroxyapatite [HAP, molecular formula of HAP is $Ca_{10}(PO_4)_6(OH)_2$]. The bone minerals also contain many substitutes containing magnesium, sodium, potassium, fluorides, chlorides and carbonate ions. This apatite mineral is closely associated with collagen fibers to yield flat plate-like nano-crystals. The organic matrix renders the tensile strength whereas the mineral components give rise to compressive strength of bone. Two bone can be distinguished: cortical bone that has approx. 90% solid bone tissue and trabecular bone that is spongy and contain 80% marrow-filled voids (Fig. 2.2). Bone is a dynamic tissue subject to

constant deposition by osteoblast activity and subsequent resorption by osteoclast. When a new surface is introduced into the bone tissue, a sequence of complex is triggered [4].
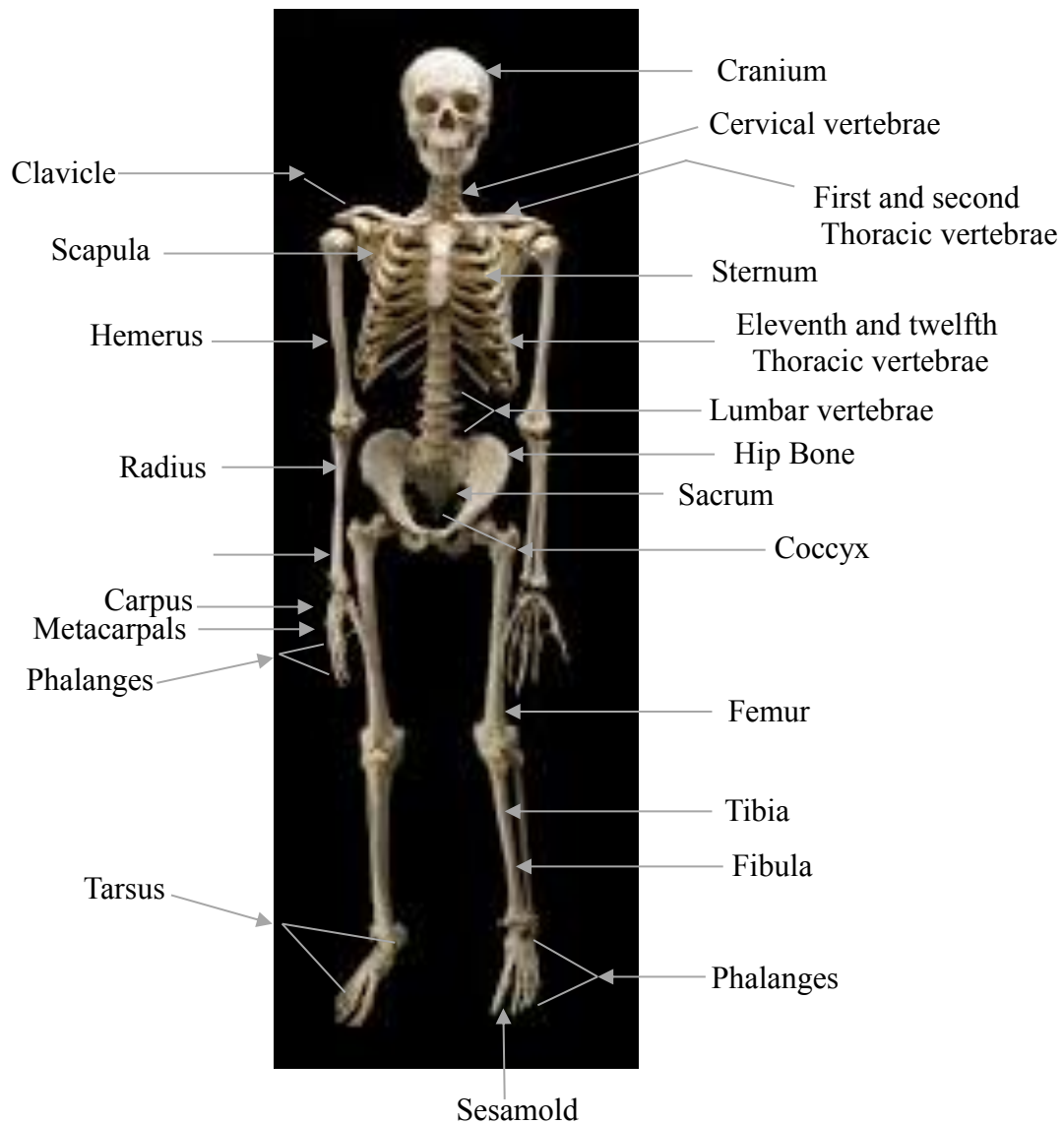
Fig. 2.1: Various Parts of the Human Skeletal Structure can be Repaired from Ceramic Material.

All prosthetic materials elicit a response from the host tissue that varies with the bulk/surface properties of that particular material. When a Bioinert/bioactive bioceramic is porous, bone in-growth occurs which mechanically attaches the bone to the material.

The type of attachment known as "biological fixation" for the damaged tissue. The bioceramic materials classification is taken over in next section.
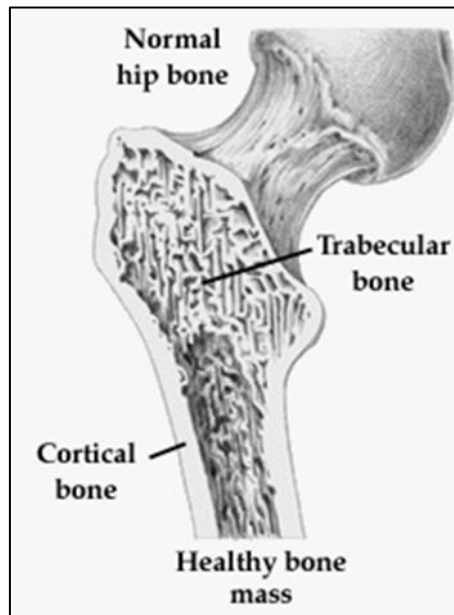
Fig. 2.2: Interior Structure of Human Bone.

2.2 Classification of Bioceramics

1. Bioinert ceramics.
2. Bioactive ceramics.
3. Bioresorbable ceramics.

The mechanism of the tissue attachment is directly related to the type of tissue response at the implant interface [5]. No material implanted in living tissue is inert, all materials are elicited a response from living tissue. Such kind of response which allows to achieve prosthetic attachment to the musculoskeletal system shown in below [6].

- ✓ If the material is toxic, the surrounding tissue dies.
- ✓ If the material is nontoxic and biologically inactive (nearly inert), a fibrous tissue of variable thickness forms.
- ✓ If the material is nontoxic and biologically active (bioactive), an interfacial bond forms.
- ✓ If the material is nontoxic and dissolves the surrounding tissue replace it.

A comparison of the relative chemical activity of these different types of bioceramics is shown in Fig. 2.3 [6].
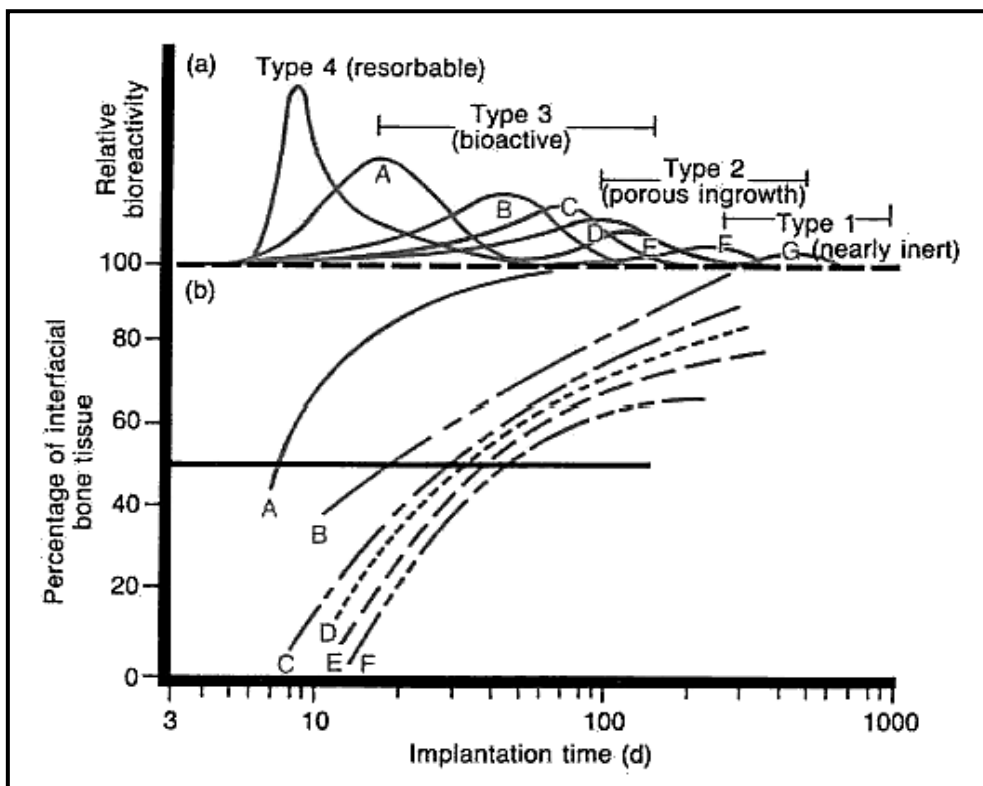
Fig. 2.3: Bioactivity Spectrum for Various Bioceramic Implants [6].

In Fig 2.3. :

(A) Relative rate of bioactivity.

(B) Time dependence of formation of bone bonding at an implant interface;

   (a) 45S5 Bioglass;

   (b) KGS Ceravital;

   (c) 55S4 Bioglass;

   (d) A/W glass-ceramic;

(e) HA;

(f) KGX ceravital;

(g) Al_2O_3-Si_3N_4;

In Fig 2.3 (a) the relative reactivity is correlates very closely with the rate of formation of an interfacial bond of implants with bone. The relative level of reactivity of an implant influences the thickness of the zone or layer of the material and tissue. Failure analysis of the implants during last few years shows failure originating from the biomaterial tissue interface [7-8].

When a material is nearly inert, and the interface is not chemically or biologically bonded (type 1 in Table 2.1 and Fig. 2.3). The concept behind almost inert, microporous bioceramics (type 2 in Table 2.1 and Fig. 2.3) is the growth of tissue into pores on the surface throughout the implants, as originated by Hulbert et al. [9]. Another approach types 2 in Table 2.1 and type 3 in Fig. 2.3 is bioactive material, the concept of bioactive materials is intermediate between resorbable and bioinert [5, 7, 8]. A bioactive material is one that elicits a particular biological response at the interface of the material that results in the formation of a bond between the tissues and the material [9]. Resorbable biomaterial (type 3 in Table 2.1 and type in Fig. 2.3) are designed to degrade gradually over a period and be replaced by the natural host tissue [10-13].

Table 2.1: Shows the Basic Attachment Mechanism of Bioceramics [1]:

Type of bioceramics	Mechanism of attachment	Type of attachment	Example
1. Bioinert	Bone growth occurs into the surface irregularities by cementing/ press fitting into a defect.	Morphological fixation	Al_2O_3 and ZrO_2
2. Bioactive	Attachment directly by chemical bonding at the surface	Bioactive fixation	Bioactive glasses/glass-ceramics/dense HAP
3. Resorbable	Slowly replaced by bone	-----	Calcium phosphate, tricalcium phosphate, and bone bioactive glasses

Ceramic materials have been given a lot of attention as biomedical implants with time as they possess some highly desirable characteristics for some specific applications. Other than their extensive medical use in the field of orthopedics, they have been used in dentistry for their inertness to body fluids, high compressive strength and resemblance to natural teeth. Also for blood interfacing applications like heart valves, the high specific strength of carbon fibres and their biocompatibility has been utilized. For artificial tendons and ligament, replacement composites ceramics materials comprising carbons fibres as reinforcing components are applied in tensile loading applications.

2.3 Applications and Characteristic Features of Bioceramics

Bioceramics are needed to alleviate pain and restore normal activity to diseased or damaged parts of the body. As people age, progressive deterioration of tissues requires replacements in many critical applications. Bone is especially vulnerable to fracture in older people because of a loss of bone density and strength [14]. After successful research and many animal-human trials, various bioceramics products are commercially available in the medical market as a substitute for the original damaged body parts and many other critical applications.

The major applications areas are as follow [15]:

1. Replacement of hip, knee, teeth, tendons and ligaments.
2. Repair for periodontal diseases.
3. Maxillofacial reconstruction.
4. Augmentation and stabilization of the jaw bone.
5. Spinal fusion, bone repair after tumour surgery.
6. Pyrolytic carbon coating for prosthetic heart valves.
7. Treatment of cancer by localized delivery through radioactive glass micropores.

Features of these application are shown in table 2.2 and characteristics are shown in table 2.3 in detailed manner.

Table 2.2: Biomedical Applications of Bioceramics [16]

Devices	Functions	Biomaterial
Artificial total hip, Knee, shoulder, elbow, wrist	Reconstruct arthritic or fractures joints	High density alumina, metal bioglass coating
Bone plates, screws, wires	Repair fractures	Bioglass-metal fibre composites, Polysulfone-carbon fibre composite
Intrameduallary nails	Align fractures	Bioglass-metal fibre composites, Polysulfone-carbon fibre composite
Harrington rods	Correct chronic spinal curvature	Bioglass-metal fibre composites, Polysulfone-carbon fibre composite
Permanently implanted artificial limbs	Replace missing extremities	Bioglass-metal fibre composites, Polysulfone-carbon fibre composite
Vertebrae Spacers and extensors	Correct congential deformity	Al_2O_3
Spinal fusion	Immobilize vertebrae to protect spinal cord	Bioglass
Alveolar bone replacements, mandibular reconstruction	Restore the alveolar ridge to improve denture fit	Polytetra fluro ethylene (PTFE) – carbon composites, porous Al_2O_3, bioglass, dense-apatite.
End osseous tooth replacement implants	Replaced diseased, damaged or loosened teeth	Al_2O_3, bioglass, dense hydroxyapatite, vitreous carbon
Orthodontic anchors	Provide post for stress application required to change deformities	Bioglass-coated Al_2O_3, bioglass coated vitallium

Table 2.3: Characteristics Features of Ceramic Biomaterials [16]

Material	Young's Modulus (GPa)	Compressive Strength (MPa)	Bond Strength	Hardness	Density g/cm^2	Klc (MPam$^{1/2}$)
Bone	3-30	130-180	60-150	NA	NA	NA
Al$_2$O$_3$	380	4000	300-400	2000-3000 (HV)	>3.9	5.0-6.0
ZrO$_2$	150-200	2000	200-500	1000-3000 (HV)	6.0	4.0-12.0
Graphite (LTI)	20-25	138	NA	NA	1.5-1.9	NA
Pyrolitic Carbon	17-28	900	270-500	NA	1.7-2.2	NA
Vitreous Carbon	24-31	172	70-207	150-200 (DPH)	1.4-1.6	NA
Bioactive HAP	73-117	600	120	350	3.1	<1
Bioglass	~ 75	1000	50	NA	2.5	0.7
AW Glass Ceramic	118	1080	215	680	2.8	2

PS – Partially Stabilized; **HAP** – Hydroxyapatite; **NA** – Not available; **AW** – Apatite Wallastonite; **HV** – Vickers Hardness; **DPH** – Diamond Pyramid Hardness.

2.4 Bioinert Ceramic -- Alumina

2.4.1. Overview on Alumina (Al_2O_3)

Alumina is very typical representative of the structural ceramics group. These materials are usually intended to serve as structural parts subjected to mechanical loads at high temperatures. The characteristic feature of structural ceramics is good mechanical behavior; therefore, efforts in developing, fabricating, and optimizing these materials are concentrated towards high strength. The objective of development of high strength ceramics is substitution of metallic materials in relevant regions. The structure of aluminum oxide consists of close-packed planes of the large oxygen ions stacked in the sequence A-B-A-B, thus forming a hexagonal close packed array of anions. The cations occupy the octahedral sites of this primary array and form another type of close packed planes which are inserted between the oxygen layers. Only two-thirds of the octahedral sites are filled with cations to maintain the charge neutrality. Fig. 2.4 (a) illustrates the packing of Al and O in the basal plane. Three different types of cation layers are possible depending on the position of the vacant cation site within layer, which may be termed as a, b and c. The stacking occurs in the sequence of a-b-c-a-b-c. This gives the complete stacking sequence of anion and cation layers of the form A-a-B-b-A-c-B-a-A-b-B-c-A. It is only reproduced after the sixth oxygen layer or after the sequence a-b-c is repeated twice Fig. 2.4 (b).

The unit cell of α-alumina defined in this way is called the crystallographic or structural unit cell. In contrast, in the morphological unit cell the cation sequence is repeated only once, and the height is half that of the structural cell. This significant difference between the two cells has given rise to some confusion in the literature dealing with crystallographic indices of sapphire [18]. The structure of α-Al_2O_3 results in coordination number of 6 and 4 for the cation and the anion, respectively. The ionic radii for this coordination are 0.053nm for Al^{3+} and 0.138nm for O^{2-}. Lattice parameters for unit cell are $a_0 = 0.7589$ and $c_0 = 12.991$Å respectively.

<div align="center">

[A]   **[B]**

</div>
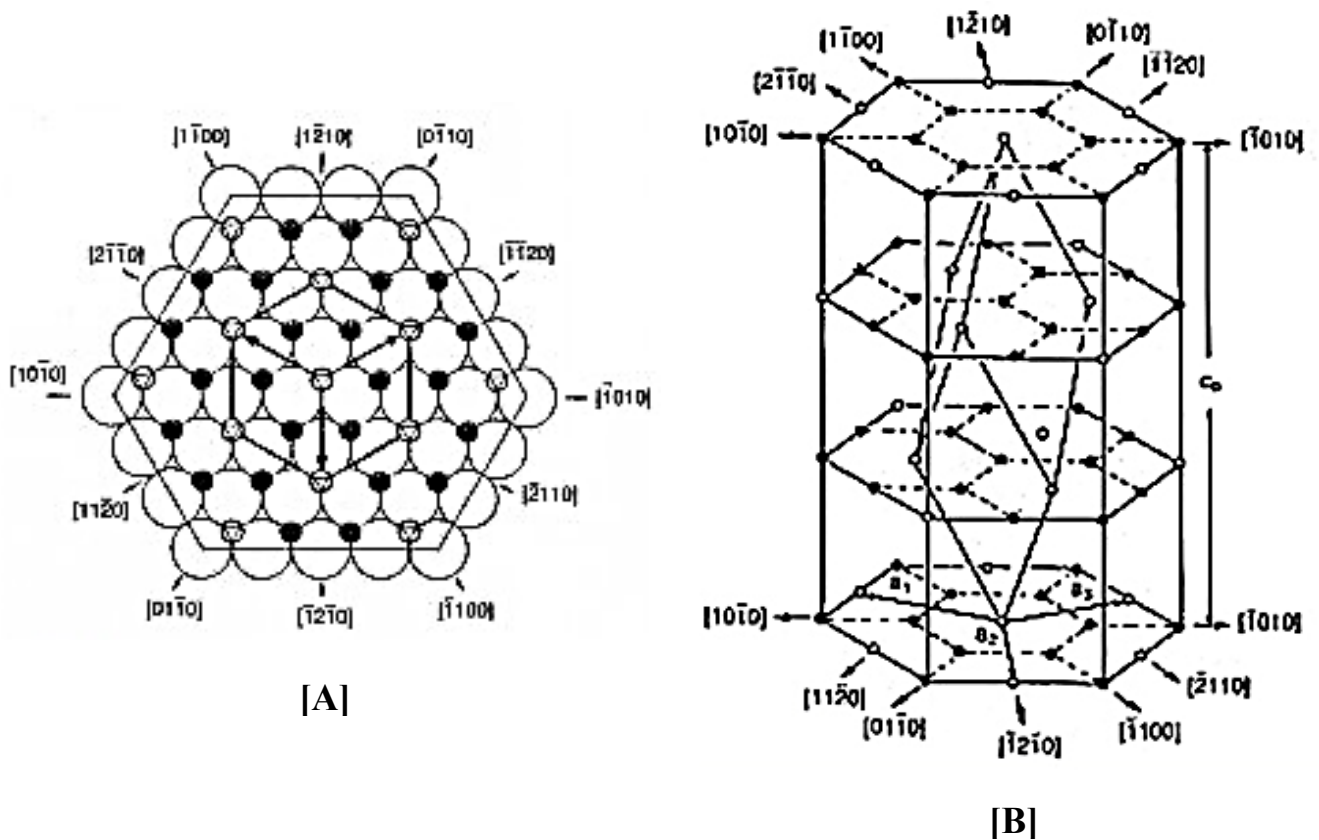
Fig. 2.4: Base plane of α-Al$_2$O$_3$ showing the hexagonal close packing anion sublattice (large open cirlces) and the cations occupying two-third of the octahedral (small filled circles); small open circles are empty octahedral interstics **(A)** The cation sublattice in α-Al$_2$O$_3$ filled circles are Al and **(B)** open circles are empty octahedral interstics [17].

2.4.2 Alumina as Bioceramics

In last 30 years alumina has proven its bio inertness. Alumina (α-Al$_2$O$_3$) is being in orthopedic surgery for more than 30 years. Such alumina implants are total hip prosthesis, dental implants, bone screws, alveolar ridge and maxillofacial reconstructions and segmental bone replacements. Fig. 2.5 shows the applications of alumina ceramic for biomedical implants.
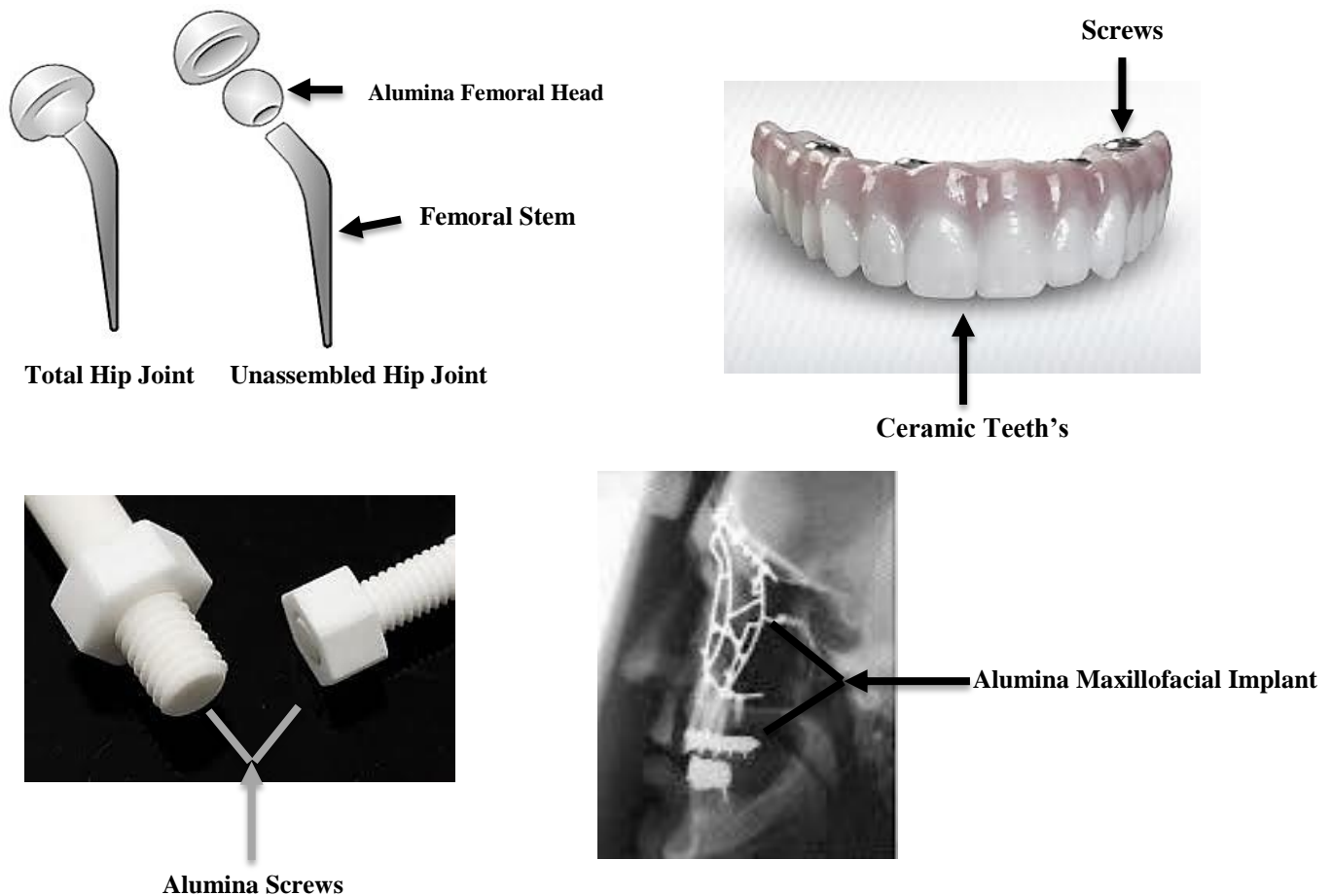
Fig. 2.5: Applications of Alumina Ceramic for Biomedical Applications.

All these are due to a combination of a range of structural properties such as corrosion resistance, biocompatibility, wear resistance, low friction and high strength [19-24]. Two major advantages of medical grade alumina over other materials are: (a) low wear rates; (b) low concentration of wear particles (debris) in the surrounding tissue. The corrosion resistance of alumina ceramics is also very high (rate of corrosion 10^{-4} g-cm^{-2} / day corresponding to maximum corrosion rate of 1mm in 10 years). Therefore, the material is termed as "Biological Inert". Superior tribological properties like, high density, small grain sizes (< 4 μm, having a very narrow size distribution) have resulted in an exceptionally low coefficient of friction and minimum wear rate [19, 20, 25]. These advantageous properties have made alumina ceramics the articulating surface in total hip / knee prostheses. Table 2.4 shows the characteristics of alumina implants with respect to ISO standard 6474 [26].

Table 2.4: Characteristics of Alumina Implants with Respect to ISO Standard 6474 [6].

Properties	Al_2O_3 Implants	ISO standard 6474
Density (g/cm^3)	> 3.93	> 3.90
Average grain size (µm)	3-6	< 7
Hardness (Vickers)	2300	> 2000
Compressive Strength (MPa)	4500	-----
Bending Strength (MPa)	550	400
Young Modulus (GPa)	380	-----
Fracture Toughness (K_{Ic}) (MPa m$^{1/2}$)	5-6	-----

2.4.3 Advantages and Disadvantages of alumina ceramic [1]

Advantages:

a) Extremely high melting point.
b) Extreme hardness.
c) Low wear resistance.
d) High strength.
e) High Hardness.

Disadvantages

a) High densification.
b) Brittle nature after sintering because of this more prone to get cracks.
c) Poor machinability.

Part B
Machinability

2.5 Machinability

The term machinability refers to the ease with which a material can be machined to an acceptable surface finish [27]. If a material x is more machinable than material y, it means that less power is required to machine x than to y. x can be cut quickly without cracking, and it could give a better surface finish while machining without wearing the tools much (free machining). Moreover, ease of chip disposal, cutting temperature, operator safety, etc. are other criteria of machinability. Therefore, to manufacture components economically, engineers are challenged to find ways to improve machinability without affecting the performance.

The condition and physical properties of the work material have a direct influence on the machinability of a work material. The various conditions and characteristics described as the condition of work material, individually and in combinations, directly influence and determine the machinability. Operating condition, tool material and geometry, and the workpiece requirement exercise indirect effects on machinability and can often be used to overcome difficult conditions presented by the work material.

2.5.1 Conditions for Machining of Work Materials

The following factors determine the condition of the work material:

1. Microstructure.
2. Grain Size.
3. Heat Treatment.
4. Chemical Composition.
5. Fabrication.
6. Hardness.

2.5.2 Physical Properties

The following physical properties affect the machining characteristics:

1. Modulus of Elasticity.
2. Thermal Conductivity.
3. Thermal Expansion.
4. Work Hardening.

2.6 Machining Operations [28]

Machining is any process in which a cutting tool is used to remove a small chip of material from the workpiece. For machining, relative motion is required between the tool and the work and the basic machining process shown in Fig. 2.6. This relative motion is achieved in most machining operation by means of a primary motion called cutting speed and a secondary motion called feed. The shape of the tool and its penetration into the work surface, combined with these motions, produce the desired shape of the resulting work surface.
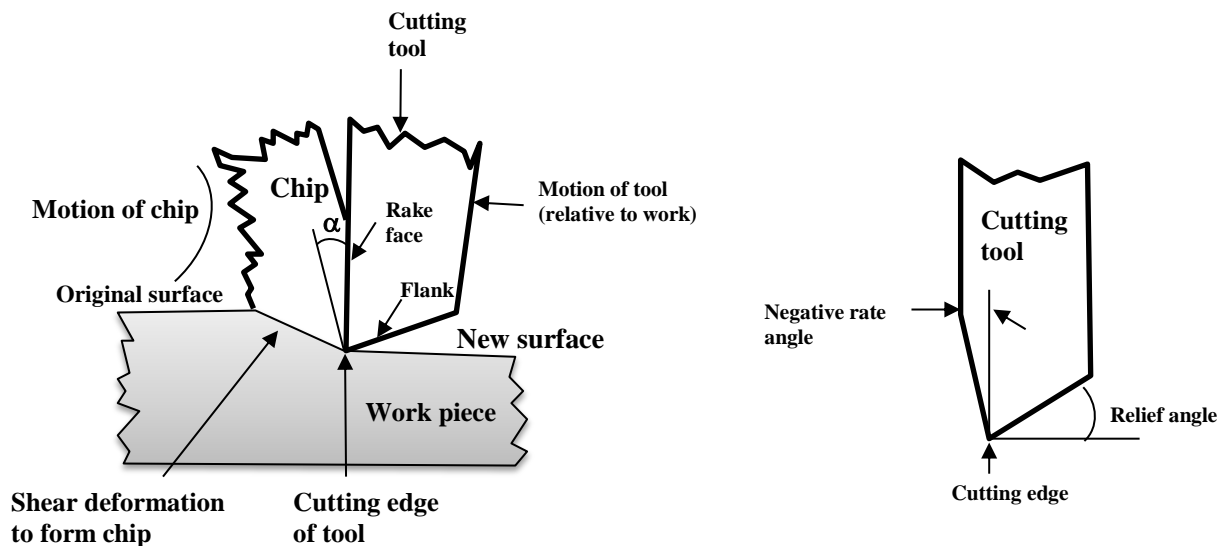
Fig. 2.6: Basic Machining Process

There are three primary machining processes classified as turning, drilling and milling. Other operations are falling into miscellaneous planning, boring, broaching and sawing.

Turning is a method in which cutting tool with a single cutting edge is used to remove material from a rotating workpiece to generate a cylindrical shape shown in Fig. 2.7. The primary motion is provided by rotating the work piece, and the feed motion is achieved by moving the cutting tools slowly in a direction parallel to the axis of rotation of the workpiece [28].
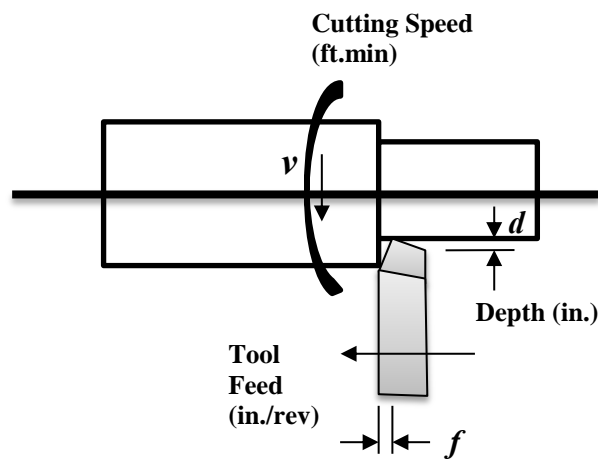
Fig. 2.7: Turning Process

Drilling is used to create a round hole. Process of drilling completed by a rotating tool that has different types of cutting edges shown in Fig. 2.8. The tool is fed in a direction parallel to its axis of rotation into the workpiece to form the round shape [28].
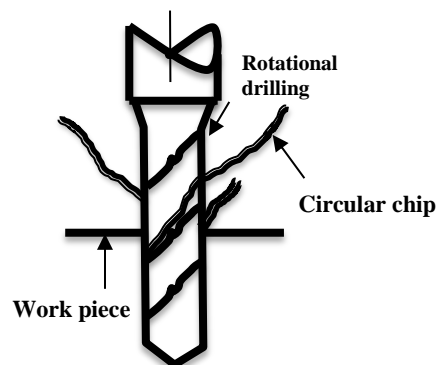
Fig. 2.8. Drilling Process

Milling is a rotating tool with multiple cutting edge is moved slowly relative to the material to generate a plane or straight surface shown in Fig. 2.9. The direction of the feed motion is perpendicular to the tools axis of rotation [29]. The rotating milling cutter provides the speed motion. The two basic forms of milling are shown in Fig. 2.10:

1. Peripheral milling.
2. Face milling.
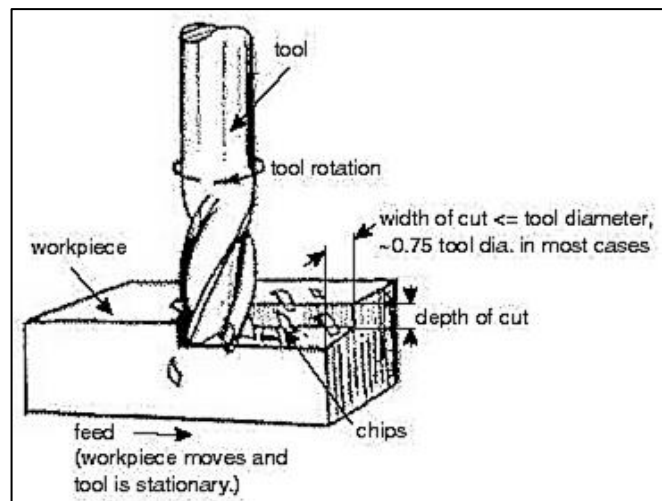
Fig. 2.9: Milling Process [29]
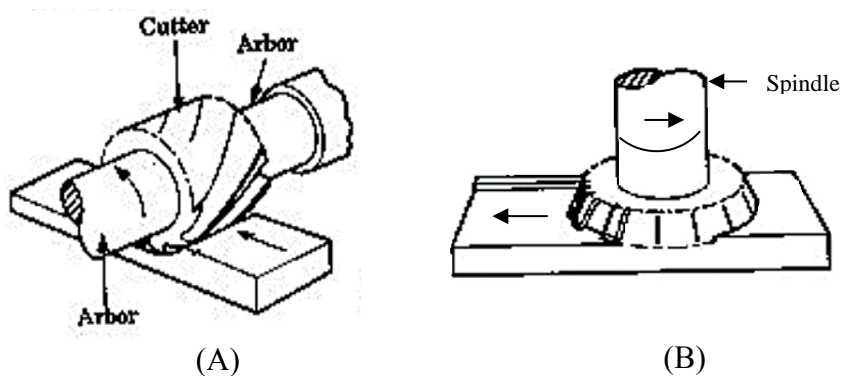
Fig. 2.10: Different Types of Milling Process (A) Peripheral Milling; (B) Face Milling [29]

Part C

Rare Earth Phosphates and Ceramic Machinability

2.7 Rare Earth Phosphates (REP)

2.7.1 Rare Earth Oxides (REO`s)

Rare earth metals or Rare earth oxides are a group of 17 elements in the periodic table. This group consists of 15 lanthanides along with scandium and yttrium shown in Fig. 2.11. Scandium and yttrium both are considered as rare earth oxide since they are likely to occur in the same ore deposits as the lanthanides and to have similar chemical properties. REO`s share many similar features, that is why they occur together in geological deposits, but their distribution and concentrations vary. These oxides were initially obtained from earths or oxides from relatively rare minerals. Thus, they were named rare earths. But despite their name, rare earth oxides (with the exceptions of the radio-activeness) are not rare but relatively plentiful present in the earth's crust [30].

Fig. 2.11: The Rare Earth Oxides Subdivided in Groups

The more abundant REO are each similar in crystal concentration to industrial metals such as chromium, nickel, copper, or lead. Even the least abundant REO, thulium, is nearly 200 times more common than gold. REO have very little tendency to become concentrated in exploitable ore deposits. Therefore, they are also referred to as "Rare" because it is not common to find them in commercially viable concentrations.

REO`s can be classified into two categories - light rare earth oxides (LREOs) and heavy rare earth oxides (HREOs) based on their electron configuration shown in Fig. 2.6. The LREO`s are defined through lanthanum to gadolinium; atomic number 57 to 64. The HREO`s are defined through terbium to lutetium, atomic number 65 to 71, and also yttrium (atomic

number 39) and scandium (atomic number 21). The principal rare-earth ores, the minerals monazite and bastnaesite, have formed the basis for historical production, with minor contributions from deposits containing xenotime [31]. Monazite, phosphate mineral, is known to exist in at least four forms, depending on whether Ce, La, Nd or Pr is the principal rare earth component.

2.7.2 Rare Earth Phosphates

Rare earth phosphates belong to the family of rare earth zircons, having high melting point (between 1900°C-2000°C) and show excellent thermal stability in both reducing and oxidizing atmosphere [32]. Rare earth phosphates are synthesized for this work by direct reaction between rare earth oxide and phosphoric acid. In a fine-grained two-phase composite, material removal should occur by the formation and link of cracks at the weak interfaces between the alumina and REP phases [33]. This is the basis for designing the current work, alumina based machinable bio-ceramics. Rare earth phosphates also have a biological role, and they have already shown non-toxicity and biocompatibility in different bio-medical applications [34-35], mainly as bio-imaging phosphor / luminescent labeling materials for bio-imaging [36-41].

2.7.2.A Lanthanum Phosphate

Lanthanum phosphate is known as Monazite, and also has long been known as a ceramic material with its high-temperature phase stability and high melting point [32]. The other properties of monazite, such as low thermal conductivity, chemical inertness and non-reactivity towards other ceramic oxides, and having thermal expansion coefficients are comparable to alumina ceramic [42]. In $LaPO_4$, 4 coordinated in a distorted tetrahedral environment. La is 9 co-ordinated by O in an unusual arrangement while O is 3 or 4 co-ordinated to 2 or 3 La and 1P [43]. The density of $LaPO_4$ is 5.13 g/cm^3. A new outlook of the material emerged recently because of investigations in the areas of photoluminescence and catalysis. For the development of photo-luminescent materials both bulk and nanometer-sized lanthanum, phosphates were found to be useful as excellent hosts/matrices [44].

The potential applications are in optoelectronic devices, solid state lasers, displays, and phosphors. Lanthanum phosphate is widely used as Lewis acid catalyst, and the catalytic property has been shown to depend on the surface area [45]. Due to the identical thermal expansion coefficients of Al_2O_3 and $LaPO_4$, their composites were widely investigated and were found to be chemically inert.

2.7.2.B Yttrium Phosphate

Yttrium phosphate is also known as Xenotime. Xenotime is used chiefly as a source of yttrium and heavy lanthanide metals (dysprosium, ytterbium, erbium and gadolinium). Sometimes gemstones are also cut from the finer xenotime crystals. Yttrium is a silvery metallic transition metal chemically similar to the lanthanides, and it has often been classified as a rare earth element [46]. Yttrium is commonly found combined with the lanthanides in rare earth minerals and is never found in nature as free elements. Most significant use of yttrium is in making phosphors, such as the red ones utilized in the television set cathode ray tube (CRT) displays and LEDs [47]. It is also utilized in the production of electrodes, electrolytes, electronic filters, laser and superconductors, various medical applications, and the tracing of different materials to enhance their properties.

Yttrium is a soft, silver-metallic, lustrous and highly crystalline transition metal in group 3. As expected from periodic trends, it is less electronegative than its predecessor in the group, scandium, and less electronegative than the next number of period 5, zirconium. Additionally, it is of comparable electronegativity to its successor in its group, lutetium, due to the lanthanide contraction. The pure element is relatively stable in air in bulk form, due to passivation resulting from the formation of a protective oxide (Y_2O_3) film on its surface.

The similarities of yttrium to the lanthanides are so strong that the element has historically been grouped with them as a rare earth element [46]. Also, it is always found in nature together with them in rare earth minerals. Yttrium is so close in size to the so-called 'Yttrium group' of heavy lanthanide ions that in solution, it behaves as if it were one of them. Even though the lanthanides are one row farther down the periodic table than the yttrium, the similarity in atomic radius may be attributed to the lanthanide contraction.

2.8 Techniques for Preparation of Rare Earth Phosphates (REP)

Literature data suggest the availability of rare earth phosphates processing techniques to achieve the pure phase of REP powder without any impurities. Most relevant synthesis process and their detail analysis related to the preparation are discussed below.

R. Wang et al. has synthesized $LaPO_4$ powder by mixing phosphoric acid with lanthanum oxide in a water bath. Lanthanum oxide was dissolved in diluted phosphoric acid with La to P of 1:1 in order to achieve $LaPO_4$ as a final product. The direct reaction between lanthanum oxide and phosphoric acid is a clean reaction with no by-product other than water according to the reaction:

$$La_2O_3 + 2H_3PO_4 \longrightarrow 2LaPO_4 + 3H_2O$$
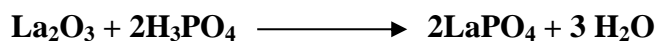
La_2O_3 powder was added slowly added to 85% H_3PO_4 (diluted by distilled water), and a large amount precipitates formed immediately at the reaction site. The synthesized powder was washed several times with de-ionized water until pH value of filtered water became close to 7 [48-50].

Lucas et al has synthesized $LaPO_4$ powder by an aqueous precipitation method from the addition of a rare earth chloride solution ($LaCl_3 \cdot 7H_2O$, $CeCl_3 \cdot 7H_2O$, $YCl_3 \cdot 6H_2O$) into a reactor containing a phosphate solution. Ammonium hydrogen phosphate used as the phosphating agent. The concentration of the solution was 0.4 mol L^{-1} for a Re/P mole ratio of the initial reagents equals to 1. They mixed 0.4 and 0.2 mol L^{-1} for a Re/P ratio of 2:1; and 0.2 and 0.6 mol L^{-1} for a Re/P ratio of 1:3. Fully automated device used for this synthesis and solution was added at a rate of 30 mL min^{-1}, using a peristaltic pump. Ammonium hydroxide solution used to maintain pH under controlled and regulated temperature and suspension continuously stirred and refluxed. After the suspension was centrifuged. The resulting precipitate was washed by centrifuging and finally dried at 80°C [51].

Nair et al. samples of ARP_3O_{10} the conventional ceramic route prepared (A=Ca or Ba; R=La, Ce or Sm). The samples were prepared by mixing the stoichiometric proportion of raw materials in the powder form followed by heating. The raw material used in the preparation of samples are $CaCO_3$ (99.9%), $BaCO_3$ (99%), CeO_2 (99%), $NH_4H_2PO_4$ (98%).

These materials were weighed, then mixed together in an agate mortar. Acetone was used for proper mixing. Then mixture was dried at 100°C. The same process was repeated three times to get a homogenous mixture. The dried powder was kept in the platinum crucible for calcined at a temperature of 750-1000°C for 3 hours in an electrically heated furnace. Calcined powder was soft grinded in an agate mortar to get a fine powder [52].

G. Gong et al. has prepared $LaPO_4$ powder by calcined rhabdophane-type $LaPO_4.0.5H_2O$ at 1300°C for 6 hours. The calcined powder was milled with silicon nitride balls in ethanol for three days and sieved through 200-mesh screen. X-ray diffraction techniques did phase conformation. The La/P atomic ratio of the calcined powder (ICP) was 0.99 [53].

Monazite type lanthanum phosphate powder was prepared by Min et al. using dry milling of rhabdophane-type $LaPO_4.0.5H_2O$ by alumina balls at room temperature in air for ten days (mechanochemical method). X-ray diffraction of the dry-milled powder showed only monazite-type $LaPO_4$. The La/P atomic ratios obtained from the chemical analysis method 0.99 [54]. They have prepared [55] rhabdophane-type $LaPO_4.0.5H_2O$ by forming $LaCl_3$ first by using La_2O_3 and HCl and further reacting this $LaCl_3$ with H_3PO_4.

Byrappa et al. has synthesized $LaPO_4$ powder by taking La_2O_3 and H_3PO_4 in ratio of 1:1.2 in a beaker containing water (14 mL) to prepare $LaPO_4$. The mixture was stirred for about 15 min, forming a white colloidal solution. The pH of the solution was adjusted to 1.4-2 using ethanol. Then the solution was autoclaved in a Teflon-lined steel autoclave at 120°C for 16-30 hours and washing the product several times in water and alcohol [35].

2.9 Machinability of Al_2O_3-REP Composites

Various researchers have developed machinability in alumina ceramics by using rare earth phosphates. Mostly all the literatures are based on Al_2O_3 - $LaPO_4$ composites. In the following most relevant processes used to prepare the composites, and their machinable properties studied the literature were discussed.

Wang et al. reported that the addition of $LaPO_4$ in alumina ceramic matrix to improve the machinability of the composites. The composites were prepared with different ratios of LP with Al_2O_3 and sintered between 1300°C to 1600°C and by X-ray diffraction proved that the Al_2O_3 and $LaPO_4$ have a separate phase and exist as a composite. Due to the layered structure of $LaPO_4$ and the weak interface between the Al_2O_3 and $LaPO_4$ phase, the 40wt. % composites can be machined by using cemented carbide drills instead of conventional diamond tools [49]. Again wang reported this work with a better result and 30 wt. % composites were machinable [50].

Gong et al. reported that pressureless sintering fabricated $Al_2O_3/LaPO_4$ composites in N_2 atmosphere. The effect of sintering temperature and sintering time on densification was investigated and also dependence of mechanical and microstructural properties of $LaPO_4$. The provided ratio of La:P was close to 1:1 and no reactions were observed at 1600°C for 2 hours in N_2 atmosphere. The 30 wt. % composite machined by using cemented carbide drills. $LaAl_{11}O_{18}$ was formed when the composites were sintered at 1700°C for 1 hour in N_2 and not machinable [53].

Min et al. reported that composites were prepared with ratios of xAl_2O_3 (x=0 to 1 mass) and (1-x) $LaPO_4$ and pressed to disk shape. Measured relative density that was larger than 94% and porosity was analyzed less than 6% were achieved when the specimens were sintered at 1600°C for 5 hours. Each sample machined with using metallic WC drills and drilling done at 2500 RPM. The sintered ceramics (x = 0 to 0.7) were found to be machinable and could drill quickly with the metallic WC drills [54].

Davis et al. reported that two-phase composites consisting of $LaPO_4$ or $CePO_4$ and alumina, mullite, or zirconia were found to be machinable, i.e. they can be drilled using by conventional tungsten carbide metal-working tools. Single-phase $LaPO_4$ was also reported to be machinable. Drilling rates, grinding rates, and normal forces are used to compare the ease of machinability. Cracking and deformation within the monazite phase was reported to be the reason for such property. The formation of a finely crushed, smeared layer of material between the workpiece and tool was analyzed after drilling all of the machinable materials [56].

Two-phase composites consisting of $Al_2O_3/LaPO_4$ were prepared by Majeed et al. with different ratio of $LaPO_4$ and subjected to ultrasonic machining, using low carbon steel tools (solid and hollow) of 3mm diameter. The effect of $LaPO_4$ on machining studied by analyzing the acoustic emission signals emitted by the workpiece during machining. The material removal rate was calculated by the time of machining. The microstructures of composites studied and the profiles of the drilled holes were plotted using a projector with magnification of 20 [57].

Wang et al. developed a new method for machinable ceramic by using composition variation and structure design methods of ceramics while retaining mechanical properties of the materials. This method also provides the fundamental design principle for the other comparable, but intrinsically different, ceramic systems based on chemical compatibility and thermodynamic properties. Graded machinable Al_2O_3-$LaPO_4$ composites were designed, fabricated and characterized [58].

Wang et al. reported that hot pressing can make the $Al_2O_3/LaPO_4$ composites, and the layered $LaPO_4$ grains inhibited densification of the composites and grain growth of Al_2O_3 due to decreasing grain boundaries. The fine and homogenous microstructure did not improve the fracture strength and elastic modulus due to the formation of weak bonding between Al_2O_3 and $LaPO_4$. But reported that the machinability of alumina matrix materials could be significantly improved by introducing an interface dispersion phase of layer structure $LaPO_4$ [59].

Zhou et al. reported a novel process to fabricate Ce-TZP/$CePO_4$ composites Sintered Ce-TZP ceramic preform with 35 vol. % open pore volume was developed by adding graphite 30 vol. %. The Ce-TZP/$CePO_4$ composites containing different amount of liquid precursor were obtained by infiltration and pyrolysis cycles. These composites can be cut and drilled by using conventional tungsten carbide metal working tools. The machinable Ce-TZP/$CePO_4$ composites containing a range from 2.3 to 7.5 vol. % $CePO_4$ has excellent machinability as well as machining outstanding mechanical properties [60].

Majeed et al reported that $Al_2O_3/LaPO_4$ composites are prepared with different ratios of $LaPO_4$ in Al_2O_3 and subjected to ultrasonic machine with low carbon steel tools (solid and hollow). Acoustic emission (AE) signal emitted by the workpiece during machinability was also analyzed. Ultra-scan inspection carried out to check for any internal defect. This work significance of $LaPO_4$ addition on machinability of $Al_2O_3/LaPO_4$ composites in the term of MRR. AE response and whole geometry and associated defects [61].

Part D
Biological Studies

2.10 *In Vitro* Cytotoxicity and Cell Viability

Cell viability and cytotoxicity will support to understand the in vivo compatibility and level of toxicity of the synthetic composites for clinical applications. Therefore, different schools are continuously evaluated and reported this phenomenon for the future development of a new of biomaterials.

Ketul et al. fabricated nanoporous alumina membrane to investigate bone cell response. Osteoblast was seeded on nanoporous alumina membranes to study both short-term adhesion and proliferation and long-term functionality and matrix production. Both the thing are done by MTT assay and cell counting. The total protein content was measured after cell lysis using the BCA assay. The results from nanoporous alumina membrane were compared with those of amorphous alumina, aluminum. Commercially available ANOPORETM and glass. Results indicate the improved osteoblast adhesion [62].

Kim et al. studied in vitro cellular response and attachment on freeze dried HA-gelatin composites. Osteoblast human osteosarcoma cells are spreading and actively proliferate on composite scaffold. The cells proliferation rate is calculated indirectly from the cells cultured on Ti discs coated with gelatin and HA-gelatin composites using MTT assay. The alkaline phosphate activities express by the cell culture on composites and HA coatings on Ti Discs enhances significantly compared with those on pure gelatin. This finding suggests that HA-gelatin composites have a high potential for use as hard tissue regeneration scaffolds [63].

Dalby et al reported the study that the original attachment of osteoblast-like cells on HA reinforced polyethylene composites (HAPE), which is designated as a second generation orthopedic biomaterial with suitable mechanical and biological characteristics for bone augmentation. Optimization of the material features like mechanical properties enhancements has a significant role for effective attachments of osteoblast cells. Polishing followed by roughing the surface of HAPE enhances osteoblast proliferation [64].

Filho et al. studied the cells attachment, cellular interaction and modulation of osteoblast cells on biocompatible material such as porous HA scaffolds. Biocompatibility of materials has been investigated through consideration of human osteoblast (HOB) cells on the fibronectin-coated glass surface and monolayers formation of HOB observed. The cellular adhesion to material interaction includes two phenomena: (a) physicochemical properties of the interacting surface and (b) molecular properties of both surfaces and also the interaction medium. The study pointed out that cell attachment is a property that depends on physical and topological features of both biomaterials and cell surfaces [65].

Part E
Motivation and Objective of the Work

2.11 Motivation of Work

In the last few decades, bioceramic materials perform tailored functional / biological / chemical activities of the living system and have significantly improved the treatment procedure through reconstructive surgeries. In such cases, alumina based bioceramics, mostly used as implants, are most prominent. There are several literatures available on the use of alumina based bioceramics, but nearly no study was found to tailor the dimensions of the implants. So that the dimensional criticality may be maintained as and when required for such applications.

Few literatures are available on the aspect of machinability of alumina-based ceramics, that too mostly using lanthanum phosphate, but no one has directed the research target towards bioceramics. Hence, such an area is found to be untouched, and that has motivated to carry out the initial study on the Machinable Alumina based Ceramics for Biomedical Applications.

The study of alumina quality, different rare earth phosphates and their contents, sintering temperatures, etc. is done with primary characterizations like machinability by drilling and behavior in biological environments. The properties are also correlated with the microstructural developments and composite nature of the sintered alumina-based ceramics.

2.12 Objective of Work
1. Preparation of pure phase REP ($LaPO_4$ and YPO_4).
2. Preparation Al_2O_3-REP ceramic matrix composites using two different alumina grades with different compositions, up to 50wt% of REP in the batch.
3. To study the sintering behaviour for optimum combination of densification, phase retention of Al_2O_3 and REP.
4. Investigate the machinability and flexural strength of composites.
5. Investigation of biocompatibility of the composites.

References:

1. J. Chakraborty, D. Basu, Bioceramics – A New Era, Transactions of Indian Ceramic Society 64 (4) 2005.

2. S. M. Best, A. E. Porter, E. S. Thain, J. Huang, Journal of European Ceramic Society 28 (2008) 1319-1327.

3. L. L. Hench, J. Wilson, An Introduction to Bioceramics, World scientific, London, UK (1993).

4. J. D. Preston, "Properties in Dental Ceramics," in: Proc. IV Int. symp. Dental Materials, Quintessa, Chicago, IL (1998).

5. L. L. Hench, E. C. Ethridge, Biomaterials: An Interfacial Approach, Academic Press, New York, 1982.

6. L. L. Hench, Journal of American Ceramic Society, 74 (7) (1991) 1487-1510.

7. L. L. Hench, "Bioactive Ceramics", p. 54 in Bioceramcis: Materials Characteristics Versus In Vivo Behavior; Vol. 523, Edited by P. Ducheyne and J. Lemons Annals of New York Academy of Sciences, New York, 1998.

8. U. Gross, R. Kinne, H. J. Schmitz, V. Strunz, The Response of Bone to Surface Active Glass/Glass-Ceramics, CRC Critical Review in Biocompatibility, 4 (1988) 2.

9. L. L. Hench, R. J. Splinter, W. C. Alien and T. K. Greenlee, Journal of Biomedical Material Research, 2 (1) (1972) 117-142.

10. K. de Groot, Bioceramics of Calcium Phosphate, CRC Press, Boca Raton, FL 1983, 1-32.

11. K. de Groot, Effect of Porosity and Physicochemical Properties on the Stability, Resorption, and Strength of Calcium Phosphate Ceramics in Bioceramics, Material characteristic Versus in *In Vivo* Behavior, Vol. 523, Edited by P. Ducheyne and J. Lemon, Annals of New York Academy of Sciences, New York, 1998.

12. K. de Groot, R. Le Geros, Significant of Porosity and Physical Chemistry of Calcium Phosphate ceramics, pp. 268-277 in Bioceramics, Material Characteristic Versus in *In Vivo* Behavior, volume 523, Edited by P. Ducheyne and J. Lemon, Annals of New York Academy of Sciences, New York, 1998.

13. K. de Groot, C.P.A.T. Klein, J.G.C. Wolke, J. de Blieck Hogervost, Chemistry of Calcium Phosphate Bioceramics, pp. 3-15 in Handbook of Bioactive Ceramics, Vol. II, Calcium Phosphate and Hydroxyapatite Ceramics, Edited by T. Yamamuro, L.L. Hench, J. Wilson, CRC Press, Boca Raton, FL, 1990.

14. L. L. Hench, Journal of American Ceramic Society, 81 (7) (1998) 1705-1728.

15. R. Sarkar, G. Banerjee, Interceram, 59 (2) (2010) 98-102.

16. T. V. Thamaraiselvi, S. Rajeswari, Trends of Biomaterials Artificial Organs, 18 (1) (2004) 9-17.

17. F. F. Lange, B. I. Davies, D. O. Raleigh, Journal of American Ceramic Society, 66 (1983) 125-127.

18. M. L. Kronberg, Acta Materialia, 5 (1957) 507-524.

19. S. F. Hulbert, J. C. Bokros, L. L. Hench, J. Wilson, G. Heimke, Ceramics in Clinical Application: Past, Present and Future: *pages 198-213*: in : High Tech Ceramics, Edited by P. Vincenzini, Elsevier, Amesterdam, The Netherlands (1987) 198-213.

20. P. Christel, A. Meunier, J. M. Dorlot, J. M. Crolet, J. Witvolet, L. Sedel, P. Boritin, Biomechanical compatibility and Design of Ceramic Implants for Orthopedic Surgery page 234: in: Bioceramics: Material Characteristics vs. *In Vivo* Behaviour, Volume 523, Edited by P. Ducheyne, J. Le,ons, Annals of New York Academy of Science, New York, USA (1988).

21. P. M. Boutin, Aview of 15 Year Result Obtained Using the Alumina-Alumina Hip Joint Replacement *page 297*: in: Ceramics in Clinical Applications, Edited by P. Vincenzini, Elsevier, New York, USA (1987).

22. J. Black, G. Hasting, Handbook of Biomaterial Properties, Champman and Hall, London, UK (1988).

23. H. Plenk, Biocompatibility of ceramics in Joint Prostheses: *pages 269-285*: in: Biocompatibility of Orthopedic Implants, Volume 1, CRC Press, Boca Raton, Florida, USA (1982).

24. A. Cahnda, D. Basu, S. Chatterjee, M. K. Basu, Wear and Friction Behaviour of Biomaterials for Total Hip Replacement, Transaction of Pow. Met. Ass. Ind., 22, 40 (1995).

25. G. Willmann, Ceramic Components for Total Hip Arthroplastry, Orthopedics Int. Edn., 5, (1997) 110-115.

26. P. N. De Aza, S. De Aza, Biological society of Ceramic Spanish, 44 (3) (2005) 135-145.

27. J. B. Davis, D. B. Marhsall, R. M. Housley, P. E. Morgan, Journal of American Ceramic Society, 81 (8) (1998) 2169-2175.

28. G. Schneider, Jr. CMfge, Cutting Tools Applications, Chapter 3, 57 (5) (2001).

29. S. Kalpakjian, S. Schmid, Manufacturing Engineering & Technology, Pearson Higher Ed. (2013).

30. W. Simon, Journal of Engineering and Mining, 10 (2010).

31. M. A. Lim, S. I. Seok, W. J. Chung, S. I. Hong, Optical Materials, 31 (2008) 201– 205.

32. Hikichi, Y. Nomura, T., Journal of American Ceramic Society, 70 (10) (1997) C-252-C-253.

33. P. E. D. Morgan, D. B. Marshall, R. M. Housley, Material Science Engineering A, 195 (1995) 215–221.

34. Y. P. Fang, A. W. Xu, W. F. Dong, Small, 1 (10) (2005) 967 – 971.

35. K. Byrappa, M. K. Devaraju, J. R. Paramesh, B. Basavalingu, K. Soga, Journal of Material Science, 43 (2008) 2229-2233.

36. N. Kodama, N. Sasaki, M. Yamaga, Y. Masui, Journal of Luminescence, 94 (2001) 19 – 22.

37. N. Kodama, Y. Tanii, M. Yamaga, Journal of Luminescence, 87 (2000) 1076-1078.

38. L. Wang, Y. Rouxue, Z. Huo, L. Wang, J. Zeng, J. Bao, X. Wang, Q. Peng, Y. Li, Angewandte Chemie International Edition, 44 (37) (2005) 6054–6057.

39. G. Yi, H. Lu, S. Zhao, Y. Ge, W. Yang, D. Chen, L. H. Guo, Nano Letter, American Chemical Society, 4 (11) (2004) 2191–2196.

40. S. F. Lim, R. Riehn, W. S. Ryu, N. Khanarian, C. Tung, Nano Letter, American Chemical Society, 6 (2) 169–174.

41. M. Yu, F. Li, Z. Chen, H. Hu, C. Zhan, H. Yang, C. Huang, Analytical Chemistry, American chemical society, 81 (3) (2009) 930–935.

42. P. E. D. Morgan, D. B. Marshall, Ceramic Composites of Monazite and Alumina, Journal of American Ceramic Society, 78 (1995), 1553-1563.

43. O. F. Mullica, W. O. Milligan, D. A. Grossie, G. W. Beall, L. A. Boatner, norg. Chim. Actu. 1984,95,231.

44. a) W. L. Wanmaker, A. Bril, J. W. ter Vrugt, J. Broos, Philips Res. Rep.1966, 21, 270. b) K. Riwotzki, H. Meyssamy, H. Schnablegger, A. Kornowski, M. Haase, Angew. Chem. Int. Ed.2001, 40, 573. c) C. Feldmann, Adv. Funct. Mater.2003, 13, 101. d) K. Riwotzki, M. Haase, J. Phys. Chem. B 1998, 102, 10129. e) H. Meyssamy, K. Riwotzki, A. Kornowski, S. Naused, M. Haase, Adv. Mater.1999, 11, 840. f) K. Riwotzki, H. Meyssamy, A. Kornowski, M. Haase, J. Phys. Chem. B2000, 104, 2824. g) M. Yu, J. Lin, J. Fu, Y. C. Han, Phys. Chem. Lett.2003, 371, 178.

45. Y. Takita, K. Sano, T. Muraya, H. Nishiguchi, N. Kawata, M. Ito, T. Ishihara, Applied Catalysis 170 (1) (1998), 23-31.

46. N G Connelly, T Damhus (with R. M. Hartshorn) Nomenclature of Inorganic Chemistry, 2005.

47. United States Occupational Safety and Health Administration, Occupational Safety and Health Guideline for Yttrium and Compounds 2007.

48. R. Wang, W. Pan, J. Chen, M. Jiang, Y. Luo, M. Fang, Ceramic International 29 (2003) 19-25.

49. R. Wang, W. Pan, J. Chen, M. Fang, J. Meng, Material Letters 57 (2002) 822-827.

50. R. Wang, W. Pan, J. Chen, M. Fang, Z. Cao, Y. Luo, Material Chemistry and Physics 79 (2003) 30-36.

51. S. Lucas, E. Champion, D. Bregiroux, D. B. Assollant, F. Audubert, Journal of Solid-State Chemistry 177 (2004) 1302-1311.

52. K. R. Nair, P. P. Rao, B. Amina, M. R. Chandran, P. Koshy, Material letters 60 (2006) 1796-1799.

53. Gong, B. Zhang, H. Zhang, W. Li, Ceramic International 32 (2006) 349-352.

54. W. Min, D. Miyahara, K. Yokoi, T. Yamaguchi, K. Daimon, Y. Hikichi, T. Matsubara, T. Ota, Material Research Bulletin 36 (2001) 939-945.

55. W. Min, K. Daimon, T. Matsubara, Y. Hikichi, Material Research Bulletin 37 (2002) 1107-1115.

56. J. B. Davis, D. B. Marhsall, R. M. Housley, P. E. Morgan, Journal of American Ceramic Society, 81 (8) (1998) 2169-2175.

57. M. A. Majeed, L. Vijayaraghavan, S. K. Malhotra, R. Krishnamoorthy, Journal of Material Processing Technology, 207 (2008) 31-329.

58. R. Wang, W. Pan, J. Chen, M. Fang, M. Jiang, Y. Luo, Ceramic International 23 (2002) 565-570.

59. R. Wang, W. Pan, J. Chen, M. Fang, M. Jiang, Z. Cao, Ceramic International 29 (2003) 83-89.

60. Z. Zhuo, W. Pan, Z. Xie, Journal of European Ceramic Society, 23 (2003) 1649-1654.

61. M. A. Majeed, L. Vijayaraghavan, S. K. Malhotra, R. Krishnamoorthy, Journal of Machine Tools and Manufacture, 48 (2008) 40-46.

62. K. C. Popat, E. E. L. Swan, V. Mukhatyar, K. I. Chantvanichkul, G. K. Mor, C. A. Grimes, T. A. Desai, Biomaterials, 26 (2005) 4516-4522.

63. H. W. Kim, J. C. Knowles, H. E. Kim, Journal of Biomedical Material Research, 72A (2005) 136-145.

64. M. J. Dalby, M. V. Kasyer, W. Bonfield, L. D. Silivo, Biomaterials, 23 (2002) 681-690.

65. F. C. Filho, G. C. Menezes, Journal of Material Science Enginnering C, 24 (2004) 637-641.

CHAPTER 3
Experimental
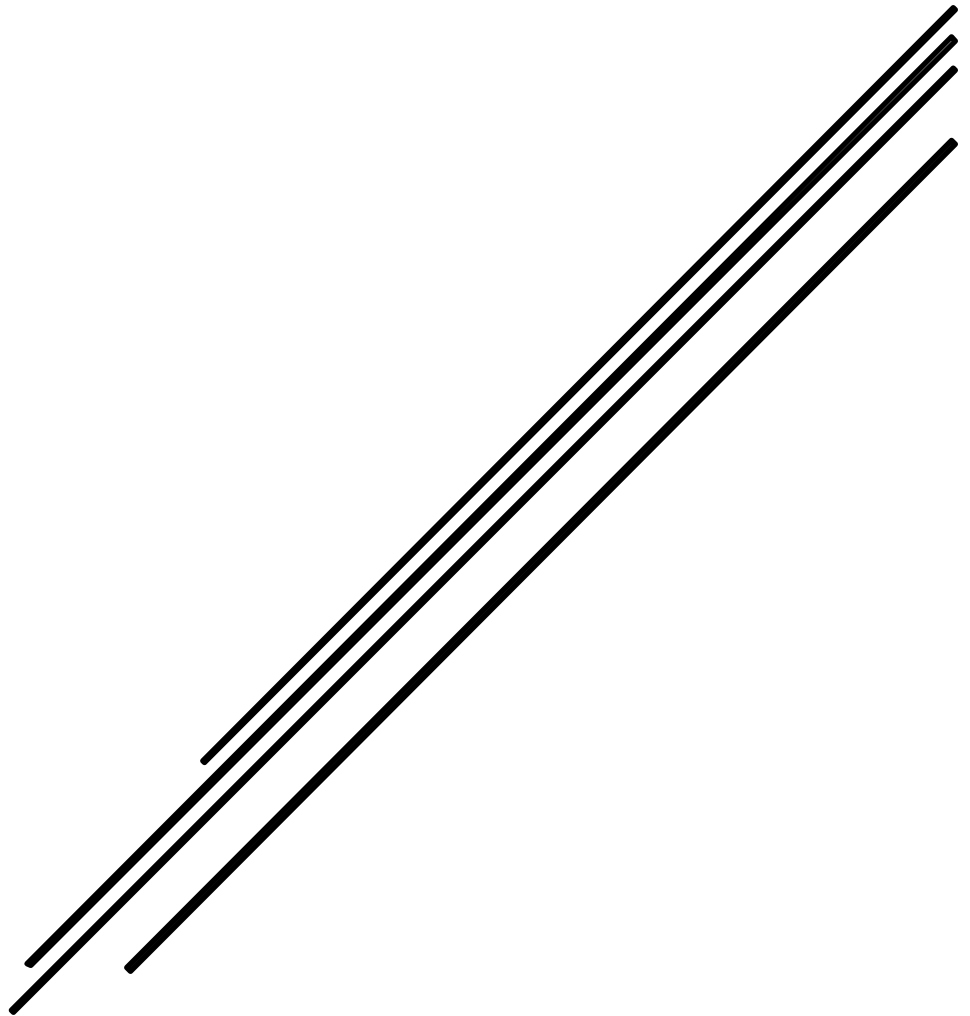
3.1 Raw materials

3.1.1 Alumina

Two different grades of alumina, namely CAl_2O_3 and RAl_2O_3 (Almatis, India) [1] were used in the study. Details of the physicochemical properties of both the aluminas are given in Table 3.1.

Properties	Unit	CAl_2O_3	RAl_2O_3
SiO_2	%	0.03	0.03
Al_2O_3	%	99.8	99.5
Fe_2O_3	%	0.02	0.03
MgO	%	0.05	0.01
CaO	%	0.02	0.02
Na_2O	%	0.07	0.10
Specific Surface Area (BET)	m^2/g	8.9	3.0
D_{50} Cilas	μm	0.4	2.6

Table 3.1: The Physico-chemical Properties of Both the Aluminas

3.1.2 Rare Earth Phosphates

Two kind of rare earth phosphates were prepared for the study, namely, lanthanum phosphate ($LaPO_4$) and yttrium phosphate (YPO_4). Both the phosphates were made from their respective oxides by reaction with orthophosphoric acid. Purity of both the lanthanum (III) oxide (La_2O_3) and yttrium (III) oxide (Y_2O_3) were 99.9% chemical grade, AR/ACS quality (Alfa Aesar, India make). Orthophosphoric acid (H_3PO_4) used was chemical grade AR quality, (Loba Chemie, India made) assay of 85%.

3.2 Preparation of Rare Earth Phosphates (REP)

Preparation of REPs was done by the wet chemical synthesis. For preparing both the rare earth phosphates same protocol was used. REP powder was synthesized by mixing of rare earth oxide with phosphoric acid in a stoichiometric amount. The direct reaction between the rare earth oxide (REO) and phosphoric acid is a clean reaction with no by-production other than water. The reactions are as follow.

$$La_2O_3 + 2H_3PO_4 \longrightarrow 2LaPO_4 + 3H_2O \text{ [2] ----------- (1)}$$
$$Y_2O_3 + 2H_3PO_4 \longrightarrow 2YPO_4 + 3H_2O \text{ [3] ------------ (2)}$$
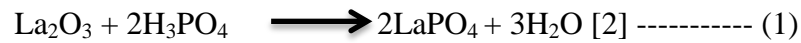
REO powder was slowly added to the H_3PO_4 (diluted by distilled water) on a magnetic stirrer. The reaction was exothermic. Precipitate form from the reaction and gradually broke into the fine particles. The precipitate was dried for 12 hours at 75°C and then double calcined at 800°C ($LaPO_4$) and 1000°C (YPO_4) for 2 hours. X-ray diffraction technique did phase identification of the calcined powders. The preparation route of the rare earth phosphates is shown in Fig. 3.1.
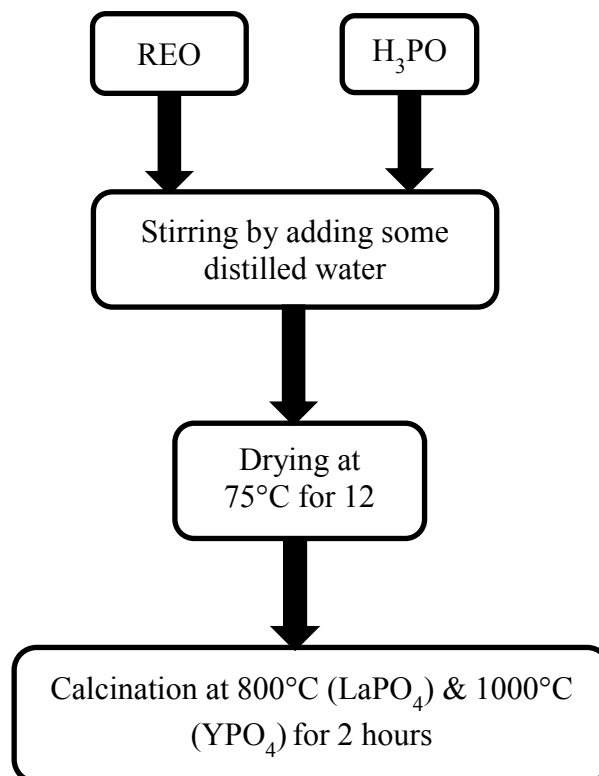
Fig. 3.1: Preparation Route for Rare Earth Phosphate

3.3 Preparation of composites

$Al_2O_3/LaPO_4$ composites were prepared by magnetic stirring method with different $LaPO_4$ content (10, 20, 30, 40, and 50 wt. %) in wet (alcohol) medium for 1 hour and then dried. Batch compositions of the Al_2O_3-REP composites are shown in Table 3.2. Mixed powders were pressed at 150 MPa in a hydraulic press (Carver, USA, make) to pellets (15mm dia x 10 mm) and bar (60 mm x 6 mm x 6 mm) shapes. 4% PVA solution (6% concentration) was used as green binder. Pressed forms were then sintered at different temperatures with a soaking period of 2 h. CAl_2O_3-REP composites were sintered at 1400, 1450, 1500, 1550 and 1600°C and RAl_2O_3-REP composites at 1500, 1550 and 1600°C (below 1500°C RAl_2O_3 was very poorly densified) in electrically heated programmable furnace (Bysakh, India, make). Sintered samples were cooled down naturally in the furnace. Fig. 3.2 shows the flow diagram for preparation route of composites.

Alumina (C and R) Wt.%	REP ($LaPO_4$ and YPO_4) Wt.%
100	0
90	10
80	20
70	30
60	40
50	50

Table 3.2: Ratios of Al_2O_3:REP in Wt.%
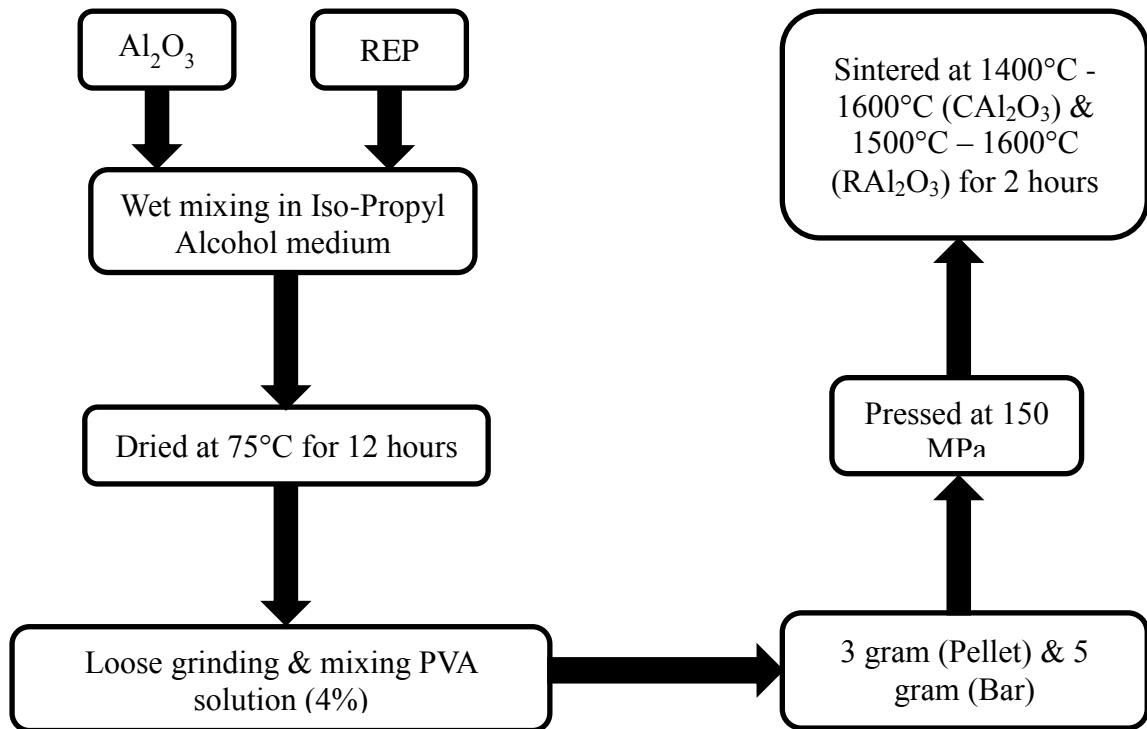
Fig. 3.2: Flow Diagram for Preparation Route of Composites

3.4 Characterization

3.4.1 Characterization of Starting Materials

3.4.1.1 Phase Analysis

Phase analysis of REP powder and the sintered composite was done the X-ray diffractions method (Rigaku, Japan) with an attachment of a Ni filter 0.154 nm and Cu-Kα as the radiation source. These X-ray diffraction techniques give some relevant parameters such as a crystal structure, chemical analysis, crystallite size, etc. the generator voltage and the current was set at 35 KV and 25 mA respectively. All composite powder were scanned in a continuous mode over a 2Ө range from 15 to 60 with a scanning rate of 5°/minute. The peak positions, phase purity, peaks of different atomic plans and the relative intensities of the powder pattern were identified in comparison with the reference powder diffraction data (JCPDS). Fig. 3.3 shows the basic setup of XRD machine used.

.

Fig. 3.3: XRD Machine (Rigaku, Japan)

3.4.1.2 Fourier Transformed Infrared Analysis (FTIR)

FTIR spectroscopy was used to characterize the chemical functional groups present in materials, based on the characteristics of vibrational and rotational energies of different molecular bonds. FTIR analyses of calcined $LaPO_4$ and YPO_4 powders were done at a resolution of 4 cm^{-1} using Spectrum RX^{-1} instrument (Perkin-Elmer) in the wavenumber range 4000 to 400 cm^{-1} using the KBr wafer technique. The mixture was ground to a finely after drying in an agate mortar. The spectrogram of the sample is observed on the computer monitor, and a graphic representation of the spectra was taken.

3.4.1.3 Microstructural Analysis

Field Emission Scanning electron microscope (FESEM) is a typical electron microscope that images formed by just scanning it with a beam of electrons. The electrons (secondary electrons, backscattered electrons (BSE) interact with the surface atoms that initiate to develop relevant information about the sample's microstructure and elemental composition. The microstructure of Al_2O_3 precursor was analyzed using scanning electron microscope (NOVA NANO SEM, FEI make) with gold coating of 240 seconds and analyzed in backscattered electron mode at 15KV sources. Several FESEM images were taken similarly of sintered composites at different temperature to determine the weak interface of REP.

3.4.2. Characterization of Sintered Products

3.4.2.1 Density Measurement

Densification study of the sintered samples was done by Archimedes principle, using a vacuum method in the water medium. Relative densification (percent theoretical density) was calculated as the ratio between bulk density and theoretical density of the composition. Theoretical density of each composition was calculated from the ideal (theoretical) density values of each component and their weight fractions used to make the composition. Dry weights of all the Al_2O_3/REP composites samples were taken by using a digital balance. Then the composite samples were kept in a beaker filled with distilled water and maintained in a vacuum desiccator for 45 minutes to remove entrapped air present in the samples. Suspended as well as soaked weights of the samples were taken using four-digit accuracy electronic balance. Bulk density and relative density of the sample were calculated as:

$$\textbf{Bulk Density} = \textbf{D/W-S} \text{ -------------- (3)}$$

$$\textbf{Relative Density} = \textbf{Bulk Desnity/Specific Gravity} \text{ --------------- (4)}$$

Were D = dry weight of the sample.

W = soaked weight of the sample.

S= suspended weight of the sample.

Percent relative densification was calculated as per the formula (Bulk density / specific gravity of the composite) x 100

Specific Gravity of the composite is calculated as, $\rho = \rho_{REP}V_{REP} + \rho_{Al2O3}V_{Al2O3}$,

Where, ρ is the specific gravity of each component and V is the volume fration of hat component in the composite mix.

$\rho_{LaPO4} = 5.07$ g/cm^3, $\rho_{YPO4} = 5.1$ g/cm^3, $\rho_{Al2O3} = 3.99$ g/cm^3.

3.4.2.2 Flexural Strength (MOR)

Determination of the flexural strength is frequently necessary as a part of the design of the structural ceramics to check compliance with established specifications or to provide information necessary to the design of an engineering structure. It is the ability of bar to resist failure in bending. The flexural strength is expressed as "Modulus of Rapture" (MOR) in MPa.

Three samples of each composition of all sintering temperatures were taken to determine the flexural strength for each test, and average values have been reported. Flexural strength was determined by standard three-point bending method in an instrument (Tinius Olsen, USA, make). The parameter for the three-point bending test was span length of 40mm with cross head speed of 0.5mm/min. The edges of the rectangular bars of 60 x 6 x 6 mm. the fundamental setup of flexural strength shown in Fig. 3.4 and Flexural strength were calculated by:

$$\sigma_{flexural} = (3FL/2BD^2) \quad \text{-------------- (5)}$$

where F = Fracture load; L =Span length; B =Width of sample and D =Thickness of the sample.
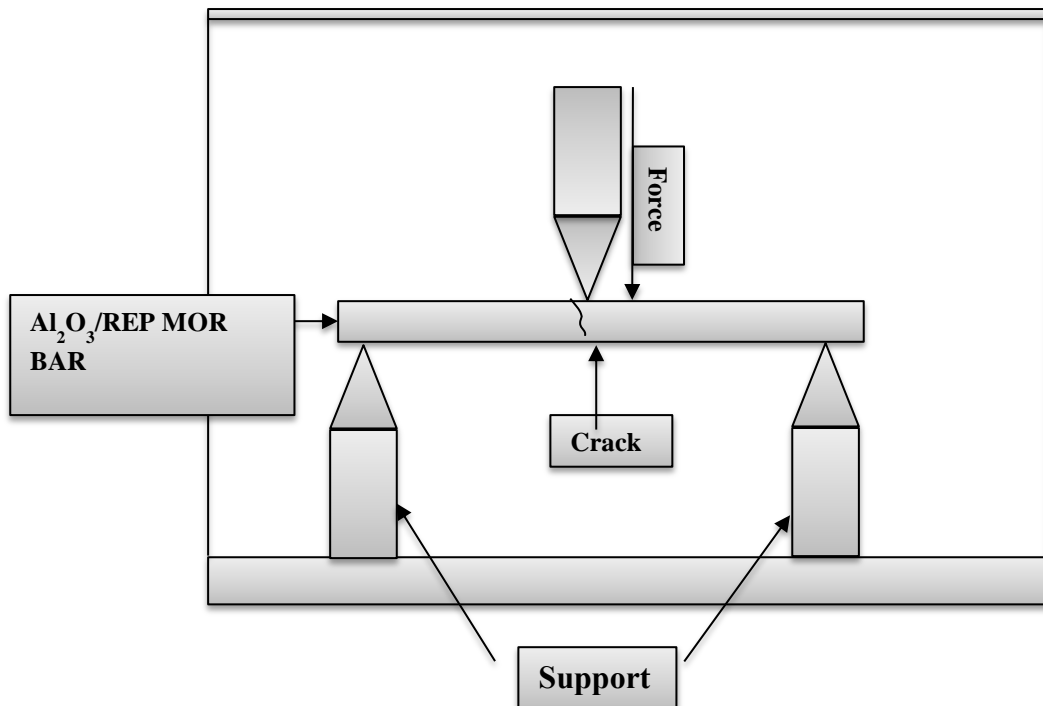
Fig. 3.4: Basic Setup of flexural strength

3.4.2.3 Machinability

The machinability of the sintered Al_2O_3/REP composites was tested by drilling using hand drill machine (Bosch make model GSB 10 RE having no-load speed of 2600 rpm). Cemented carbide drill bit, 4 mm dia. was used for the drilling purpose. Water was used at the drill tip to reduce the friction heat. Fig. 3.5 shows the hand drill machine that was used for drilling.

Cemented Carbide Drill Bit (4mm)

Fig. 3.5: Bosch Hand Drill (GSB 10 RE)

3.4.2.4 *In vitro* cytotoxicity test

An in vitro cytotoxicity test of steam sterilized Al_2O_3/REP composites (powder) was performed using MG 63 Osteoblast Cell line by direct contact method as per ISO-10993-5 guideline [11]. Osteoblast cells were employed in the present study because it can be easily cultured in a reproducible manner and also this cell line is widely used for many biocompatibility tests.

It has ease rate of proliferation with most of the biomaterial surface because it more resistance to survive in the atmosphere as compared to other cells. In the beginning, guideline Osteoblast cells were subcultured, trypsinized and seeded onto multiwell tissue culture plates. The Osteoblast cells were cultured with DMEM (Dulbecco's Modified Eagle Medium), 10% FBS (Fetal Bovine Serum) and incubated at 37°C in 5% CO_2 atmosphere till formation of a cell monolayer. The test specimen (Al_2O_3/REP) was incubated at 37°C for 24 to 26 hrs. The Al_2O_3/REP was examined using inverted microscope for cellular response to the requisite incubation. In vitro cytotoxicity of the test, specimen was also compared with the positive

control Osteoblast cells and Pure Al_2O_3. Cell was examined by inverted microscopy to check the response of the cells around the test specimens (composites).

3.4.2.5 Cell Viability study

The MTT assay was performed to measure the metabolic activity of cells and assessed through, 'color-change' phenomenon from yellow colored tetrazolium salt, MTT {3-(4,5-diamethyl thiazol-2-yl)-2,5-diphenyltetrazolium bromide} to purple colored formazan. Fresh test specimens Al_2O_3/REP (powder) composites were sterilized by steam sterilization 20 minute, and extract was prepared after 24–26 hrs. incubation at 37°C in 1 ml culture medium containing serum protein. The extract solution was further diluted to 10, 5 and 2.5% in same culture medium. Equal volume (100 µl) of extract as obtained from Al_2O_3/REP composites (powder), positive control Osteoblast cells and pure Al_2O_3. The cells were placed on a subconfluent monolayer of Osteoblast cells and incubated for 24 at 37°C. The cultured cells were treated with 50 µl of MTT and further incubated at 37°C for 4 h in humidified and 5% CO_2 atmosphere. Aspiration removed the excess amount of MTT, and formazan crystals were dissolved by adding 100 µl of isopropanol. Cytotoxicity tests were performed in triplicate. The color exchange was quantified by measuring absorbance at 570 nm using a spectrophotometer. Representation of cell viability index is done against the batch composition.

References:

1. Alumina's for ceramic applications, Product catalogue, Almatis Inc., USA.
2. W Ruigang, P. Wei, C. Jian, F. Minghao, C. Zhenzhu, L. Yongming, Journal of Material Chemistry and Physics, 79 (2003) 30-36.
3. S. Lucas, E. Champion, D. B. Assollant, G. Leroy, Journal of Solid State Chemistry; 177 (2004) 1312-1320.
4. C. Tas, Biomaterials, 21 (2000) 1429-1438.
5. P. Li, I. Kangasniemi, K. de Groot, T. Kokubo, Journal of American Ceramic Society, 77 (1994) 1307-1312.
6. P. Li, K. Nakanishi, T. Kokubo, K. de Groot., Biomaterials, 14 (1993) 963-968.
7. P. Li, I. Kangasniemi, K. de Groot, T. Kokubo, AU. Yli-Urpo, Journal of Non-Crystalline Solids, 168(1994) 281-286
8. S. Cho, K. Nakanishi, T. Kokubo, N. Soga, C. Ohtsuki, T. Nakamura, T. Kitsugi, T. Yamamuro, Journal of American Ceramic Society,78 (1995) 1769-74.
9. T. Kokubo, F. Miyaji, H. M. Kim, T. Nakamura, Journal of American Ceramic Society 79 (1996) 1127-1129.
10. T. Kokubo, H. Takadama, Biomaterials, 27 (2006) 2907-2915.
11. I.S.O. 10993-5, Biological evaluation of medical products test for in vitro cytotoxicity Part 5 (1999).

CHAPTER 4

Results & Discussion

Part A: Raw Material Characterization
Part B: Characterization of Sintered Composites
Part C: Cytotoxicity of Composites
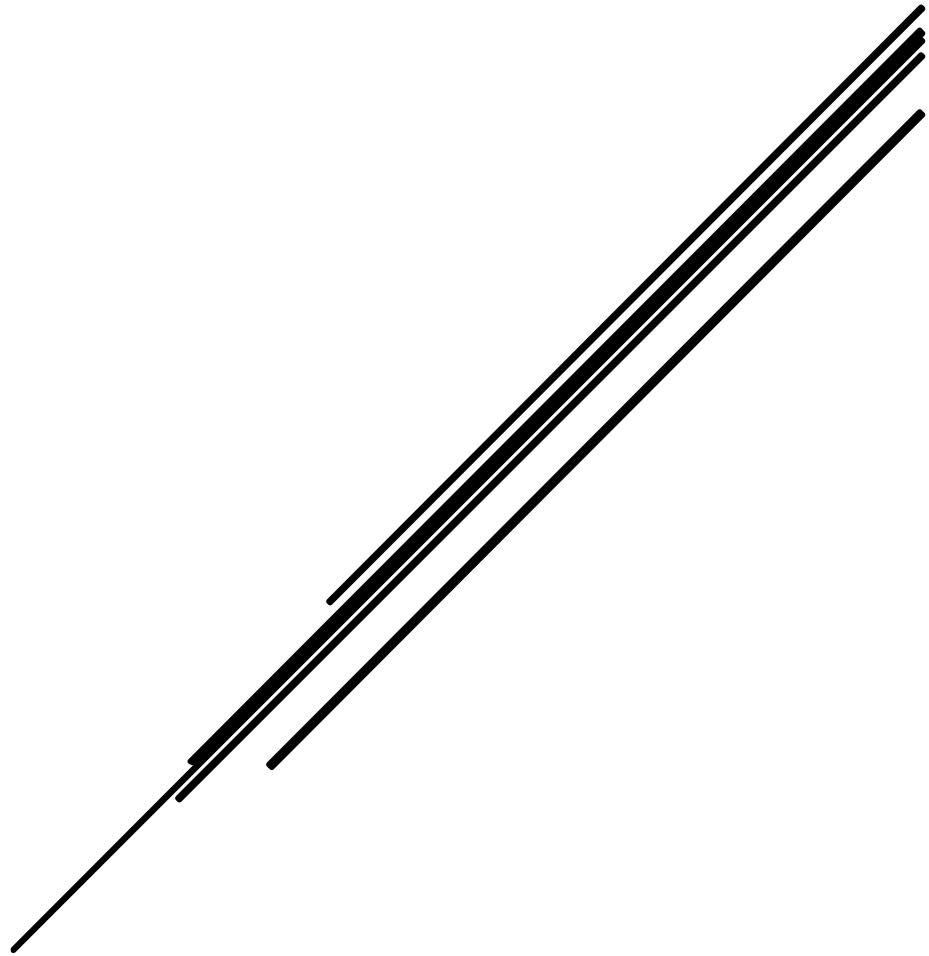
This chapter deals with the preparation and different characterizations of REPs used in the study. Next the sintered composites of different Al_2O_3-REP compositions were characterized. Composite nature of the sintered compositions is confirmed by phase analysis; densification behavior was characterized by measuring the bulk density and relative densification; 3 point modulus of rupture (flexural) testing for measuring the strength; machinability was studied by drilling method using a conventional drill bit; microstructural features was investigated under electron microscope with elemental distribution study of the relevant elements and also the biological compatibility of the sintered compositions were studied by cytotoxicity measurement.

Four different compositions prepared with REP and the sintering kinetics of composites at various temperature as given in Table 4.1. In in this table, CAl2O3 is calcined and RAl2O3 reactive alumina (Commercial grade alumina).

Table 4.1: Sintering Schedule of Composites

Composition	Temperature
CAl_2O_3-$LaPO_4$	1400°C – 1600°C (2 hours)
RAl_2O_3-$LaPO_4$	1500°C – 1600°C (2 hours)
CAl_2O_3-YPO_4	1400°C – 1600°C (2 hours)
RAl_2O_3-YPO_4	1500°C – 1600°C (2 hours)

Part A
Raw material Characterization

4.1 Properties of Alumina's

Two types of alumina powders were used in this study namely CAl_2O_3 and RAl_2O_3. Details of the two aluminas are given in Table 3.1. From the values, it can be seen that both the aluminas are highly pure but CAl_2O_3 is relatively finer and reactive as compared to that of RAl_2O_3 [1].

4.2 Characterizations of REP

4.2.1. Phase Analysis of Rare Earth Phosphates (REP`s)

Two different types of REP`s were used in this study. Both REP`s prepared by using wet chemical synthesis and direct chemical reaction between respective rare earth oxides and H_3PO_4. La_2O_3 and Y_2O_3 were used to make $LaPO_4$ and YPO_4 respectively. The reaction product obtained was dried and then double calcined at 800°C ($LaPO_4$) and 1000°C (YPO_4) and checked for phase analysis by X-ray diffraction technique. Fig. 4.1 shows the phase analysis of double calcined lanthanum phosphate ($LaPO_4$) and yttrium phosphate (YPO_4). Phase analysis shows only $LaPO_4$ (32-0493) and YPO_4 (84-0335) phases with no other impurity phosphate phase or oxide phase [2-5].

(A)   **(B)**
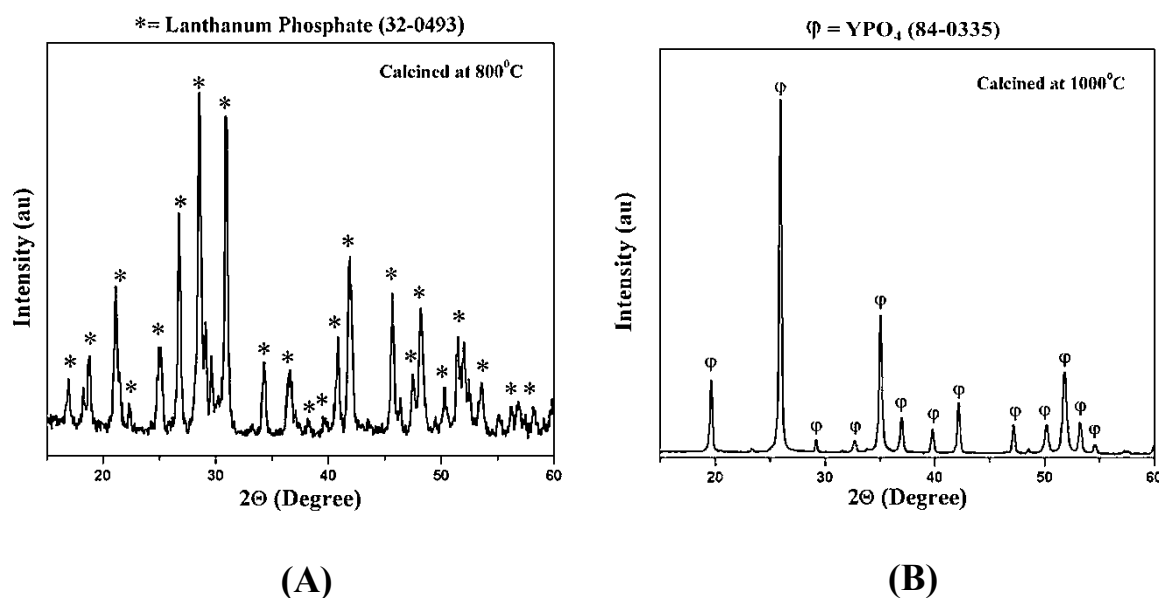
Fig. 4.1: Phase Analysis of the REPs (A) $LaPO_4$; (B) YPO_4

4.2.2 Fourier Transformed Infrared (FTIR) Analysis

FTIR analysis of both the prepared phosphates was done to measure the characteristics energy absorption peaks of different molecular bonds in the infra-red region. Fig. 4.2 (A) shows the FTIR analysis of $LaPO_4$. The very first band is characteristics of the vibration of phosphates group at about 584 cm^{-1} for v_4, after this a stretch of v_1 and v_3 at 1050 cm^{-1} and the v_2 is observed in the investigated range of wavenumbers. The broad band at 3455 cm^{-1} and the bands 1639 and 1458 cm^{-1} are associated with H_2O [5]. A small band at 2005 cm^{-1} can be corresponding to the La - O [6-7].

The spectra of YPO_4 is shown in Fig. 4.2 (B); the peak appearing at 525 – 641 cm^{-1} and 1049 and 1258 cm^{-1} are corresponded to the bending vibration (*u*4 region) and stretching vibration (*u*3) of PO_4 group. A band at 2922 cm^{-1} can be assigned to stretching vibration of Y - O. Peak centered at 1650, 2020 and 3408 cm^{-1} belong to the bending and stretching vibrations of O-H group [5].
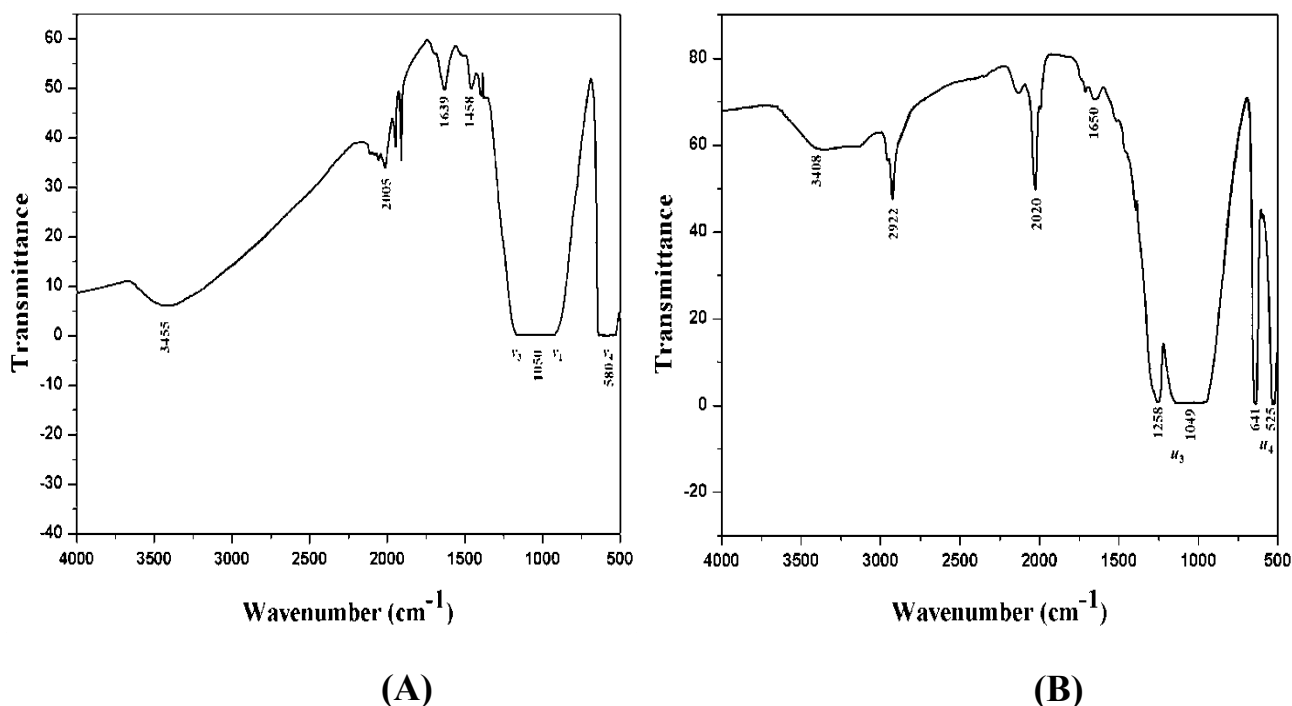
Fig. 4.2: FTIR Analysis of REP`s (A) $LaPO_4$; (B) YPO_4

4.2.3 Microstructure of Rare Earth Phosphates

Calcined REP powders were studied for the microstructural characterization and the photomicrographs are shown in Fig 4.3 and 4.4. The morphology of $LaPO_4$ shows micron sized particles [Fig. 4.3 (A) low-magnification], which are found to have a sponge-like structure on high-magnification [Fig. 4.3(B)]. Calcined YPO_4 particles show a needle or rod-like structure [5] and the morphology shows high aspect ratio of the individual rod like grains [Fig. 4.4 (A) & (B)].

(A)   (B)
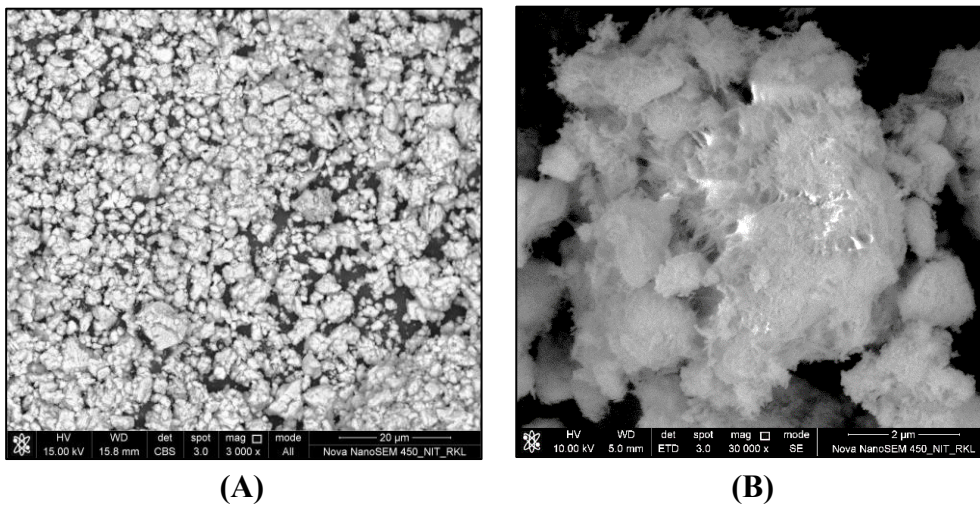
Fig. 4.3: FESEM Photomicrographs of Calcined $LaPO_4$ (A) Low Magnification; (B) High Magnification

(A)   (B)
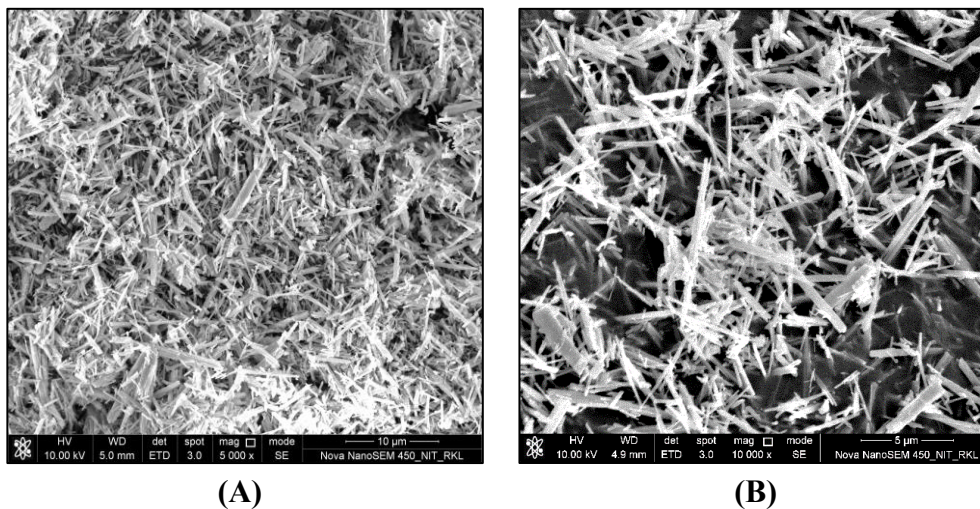
Fig. 4.4: FESEM Photomicrographs of Calcined YPO_4 (A) Low Magnification; (B) High Magnification

Part B

<u>Characterizations of Composites</u>

4.3 Densification Study of Composites

Densification behavior is studied by the Archimedes principle using a vacuum method in the water medium. For pure alumina compositions, CAl_2O_3 is highly sinterable (about 97% densification was obtained at 1600°C compared to that of RAl_2O_3, due to its increased reactivity from finer particle sizes. But it is observed that the addition of REP reduces the extent of densification of the composites for all the sintering temperatures. Again increasing amount of REP is found to decrease the density values gradually (Fig. 4.5 – Fig. 4.8). This is due to the presence of REP particles in between the alumina particles that act as a weak interphase material, results in interfacial debonding and reduced sintering / densification [8-9].

Increasing amount of REP content in the compositions, increases the presence of REP particles in the alumina matrix; hence greater extent of debonding and desintering of alumina ceramics occur, resulting in further lower density values. But the increase in sintering temperature, helps in increasing the sintering effect, thus results in higher density values for all the different composition and REP contents.

The fall in relative densification against rare earth content for both the types of alumina and REPs is much prominent compared to that of the bulk density plot. As the REPs have higher true density (specific gravity) values and increasing amount of REP increases the theoretical density of the compositions.
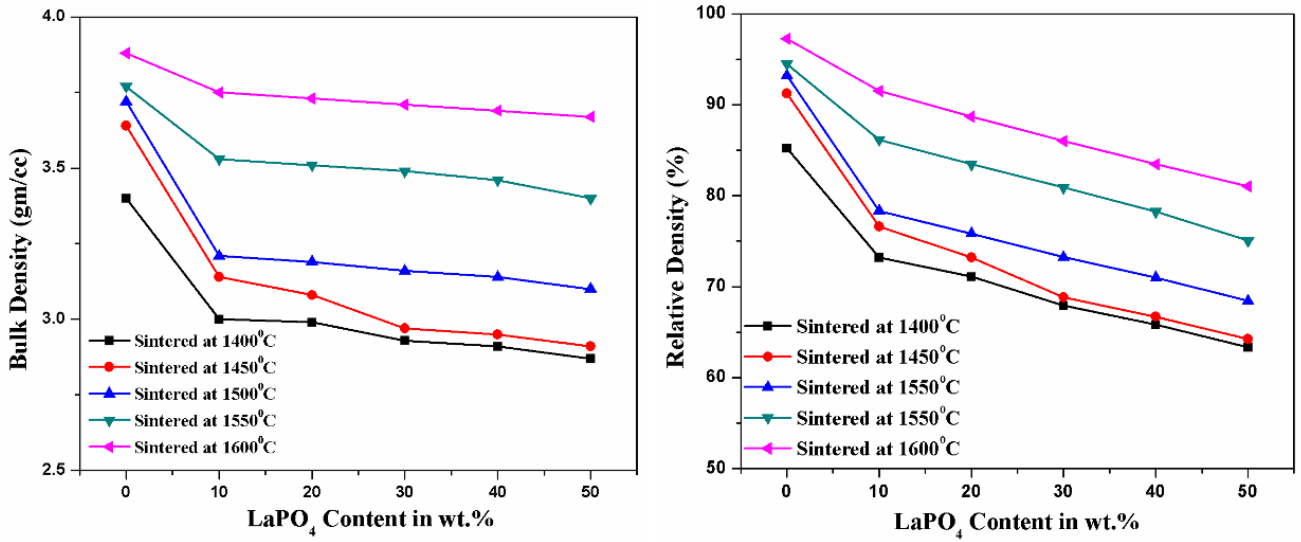
Fig. 4.5: Bulk Density and Relative Density Plot of CAl_2O_3 – $LaPO_4$ Against the Temperature
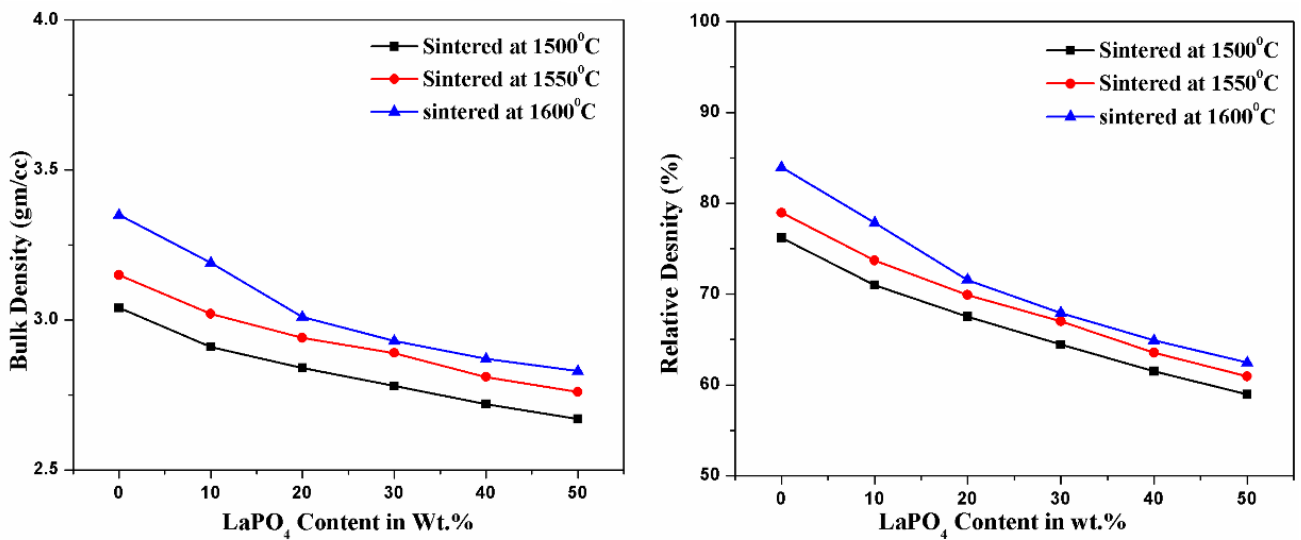
Fig. 4.6: Bulk Density and Relative Density Plot of RAl_2O_3 – $LaPO_4$ Against the Temperature
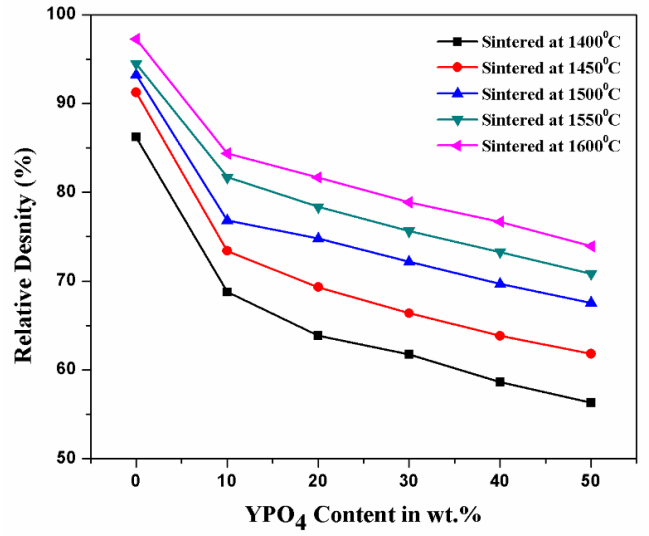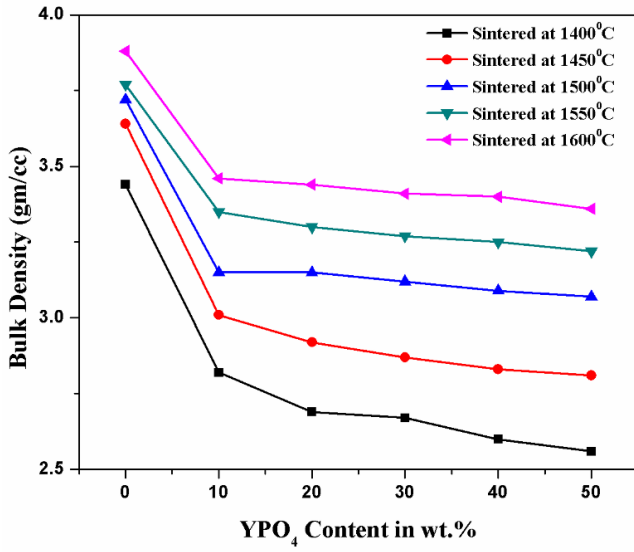
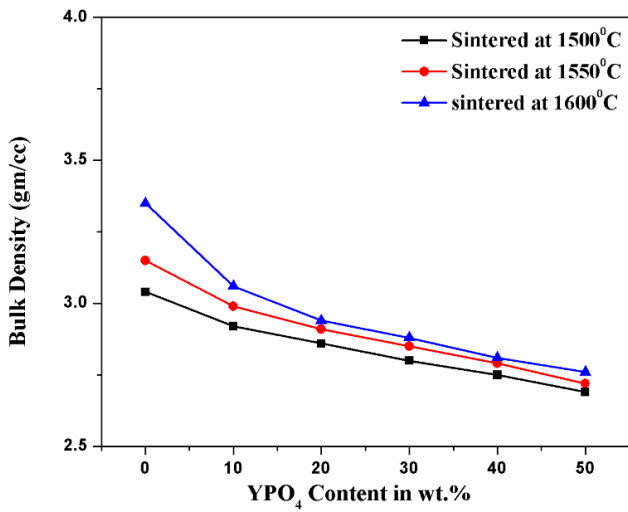Fig. 4.7: Bulk Density and Relative Density Plot of $CAl_2O_3 - YPO_4$ Against the Temperature
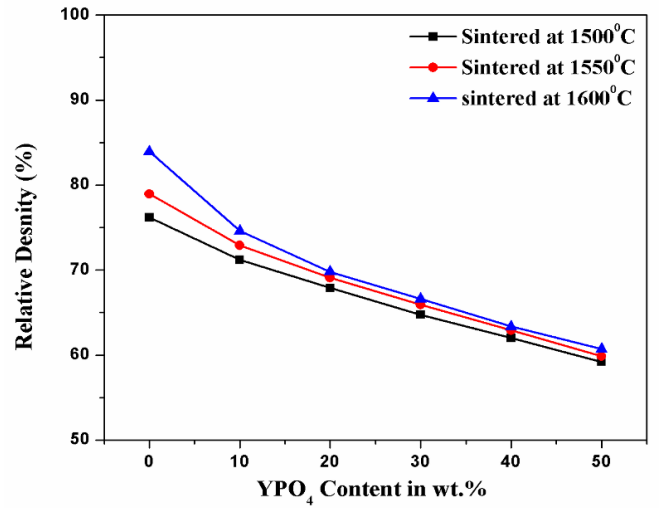
Fig. 4.8: Bulk Density and Relative Density Plot of RAl_2O_3-YPO_4 Against the Temperature

4.4 Phase Analysis of Composites

Phase analysis study of the sintered composites sintered at different temperatures shows only the peaks of the reactant phases, namely Al_2O_3 and REP and no other reaction product phases are observed. This trend is found for both the types of alumina, both the REPs, for all the REP contents and all the sintering temperatures. Increase in REP phase intensity is observed as the REP content is increased in the compositions. Phase analysis studies of 10 wt. % to 50 wt. % of REP ($LaPO_4$ and YPO_4) containing composites sintered at different temperatures are shown in Fig. 9 - Fig. 12 respectively.

Presence of separate and individual reactant phases and absence of any other phases indicate that no reaction has occurred between the reactant phases within the sintered composites for all the different contents of REP sintered at various temperatures. Hence, the sintered products are composite in nature for both the REP containing batches, even after sintering at different temperatures. REP phases are present as un-reacted one in the sintered compositions and remain as an interphase material.

$*$ = $LaPO_4$ (32-0493)

$\blacklozenge$ = Al_2O_3 (42-1468)
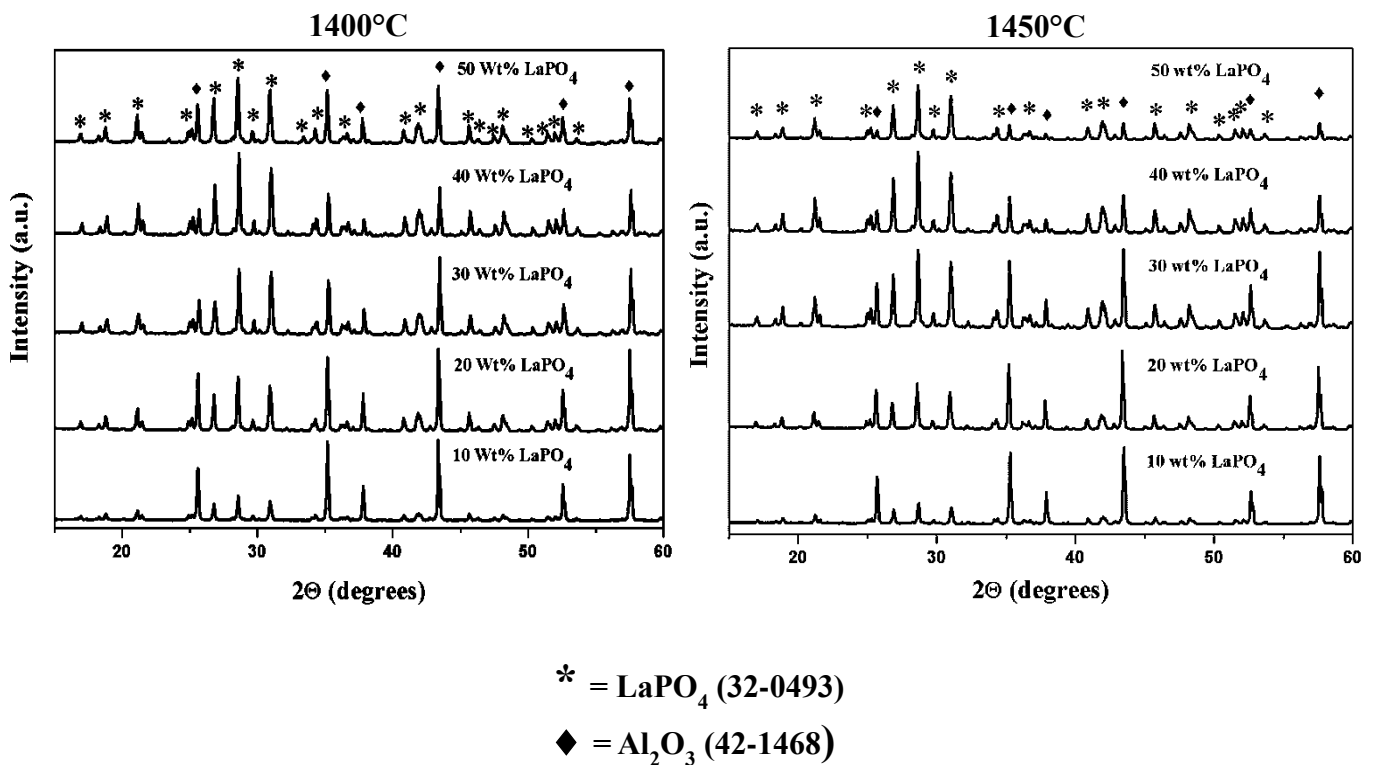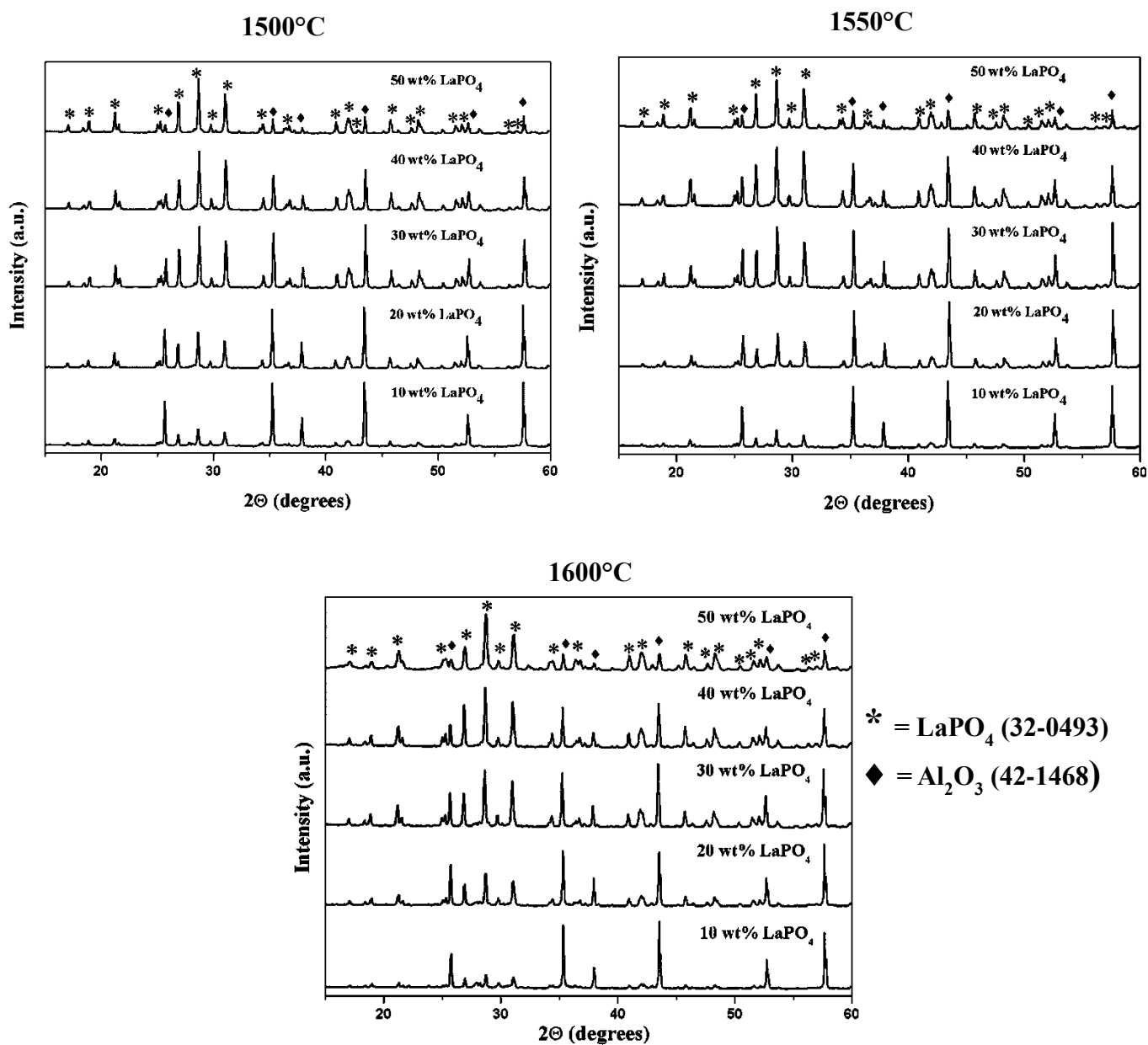
Fig. 4.9: XRD Pattern of CAl_2O_3-$LaPO_4$ Composites Containing 10 wt. % - 50 wt. % of $LaPO_4$ Sintered at Different Temperatures
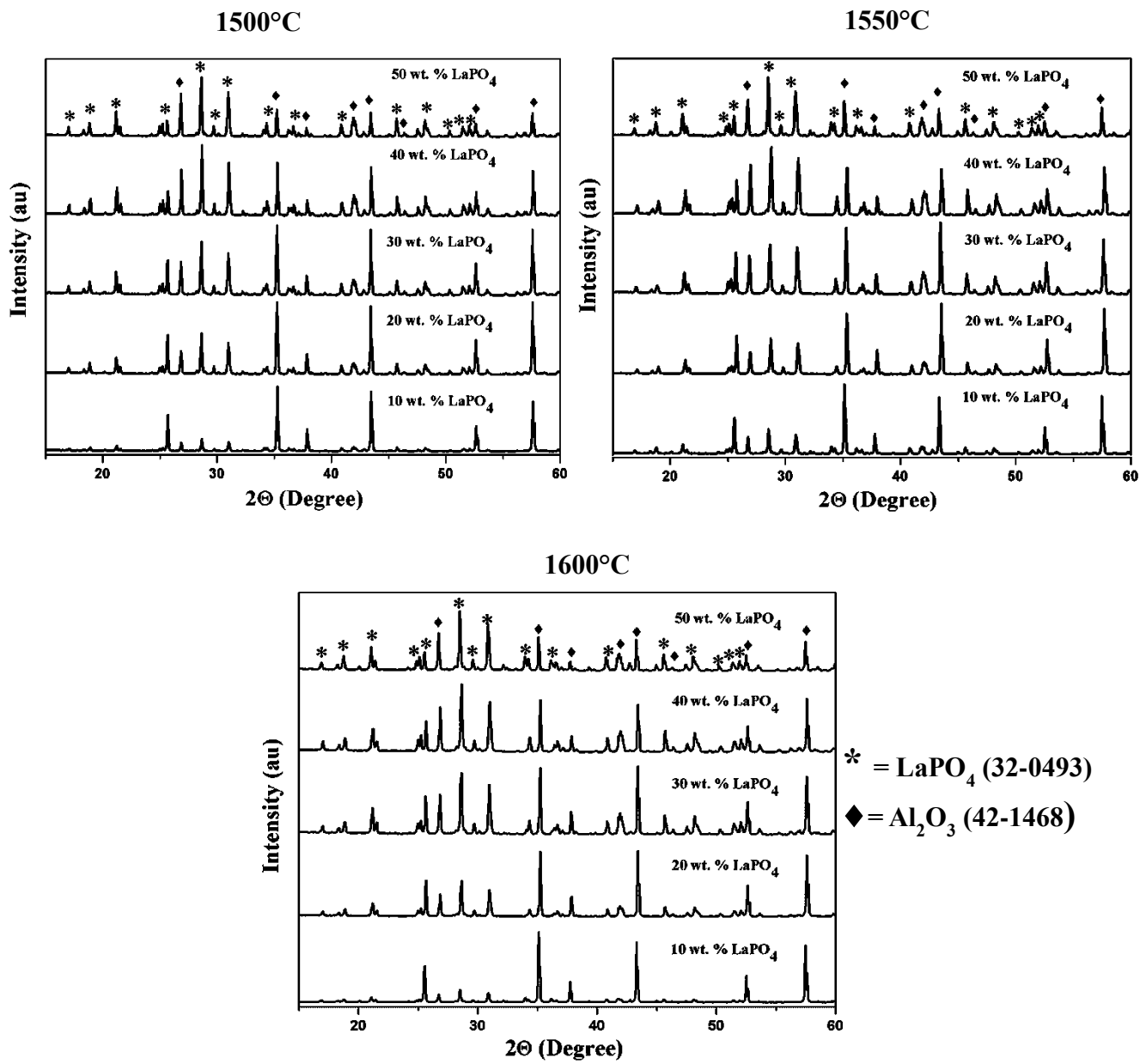
Fig. 4.10: XRD Pattern of RAl_2O_3-$LaPO_4$ Composites Containing 10 wt. % - 50 wt. % of $LaPO_4$ Sintered at Different Temperatures

Fig. 4.11: XRD Pattern of CAl_2O_3-YPO_4 Composites Containing 10 wt. % - 50 wt. % of YPO_4 Sintered at Different Temperatures
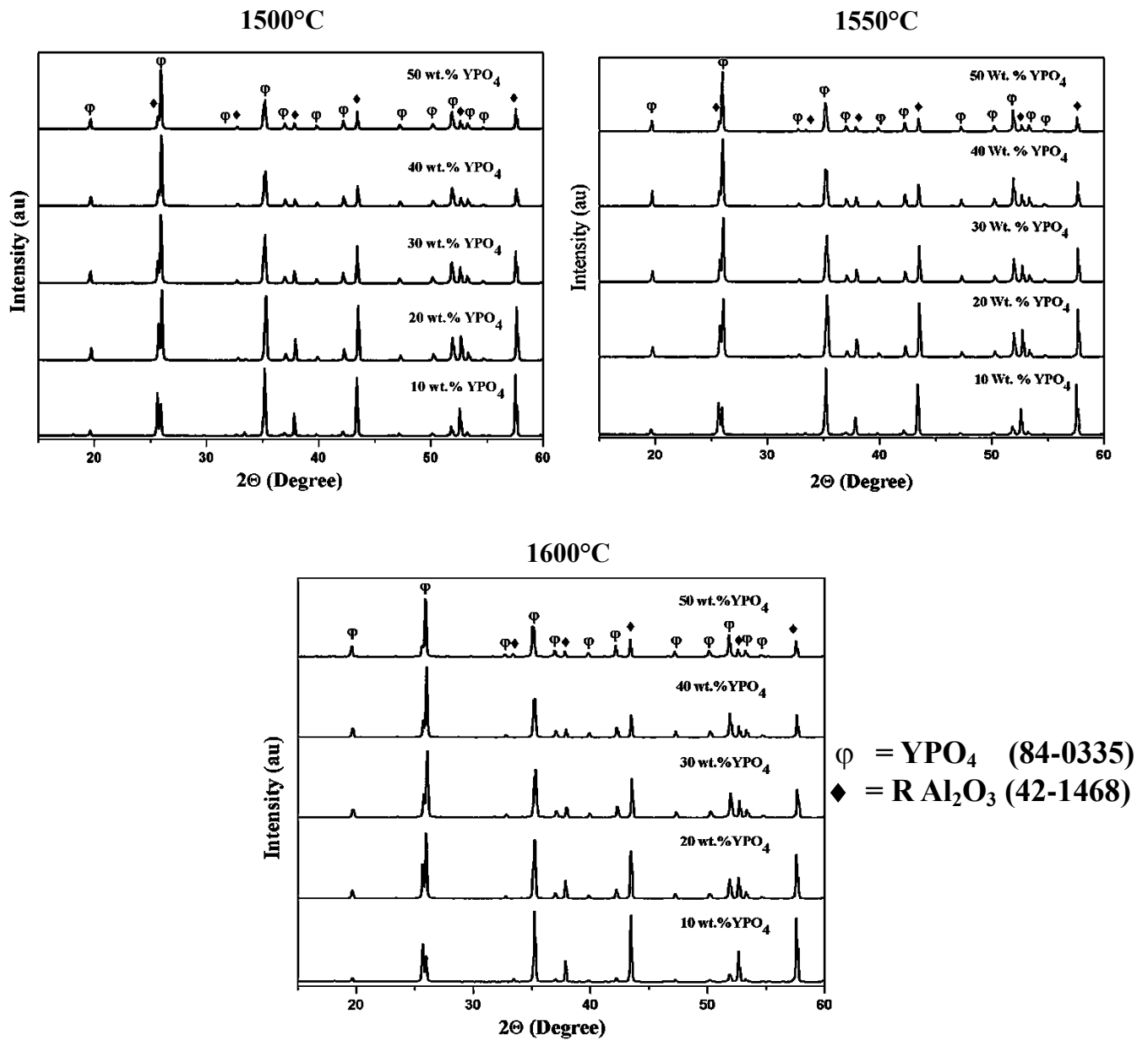
$\varphi = YPO_4$ (84-0335)

$\blacklozenge = C\ Al_2O_3$ (42-1468)

1500°C

1550°C

1600°C

φ = YPO$_4$ (84-0335)
$\blacklozenge$ = R Al$_2$O$_3$ (42-1468)
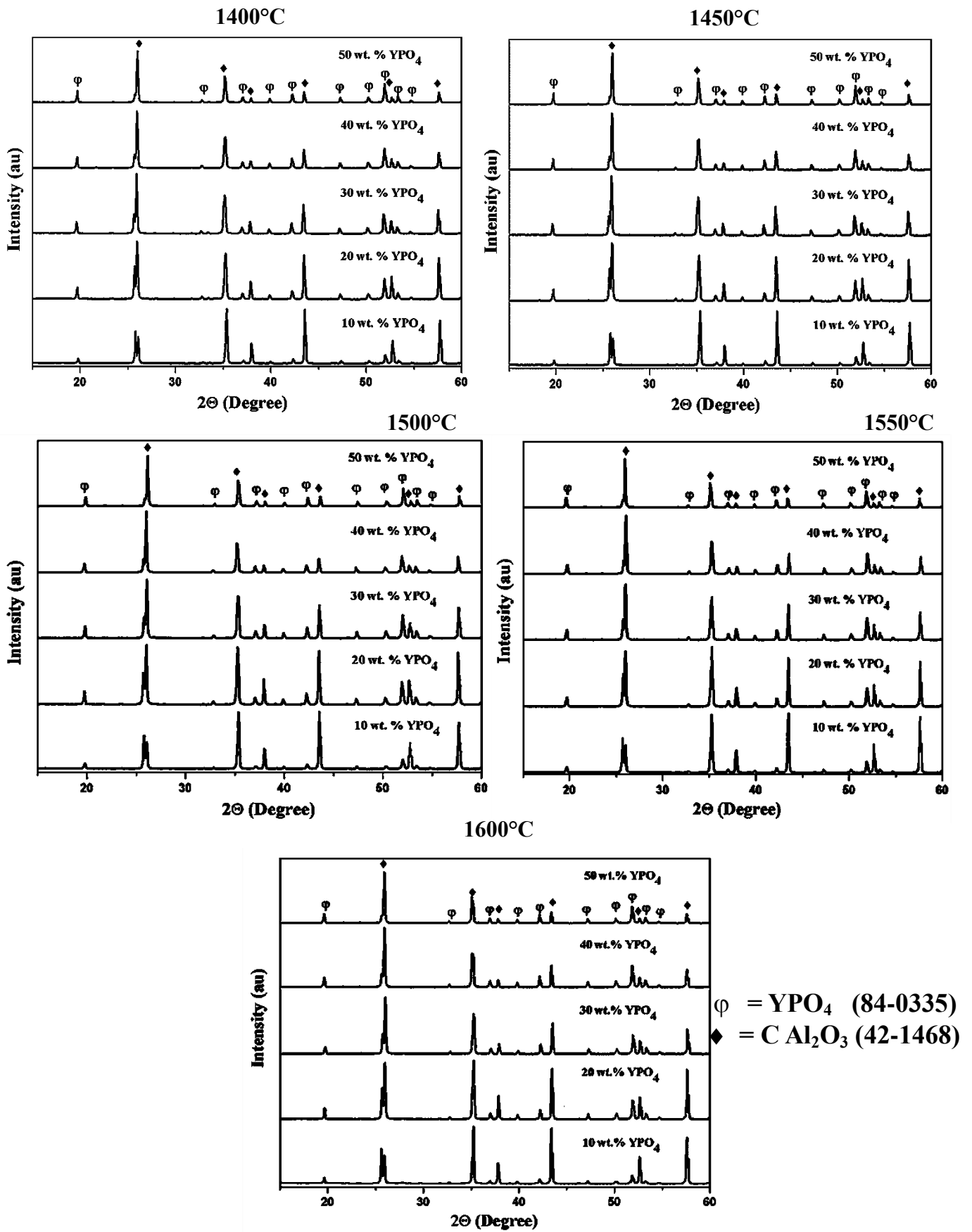
Fig. 4.12: XRD Pattern of RAl$_2$O$_3$-YPO$_4$ Composites Containing 10 wt. % - 50 wt. % of YPO$_4$ Sintered at Different Temperatures

4.5 Flexural Strength of composites

The Flexural strength of the composites is characterized by 3-point bending test method on bar samples of 60x6x6 mm dimension. A gradual decrease in the strength values is observed for both the aluminas with the increasing addition of REP. Flexural strength values of the composites are shown in Fig. 4.13 – Fig. 16. This gradual and continuous decrease in strength with increasing amount of REP is due to the increasing presence of REP particles in the alumina matrix causing increasing effect of desintering/debonding. Presence of REP particles reduces the sintering in the compositions, thus deteriorated the densification (as already described) and the corresponding strength. Increase in sintering temperature is found to increases the strength values for all the compositions, which is associated with the increased sintering effect resulting in greater densification and strength. CAl_2O_3 shows a higher strength values compared to that of RAl_2O_3 for all the sintering temperatures and all the REP containing conditions. This is due to the increased sintering and densification of CAl_2O_3.
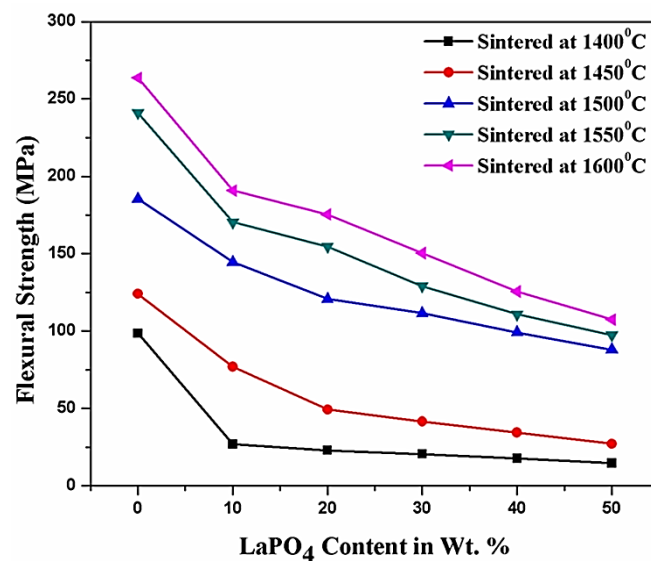
Fig. 4.13: Flexural Strength Plots of CAl_2O_3 – $LaPO_4$
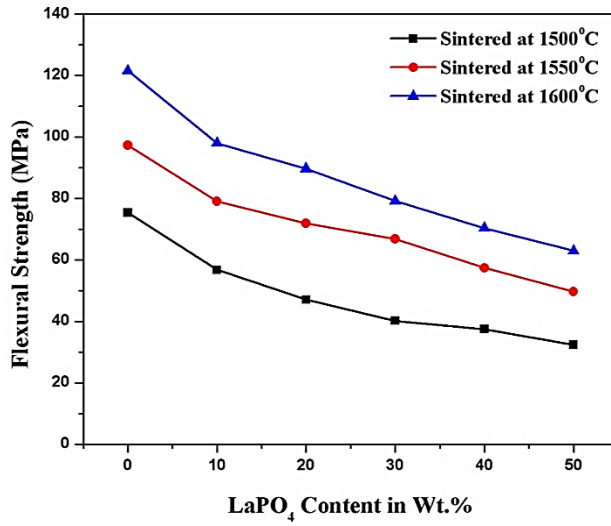
Fig. 4.14: Flexural Strength Plots of $RAl_2O_3 - LaPO_4$
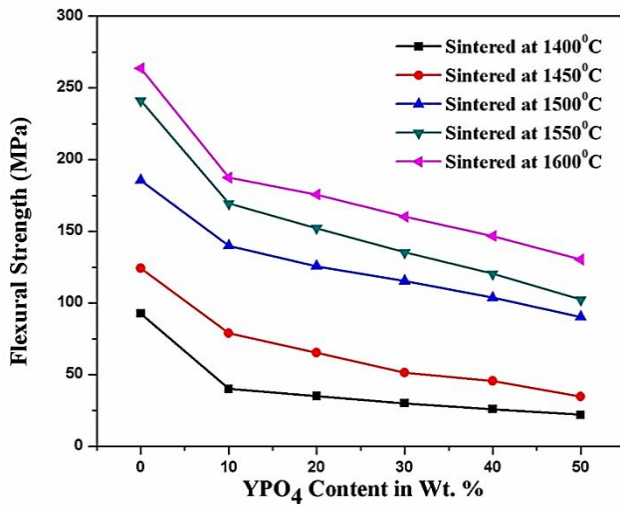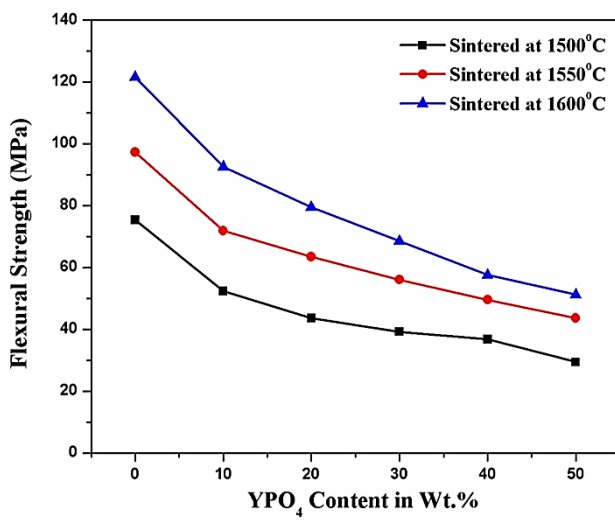

Fig. 4.15: Flexural Strength Plots of $CAl_2O_3 - YPO_4$

Fig. 4.16: Flexural Strength Plots of $RAl_2O_3 - YPO_4$

4.6 Microstrucutre Analysis

Microstructural developments of sintered Al_2O_3-REP composites with different REP content are shown in Fig. 17 – Fig. 20. All the different compositional variations are studied and only 1600°C sintered products are shown as representative ones. In each of the CAl_2O_3 and RAl_2O_3 composites containing both the REPs, two different phases can be distinguished easily. Higher scattering of the incident electron (for both backscattered and secondary electrons) by the REP phases (due to the presence of rare earth elements having higher atomic number) resulting in higher brightness of the REP particles. The rod-like feature of the YPO_4 particles is also observed in different composites containing various types of aluminas. This feature also indicates the presence YPO_4 as a separate entity in the sintered products, showing the composite character even after sintering.

Again, the size of the REP grains were found to be in the range of 1-2 micron but the size of alumina grains were found to be reduced by increasing amount of REP content in the sintered composites. This is common for both the aluminas and both the different types of REPs. This may be due to the higher extent of the restriction in the diffusion path of alumina for grain growth in increased presence of the REP particles in between them. In general, REP grains, distributed in the Al_2O_3 matrix and refines the grain size of Al_2O_3 [3] and reduces the size of alumina grains after sintering.

Elemental distribution mapping of different elements present in the sintered composites is shown in Fig. 21 – Fig. 24. It can be seen that elements like Al, P, O and rare earth (like La or Y) are well distributed in the photomicrographs. This confirms the well distribution of the elements, and so the respective oxides, namely Al_2O_3 and REP in the sintered composites
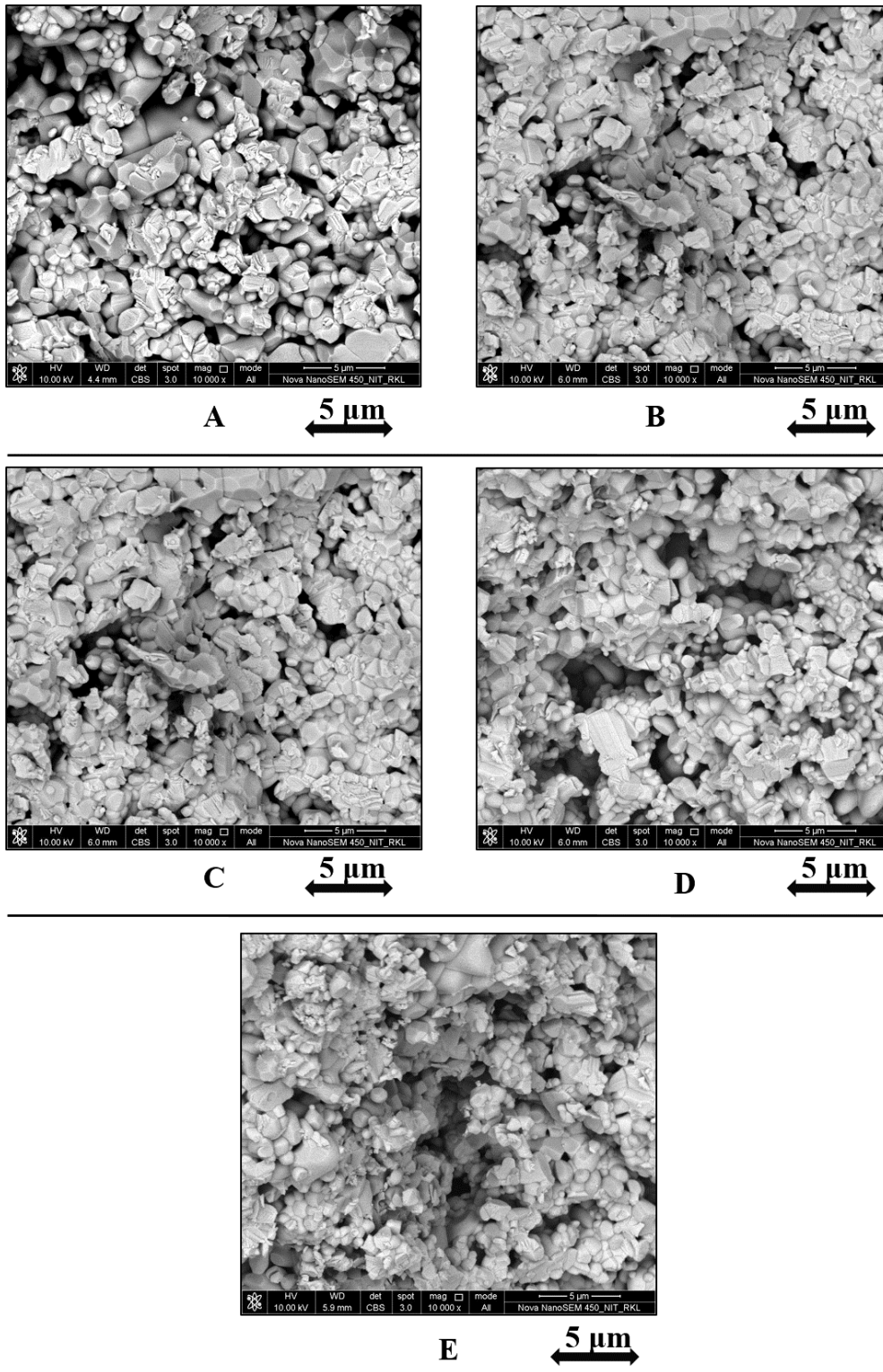
Fig. 4.17: FESEM Micrographs of the Fractured Surface of CAl_2O_3-$LaPO_4$ Composites Sintered at 1600°C (back-scattered); (A) 10 wt.% $LaPO_4$; (B) 20 wt.% $LaPO_4$; (C) 30 wt.% $LaPO_4$; (D) 40 wt.% $LaPO_4$; (E) 50 wt.% $LaPO_4$
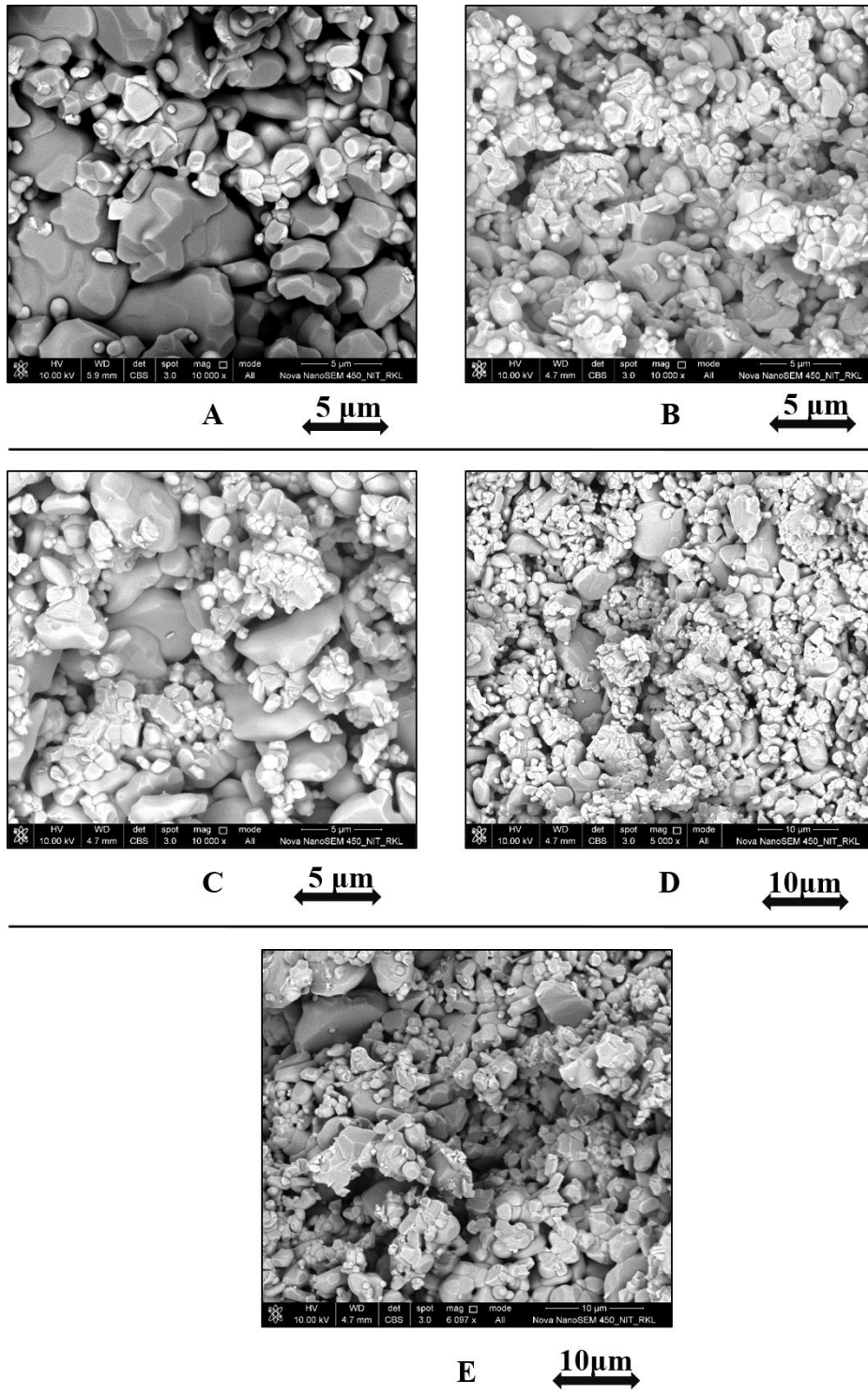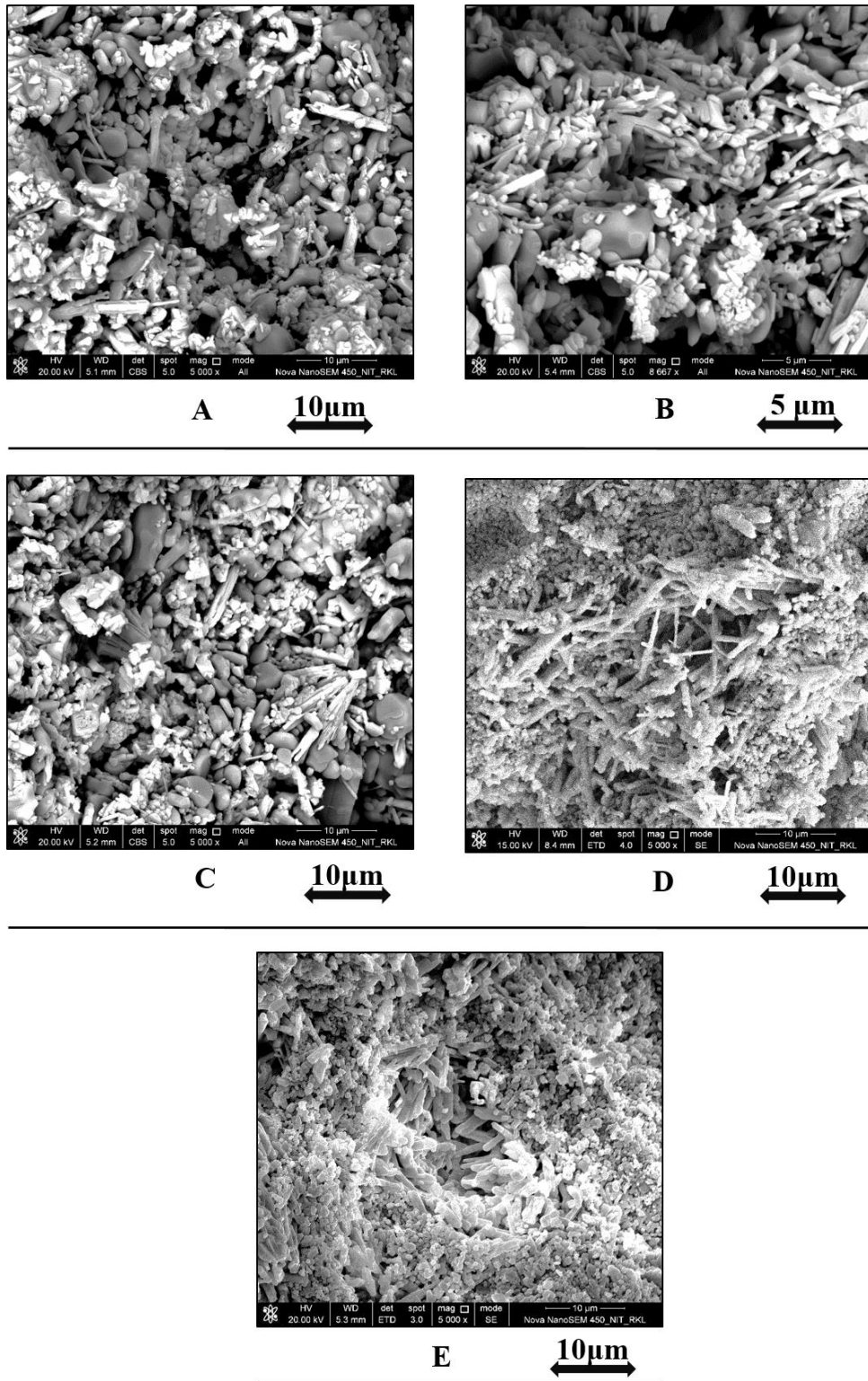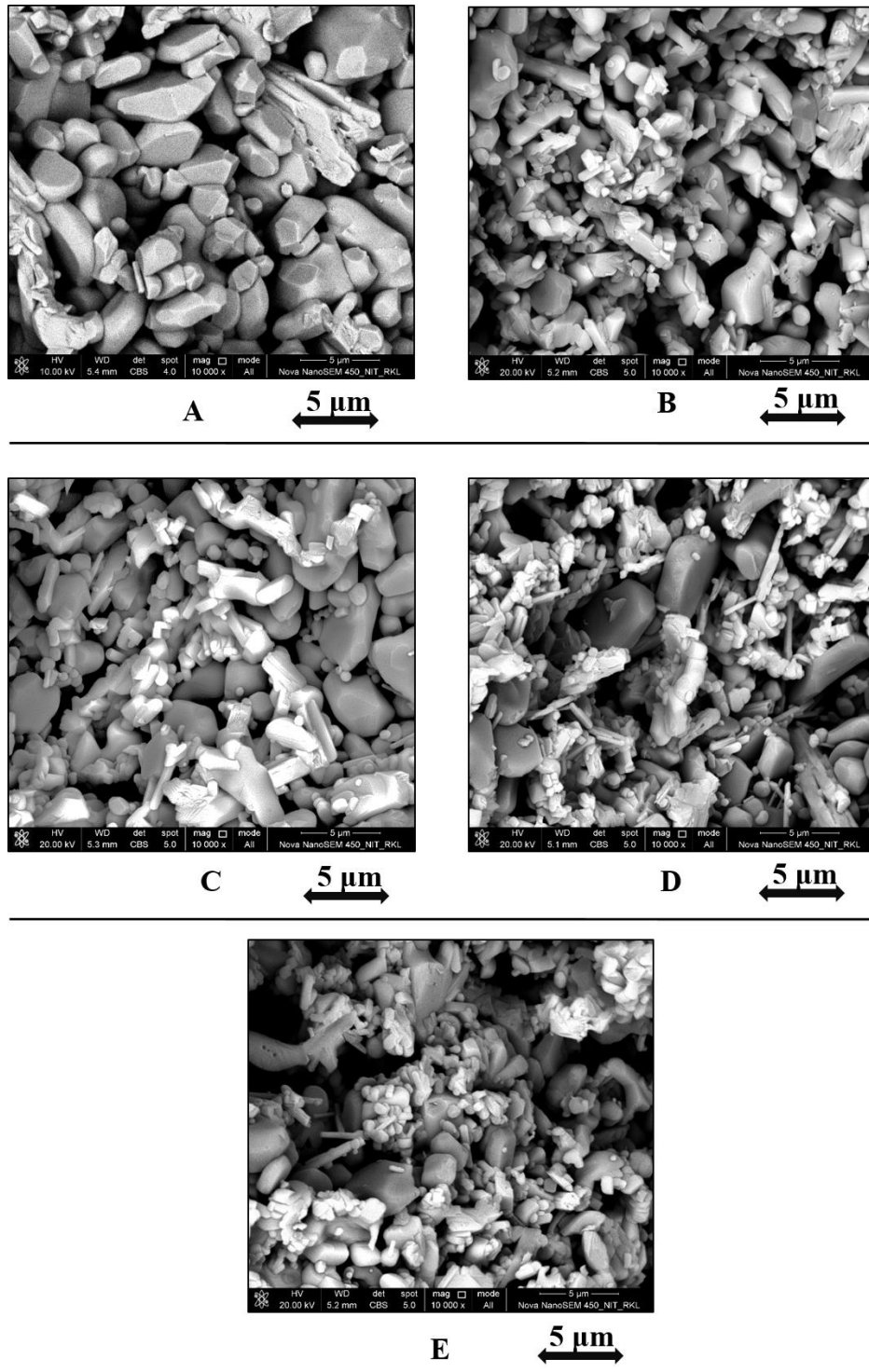
Fig. 4.18: FESEM Micrographs of the Fractured Surface of RAl_2O_3-$LaPO_4$ Composites Sintered at 1600°C (back-scattered); (A) 10 wt.% $LaPO_4$; (B) 20 wt.% $LaPO_4$; (C) 30 wt.% $LaPO_4$; (D) 40 wt.% $LaPO_4$; (E) 50 wt.% $LaPO_4$.

Fig. 4.19: FESEM Micrographs of the Fractured Surface of CAl$_2$O$_3$-YPO$_4$ Composites Sintered at 1600°C (back-scattered); (A) 10 wt.% YPO$_4$; (B) 20 wt.% YPO$_4$; (C) 30 wt.% YPO$_4$; (D) 40 wt.% YPO$_4$; (E) 50 wt.% YPO$_4$
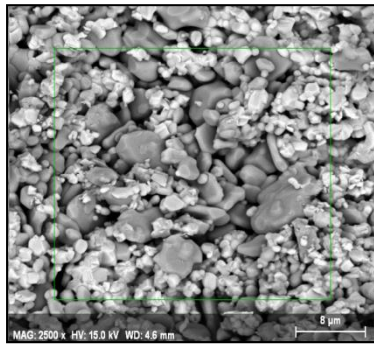
Fig. 4.20: FESEM Micrographs of the Fractured Surface of RAl_2O_3-YPO_4 Composites Sintered at 1600°C (back-scattered); (A) 10 wt.% YPO_4; (B) 20 wt.% YPO_4; (C) 30 wt.% YPO_4; (D) 40 wt.% YPO_4; (E) 50 wt.% YPO_4
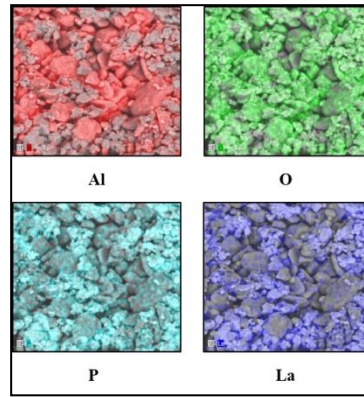
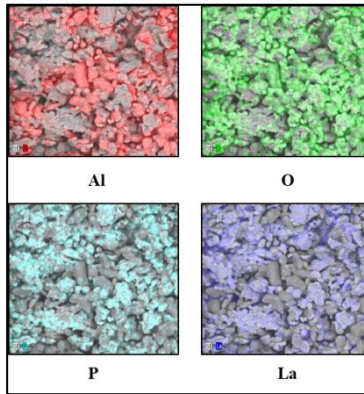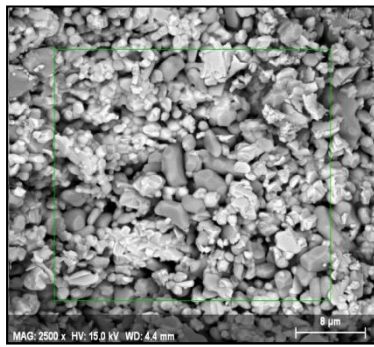Fig. 4.21: Elementary Mapping of $CAl_2O_3/LaPO_4$ Composite Sintered at 1600°C

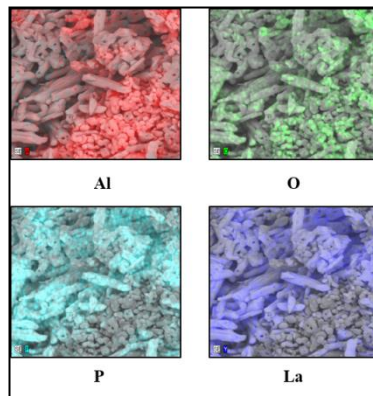Fig. 4.22: Elementary Mapping of $RAl_2O_3/LaPO_4$ Composite Sintered at 1600°C
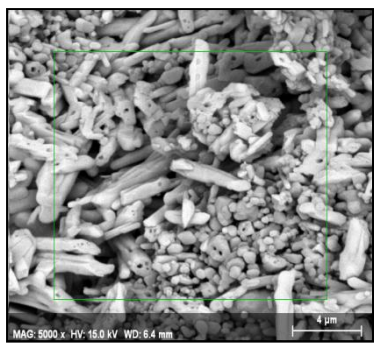

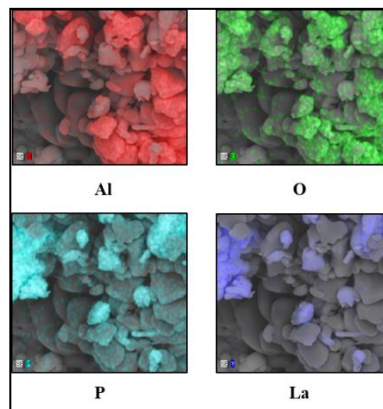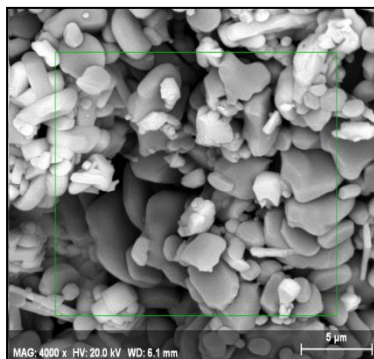Fig. 4.23: Elementary Mapping of CAl_2O_3/YPO_4 Composite Sintered at 1600°C

Fig. 4.24: Elementary Mapping of RAl_2O_3/YPO_4 Composite Sintered at 1600°C

73

4.7 Machinability study

The machinability study by drilling of different sintered samples is investigated by the cemented carbide drill bits. Fig. 4.25 shows the drilling study of pure Al_2O_3 sintered samples. It shows that pure alumina is not drillable and cracks/ breaks during the drilling operation under cemented drill bits. Strong bonding in pure alumina samples after sintering resulted in poor machinability and so the sintered samples were broken due to failure.
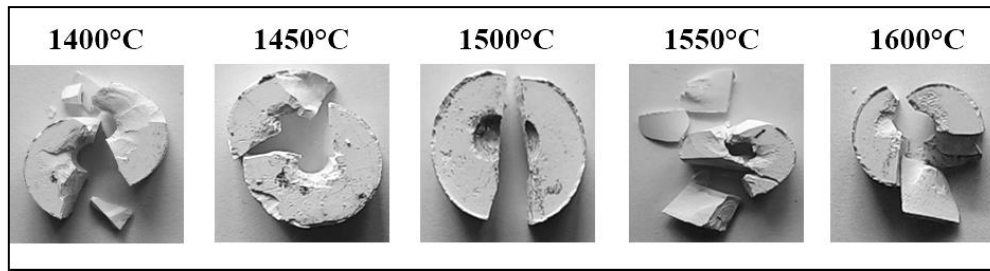
(A)
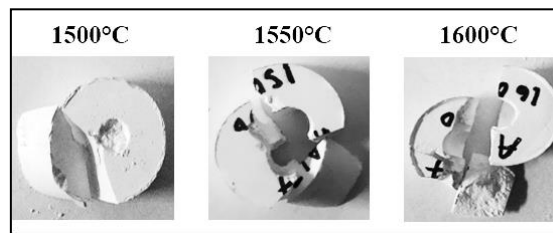
(B)

Fig. 4.25: Photographs of Pure Alumina Samples, Without Any REP (A) CAl_2O_3 ; (B) RAl_2O_3

Drilling study of the sintered composites with different aluminas and different amounts of $LaPO_4$ and YPO_4 are shown in Fig. 4.26 – Fig. 4.27. Grossly, the incorporation of REPs in alumina makes the sintered composites drillable. The holes are cleanly drilled, with no evidence of large-scale cracking or chipping

The addition of REP serves two purposes: (i) It forms a fine, highly stable REP phase, which pins the boundaries of Al_2O_3 and refines the grain size of Al_2O_3. (ii) It segregates at the Al_2O_3 grain boundaries and does not react with Al_2O_3 even at high temperature (1600°C).

This enhances the machinability of the composites by crack deflection along the weak interface between REP and Al_2O_3 and along layer plane of REP phase during drilling [2]. Microstructural photographs and elemental distribution of the elements present confirmed that REP particles are well distributed in the alumina matrix. They are acting as a weak interphase material in between the alumina particles, causing de-sintering and debonding effect and resulting in crack deflection and machinability.

REP grains possess a layered crystal structure, and they get readily delaminated due to its low cleavage energy, fractures propagate parallel to the layer crystals [2]. Crack deflections, branching and blunting during machining of these layered crystals help to prevent macroscopic fractures from propagation beyond the local cutting area. For the Al_2O_3-REP composites, the layered structure REPs surrounding the Al_2O_3 grains is the main feature in the microstructure of this composite. Microstructural photomicrographs showed in Fig. 4.17 – 4.20 indicate that most of the fracture mode belongs to inter-granular fracture, which confirms the formation of weak Al_2O_3-REP interfaces and is the primary reason of the improved machinability of this composite.

Hence, the layered structure REP and the weak interface at the Al_2O_3- REP grain boundaries are the primary reason for the improvement of the machinability. Both of them enhance the crack deflection and avoid the catastrophic failure of the material during drilling. In the two-phase mixtures of Al_2O_3 and REPs easy material removal by formation and linking of cracks at the weak interfaces between the two phases makes the composites machinable [2][8].

Drilling study also showed that for CAl_2O_3, which shows greater sinterability compared to RAl_2O_3, there is a threshold amount of REP content for the composite to be machinable at higher temperatures [Fig. 4.26A – Fig. 4.27A]. For the CAl_2O_3 composites sintered at 1550°C, a minimum of 20 wt. % of REP and for composite sintered at 1600°C, minimum of 30 wt. % of REP is found to be required to become drillable. This may be associated with the greater extent of densification of fine alumina at higher temperatures, which is reducing the desintering and debonding effect of REP and requiring threshold content for drillability.
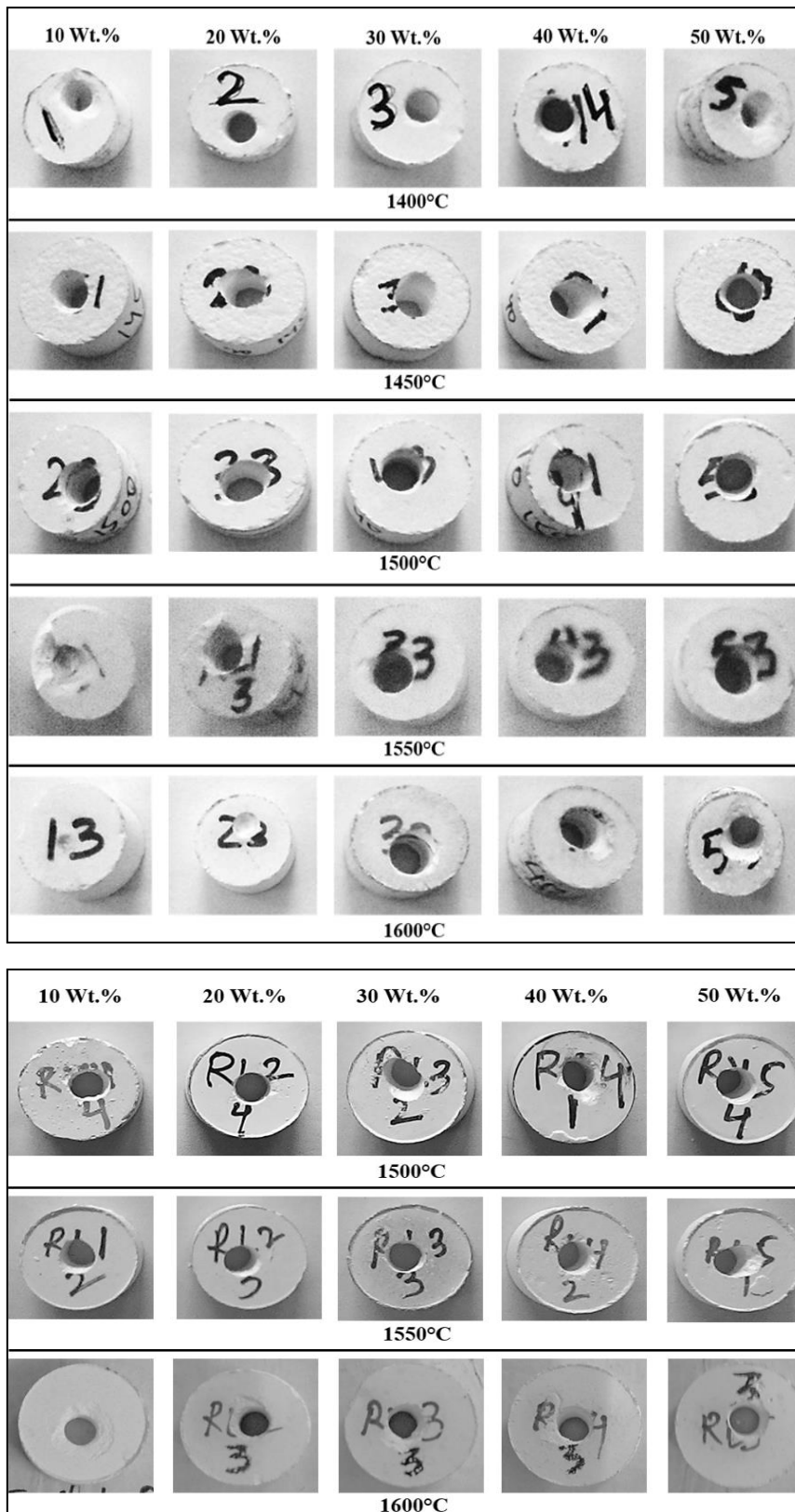
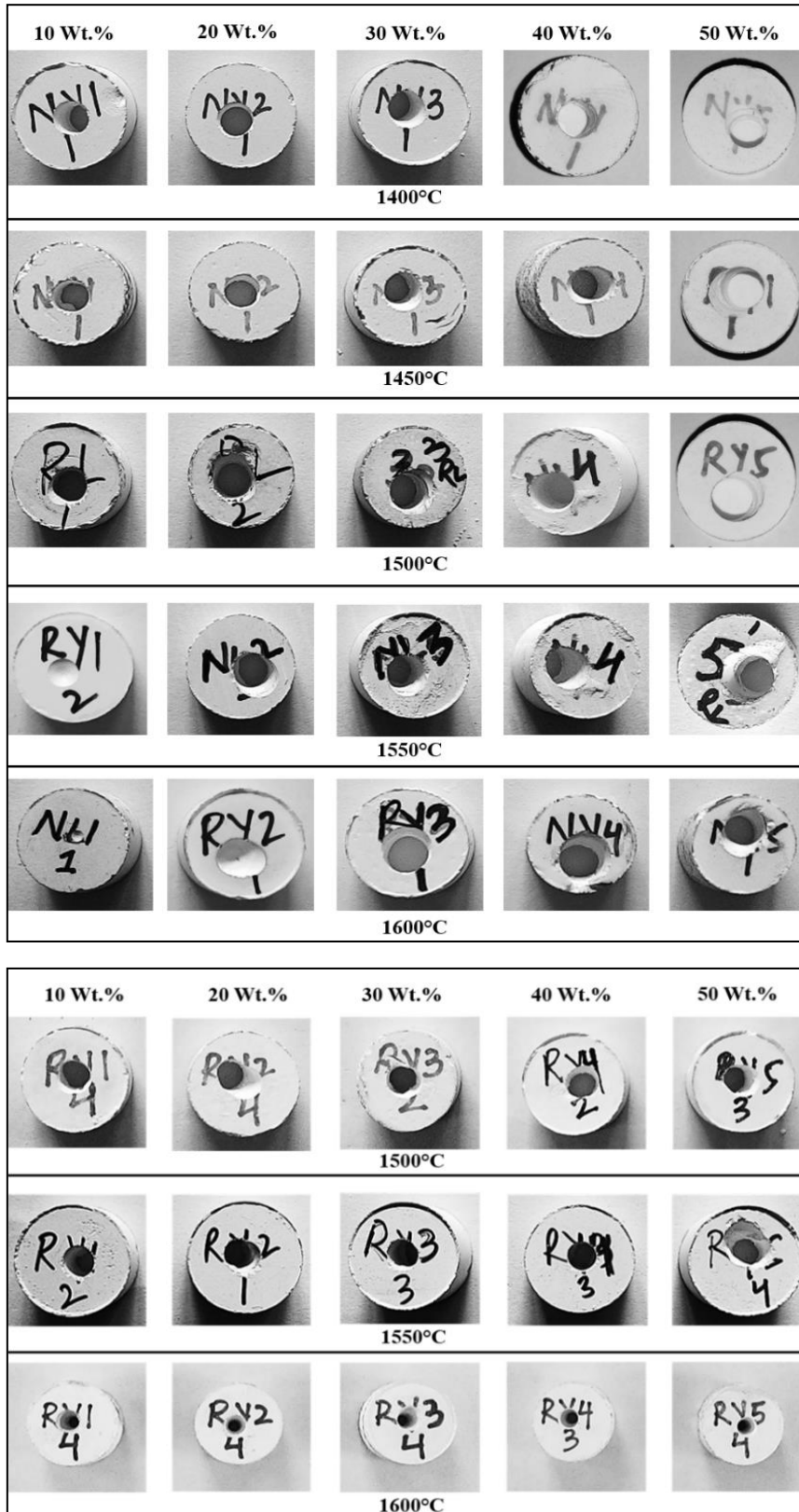Fig. 4.26: Photographs of Drilled Composites (A) CAl$_2$O$_3$-LaPO$_4$; (B) RAl$_2$O$_3$-LaPO$_4$

Fig. 4.27: Photographs of Drilled Composites (A) CAl$_2$O$_3$-YPO$_4$; (B) RAl$_2$O$_3$-YPO$_4$

4.8 Cytotoxicity of composites

The concept of biocompatibility, associated with a set of In vitro standard tests. It is introduced to confirm the biological behavior of the synthetic material. When the synthetic materials are first used in biomedical applications, the only requirement is to achieve a suitable condition such as combination of physical properties to match those of the replaced tissue with minimal toxic response of the host. Bioactivity is the ability to interact with a biological environment to enhance the biological response [10-11]. Confirmation of In vitro cytotoxicity of bioceramic material is to evaluate cell response of the composites [10] [12]. Biomaterials once implanted will help the body to heal itself. Capability of bioceramic within living bone and host material are mandatory to develop new bioactive ceramics for load bearing bone repair applications. Here in, In vitro cytotoxicity and cell viability is analyzed using MG 63 osteoblast cells.

4.8.1. In Vitro Cytotoxicity

In vitro cytotoxicity of composites (sintered at 1600°C) carried out direct contact with MG 63 osteoblast cells is represented in the Fig. 4.28 – Fig. 4.31. The cytotoxicity of the composites evaluated with following the ISO-10993-5 [13]. The test result performed on the composites (powder) exhibits small spherical and long tail morphology characteristics of MG 63 osteoblast cell line and analyzed with pure Al_2O_3, 10 and 50 wt. % of REP. The positive control and pure Al_2O_3 are found to adhere and expand on composite powder. The fraction of long shaped cells is similar to a positive control and composites. Morphology of the MG 63 osteoblast cells (Dead & Live) are marked in Fig 4.28 and same for all respective ones. Generally dead cell are look like open envelope and live cells poses there original tail like structure. The results of the cytotoxicity test reveal that the extract of composites does not affect the cell viability and proliferation.
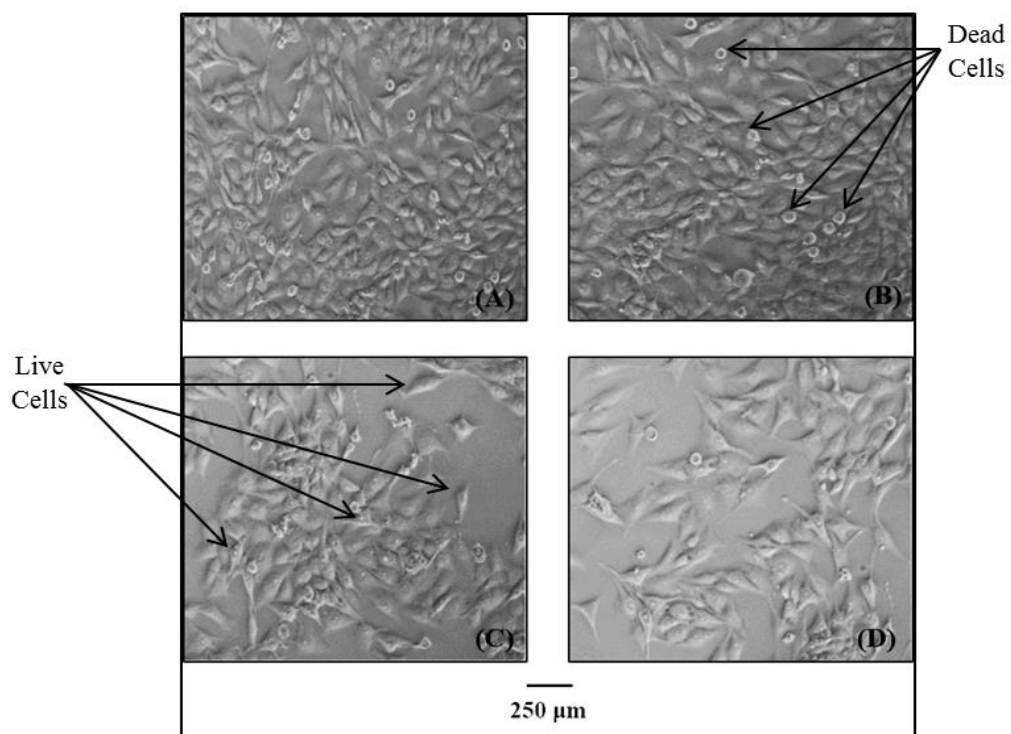
Fig. 4.28: Inverted Microscope Images of MG 63 Osteoblast Cell Adhesion on CAl_2O_3-$LaPO_4$ Composites Sintered at 1600°C (A) Control; (B) Pure CAl_2O_3; (C) 10 wt. % of $LaPO_4$; (D) 50 wt. % of $LaPO_4$

Fig. 4.29: Inverted Microscope Images of MG 63 Osteoblast Cell Adhesion on RAl_2O_3-$LaPO_4$ Composites sintered at 1600°C (A) Control; (B) Pure RAl_2O_3; (C) 10 wt. % of $LaPO_4$; (D) 50 wt. % of $LaPO_4$
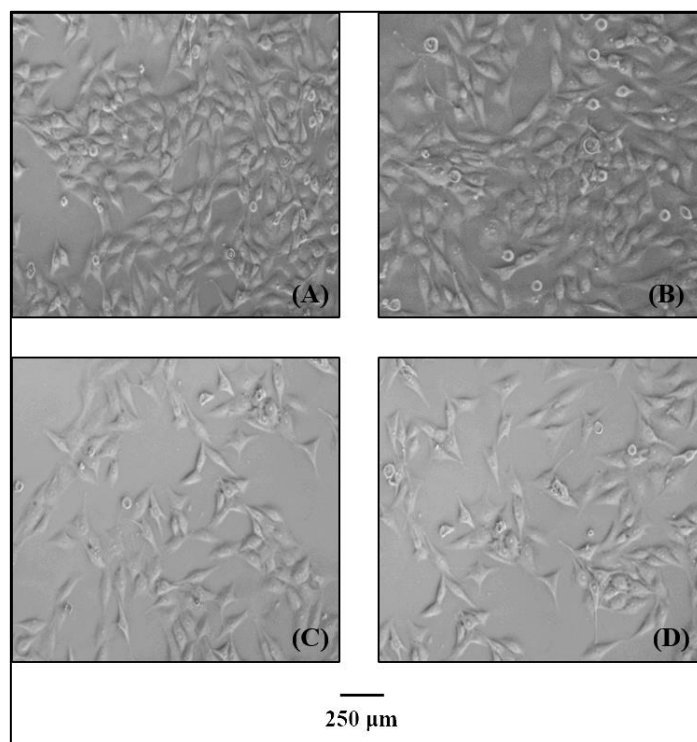
Fig. 4.30: Inverted Microscope Images of MG 63 Osteoblast Cell Adhesion on CAl_2O_3-YPO_4 Composites Sintered at 1600°C (A) Control; (B) Pure CAl_2O_3; (C) 10 wt. % of YPO_4; (D) 50 wt. % of YPO_4
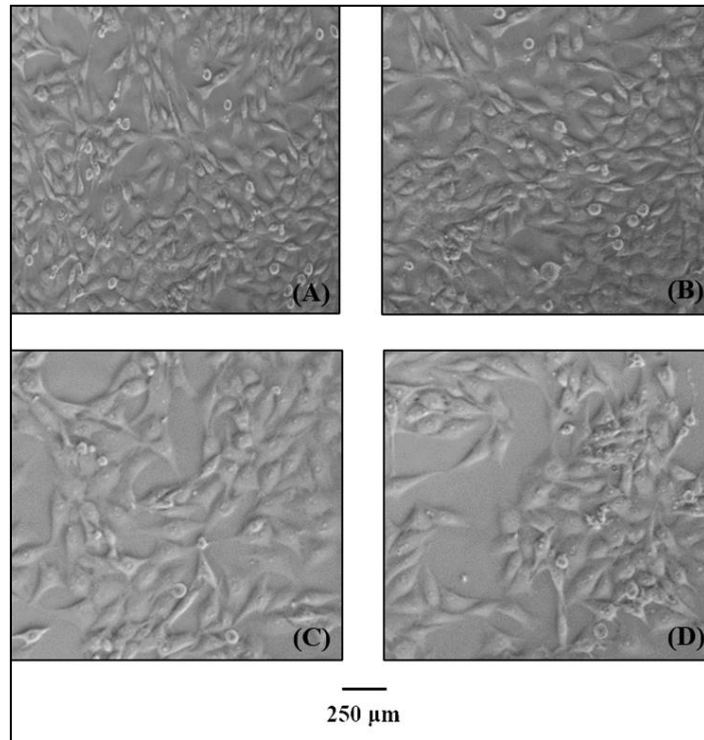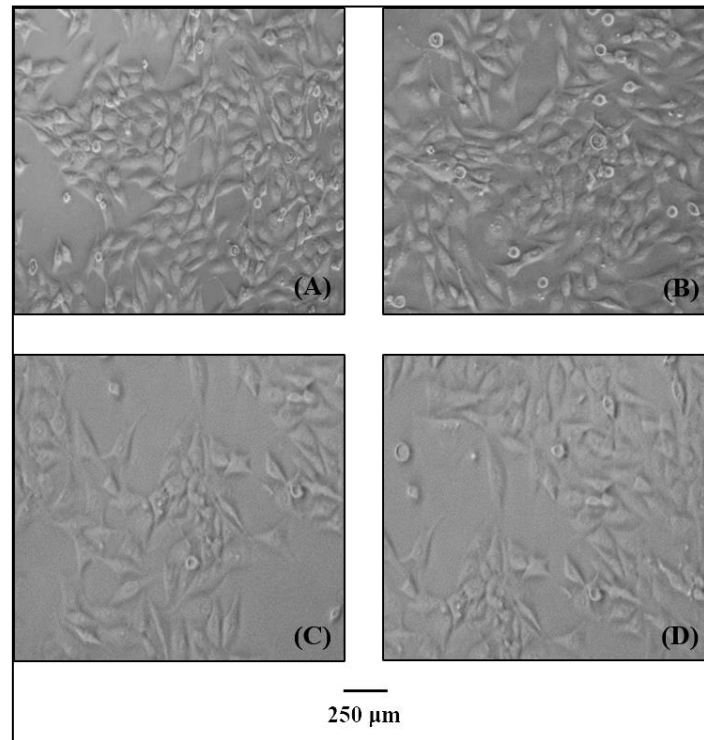

Fig. 4.31: Inverted Microscope Images of MG 63 Osteoblast Cell Adhesion on RAl_2O_3-YPO_4 Composites Sintered at 1600°C (A) Control; (B) Pure RAl_2O_3; (C) 10 wt. % of YPO_4 (D) 50 wt. % of YPO_4

4.8.2 Cell viability study

Metabolic study of the composites (10 and 50 wt. % of REP in both the Al_2O_3) sintered at 1600°C has been investigated by MTT assay using MG 63 Osteoblast cells. The difference in the cell viability index amongst the sintered composites is shown in Fig. 32 – Fig. 35. The cell viability index of pure alumina and composites containing 10 and 50 wt. % of REPs is evaluated by controlled tissue culture plate and then compared. Clearly, it shows that different ratios of REP supports the growth of the MG 63 cells and also proves that higher amount of REP also supports the growth of cells. Results show that composites are non-toxic and have biocompatible nature.
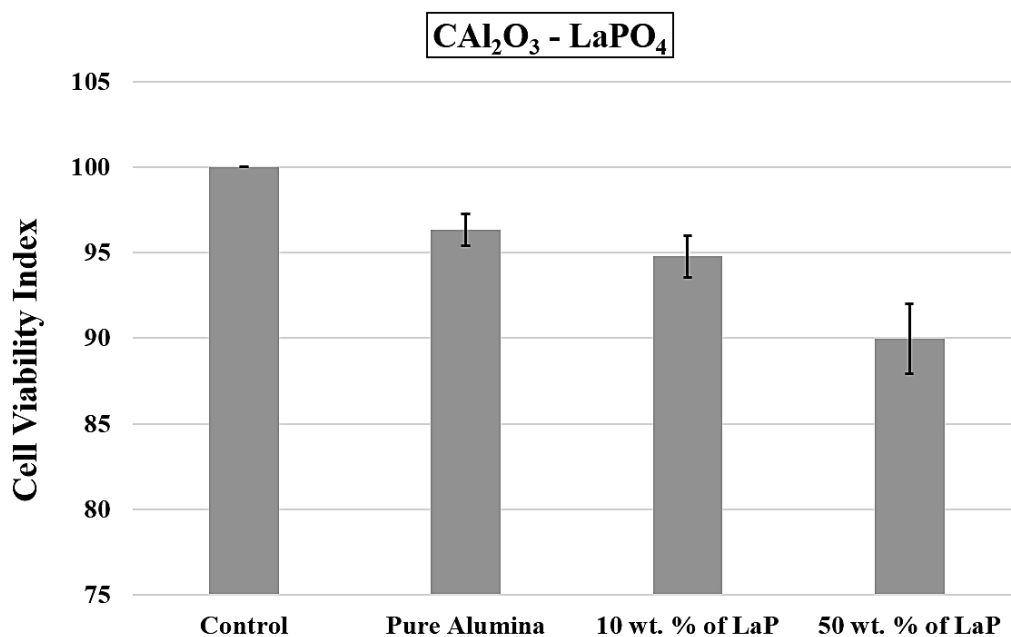

Fig. 4.32: Cell Viability Index of Composites (10 & 50 wt. % of $LaPO_4$) Sintered at 1600°C $CAl_2O_3/LaPO_4$
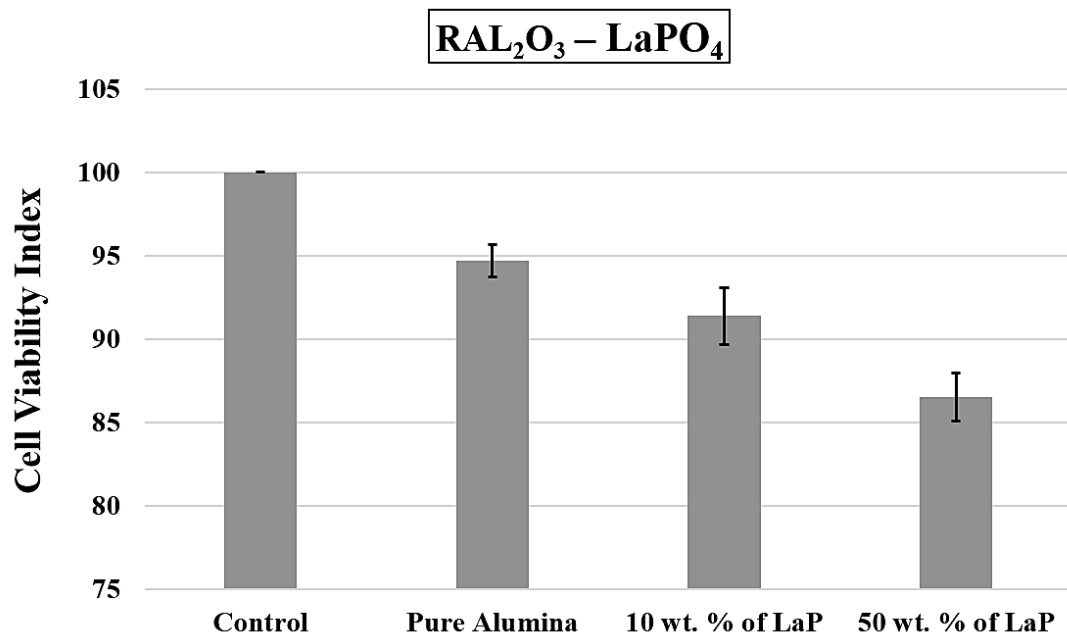
Fig. 4.33: Cell Viability Index of Composites (10 & 50 wt. % of LaPO$_4$) Sintered at 1600°C RAl$_2$O$_3$/LaPO$_4$
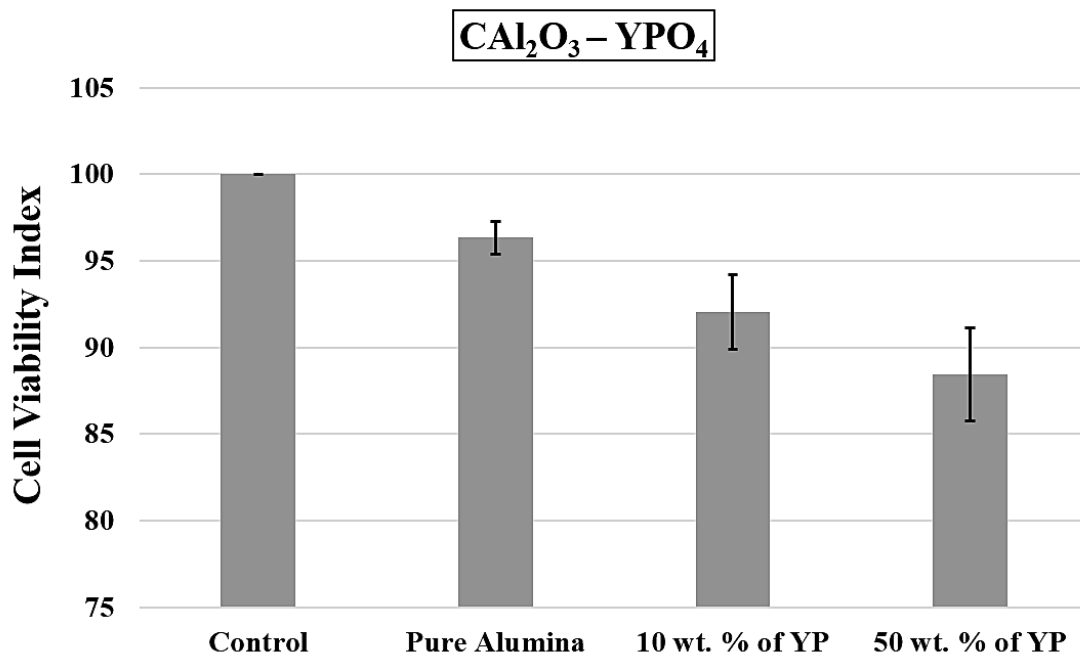

Fig. 4.34: Cell Viability Index of Composites (10 & 50 wt. % of YPO$_4$) Sintered at 1600°C CAl$_2$O$_3$/YPO$_4$
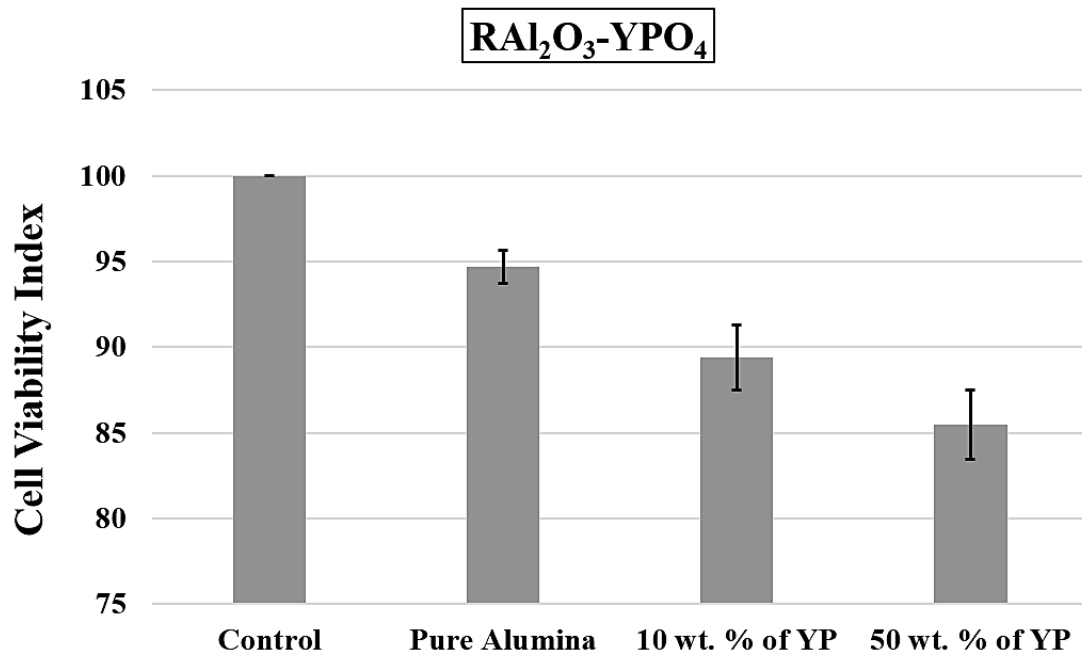
Fig. 4.35: Cell Viability Index of Composites (10 & 50 wt. % of YPO_4) Sintered at 1600°C RAl_2O_3/YPO_4

References:

1. Alumina's for ceramic applications, Product catalogue, Almatis Inc., USA.

2. R. Wang, W. Pan, J. Chen, M. Jiang, Y. Luo, M. Fang, Ceramic International 29 (2003) 19-25.

3. R. Wang, W. Pan, J. Chen, M. Fang, J. Meng, Material Letters 57 (2002) 822-827.

4. R. Wang, W. Pan, J. Chen, M. Fang, Z. Cao, Y. Luo, Material Chemistry and Physics 79 (2003) 30-36.

5. S. Lucas, E. Champion, D. Bregiroux, D. B. Assollant, F. Audubert, Journal of Solid-State Chemistry 177 (2004) 1302-1311.

6. J. D. Donaldson, A. Hezel, S. D. Ross, J. Inorg. Nucl. Chem., 29 (1967).

7. H. Lai, Y. Du, M. Zhao, K. Sun, L. Yang, Ceramic International, 40 (2014) 1885-1891.

8. Davis J. B., Marshall D. B., Houslwy R. M., Morgan P. E. D., Journal of American Ceramic society, 81 (8) (1998), pp. 2169–2175.

9. Majeeda M. A., Vijayaraghavan L., Malhotra S. K., krishnamorthy R., Journal of Materials Processing Technology, 209 (5) (2009), pp. 2499–2507.

10. T. Kokubo, H. Takadama, Biomaterials, 27 (2006) 2907-2915.

11. L. L. Hench, Biomaterials, Science 208 (1980) 826-831.

12. S. Nath, R. Tu, T. Goto, Surface Coatings Technol., 206 (2011) 172-177.

13. I.S.O. 10993-5, Biological evaluation of medical product, test for in vitro cytotoxicity Part 5 (1999).

CHAPTER 5
Conclusion
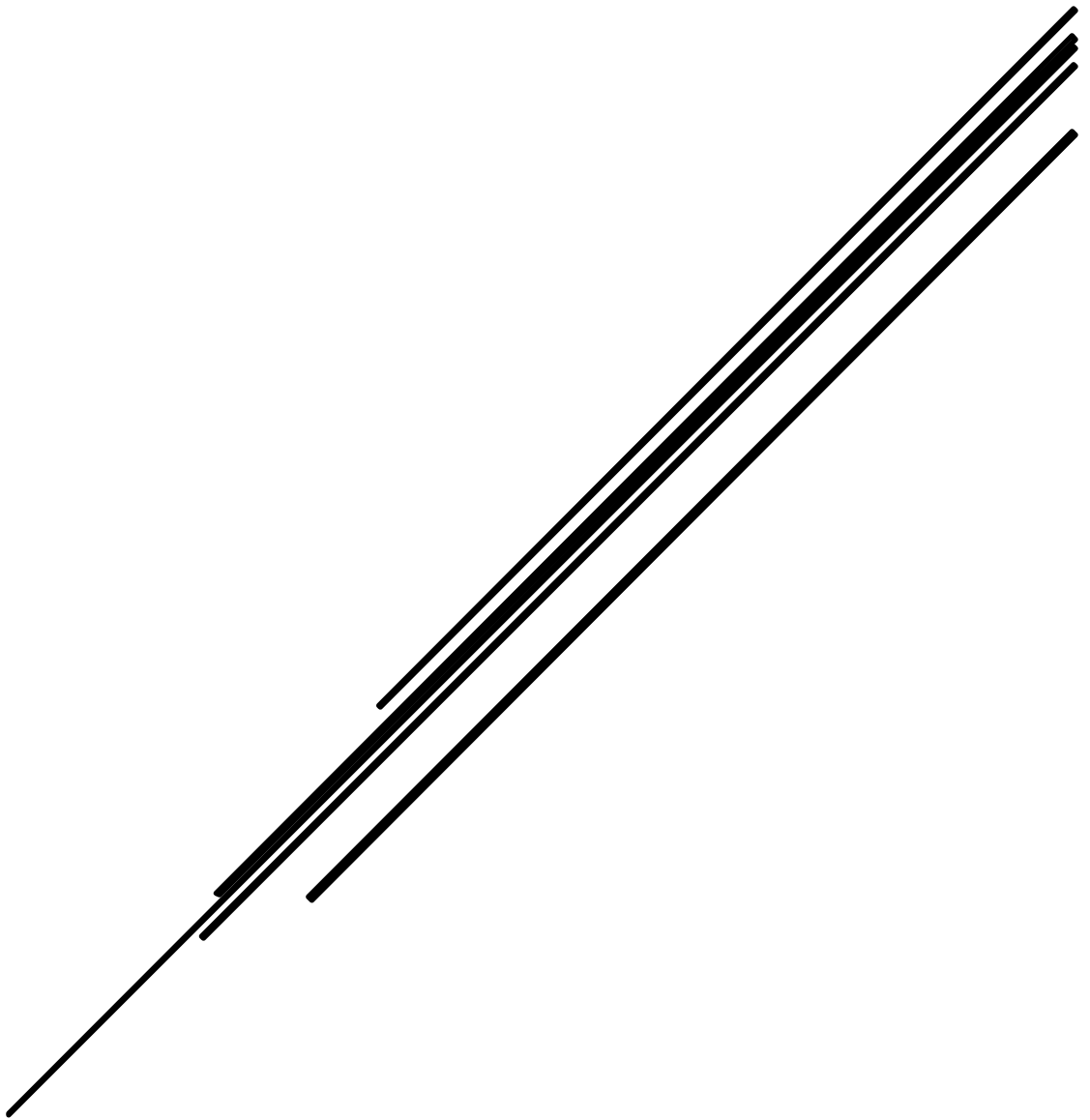
5.1 Conclusion

1. Phase pure rare earth phosphates (REP), namely $LaPO_4$ and YPO_4 were prepared used reaction synthesis technique and calcination. The preparation of rare earth phosphates is scalable process and can be produced in laboratory in maintained neat and clean atmosphere. Synthesized phosphates were characterized and confirmed by phase analysis, FTIR and microstructural characterization.

2. Two grades of commercially available synthetic and pure alumina, namely CAl_2O_3 and RAl_2O_3 were used to Al_2O_3-REP composites by solid mixing in wet medium, pressing and sintering between 1400 to 1600°C. REP content in the compositions were varied between 10 to 50 wt. %.

3. Densification and strength study of the different composites showed that the sinterability and strength of Al_2O_3/REP composites were dependent on the REP content. Increasing amount of REP content was found to decrease the densification and strength of the composites and increasing sintering temperature resulted in increased values.

4. Phase analysis study of the sintered composites confirmed the presence of only alumina and REP phases irrespective of REP content and sintering temperature. This indicates no reaction between the components has occurred, and the sintered products are composites in nature.

5. Microstructural study and elemental distribution confirmed the well distribution of Al_2O_3 and REP particles in all the compositions. REP particles have also retained their features even after sintering, showing their thermal stability and non-reactivity with alumina. Thus, the sintered samples are composites in nature.

6. The machinability of composites is markedly improved due to the presence of weak interphase material REP in between the Al_2O_3 particles. Hence, the sintered composites are drilled by using conventional cemented carbide drill bits. But pure alumina, without any REP content, were found to be not drillable and cracked during drilling in the same drill bits.

7. Al$_2$O$_3$/REP composites also showed the positive results in cytotoxicity testing and cell viability study supports the growth of cells on the sintered composited and showed good compatibility.

8. CAl$_2$O$_3$ showed better result as compare to the other alumina in all aspects.

9. CAl$_2$O$_3$ with 30wt. % REP content sintered at 1600°C was found to be machinable with a densification of >85% and strength >150MPa, may be reported as the optimum batch with desired properties.

10. Both rare earth phosphates are biocompatible. REPs are being used in biomedical fields, mainly as bio-imaging phosphors. Most of the rare earth oxides are radioactive in nature but these do not have much radio activeness. Both REPs with CAl$_2$O$_3$ showed better result as compare to other REP/alumina composites.

5.2 Future Scope of Work

➢ Machinability study of ceramic materials is not common and so the simplest and easiest techniques, drilling, are studied here. Sintered composited prepared in the study were found to be well machinable by drilling, but further machinability study may be proposed as future scope of the work.

➢ CAl$_2$O$_3$ with 30 wt. % REP content sintered at 1600°C was found to be machinable with a densification of >85% and strength >150MPa. But all the properties of this composition and also other compositions may also be improved by incorporating better processing techniques, like isostatic pressing, hot pressing, etc. Study with these advanced processing techniques may be taken up as future scope of the work.

➢ Cytotoxicity and cell viability study was done as the biological study of the sintered composites. However, further detailed biological study, including in-vivo characterization, may be taken up as the future scope of the work.

List of Publications from this work

1. **A. Badolia**, R. Sarkar, S. K. Pal, Lanthanum Phosphate Containing Machinable Alumina Ceramic for Bio-Medical Application, Transactions of Indian Ceramic Society, 73 (2) (2014) 115-120.

2. **A. Badolia**, R. Sarkar, Effect of $LaPO_4$ content on the machinability, microstructure and biological properties of Al_2O_3, Accepted, Interceram (13-06-2015).

3. **A. Badolia**, R. Sarkar, Reactive Alumina-$LaPO_4$ Composite as Machinable Bioceramics, Bulletin of Material Sciences, Article 955 (BOMS-D-15-0031.1) (02-07-2015).

4. **A. Badolia**, R. Sarkar, Alumina Based Machinable Bioceramic: Addition of YPO_4, Accepted, Ceramic Forum International CFI 9/2015.

5. **A. Badolia**, R. Sarkar, Alumina Yttrium Phosphate Machinable Bioceramic Composites, Communicated to Journal of Applied Ceramic Technology (2015).

Conferences Attended

1. International conference of Indian Ceramic Society, presented paper title "Lanthanum Phosphate Containing Machinable Alumina Ceramic for Bio-Medical Application", at Jamshedpur Dec 2013.

Curriculum Vitae

Abhishek Badolia
S/O: Shri Krishan Lal Badolia
3A/11, W.E.A., Karol Bagh,
Near Pusa Road, New Delhi,
Delhi-110005
Phone: +91-9692701883, 9968806149
Email: rite2badolia@rediffmail.com

Date of Birth: 07-09-1990

Education: B.Tech (Bio-medical Engineering), 2012, P.D.M. College of Engineering, Haryana, INDIA

Research Interest: Bioceramics, Machinable Ceramics, Biomaterials

Publications:

1. **A. Badolia**, R. Sarkar, S. K. Pal, Lanthanum Phosphate Containing Machinable Alumina Ceramic for Bio-Medical Application, Transactions of Indian Ceramic Society, 73 (2) (2014) 115-120.

2. **A. Badolia**, R. Sarkar, Effect of $LaPO_4$ Content on the Machinability, Microstructure and Biological Properties of Al_2O_3, Accepted, Interceram (13-06-2015).

3. **A. Badolia**, R. Sarkar, Reactive Alumina-$LaPO_4$ Composite as Machinable Bioceramics, Bulletin of Material Sciences, Article 955 (BOMS-D-15-0031.1) (02-07-2015).

4. **A. Badolia**, R. Sarkar, Alumina Based Machinable Bioceramic: Addition of YPO_4, Accepted, Ceramic Forum International, CFI 9/2015.

5. **A. Badolia**, R. Sarkar, Alumina Yttrium Phosphate Machinable Bioceramic Composites, Communicated to Journal of Australian Ceramic Society (2015).

Conferences:

1. **A Badolia**, R Sarkar, S Pal, "Lanthanum Phosphate Containing Machinable Alumina Ceramic for Bio-Medical Application" presented orally in International conference of Indian Ceramic Society, at Jamshedpur Dec 2013.